ESL-TR-88-50

# CHARACTERIZATION OF CHEMICALS ON ENGINE EXHAUST PARTICLES

M.R. KUHLMAN, J.C. CHUANG

BATTELLE COLUMBUS DIVISION
505 KING AVENUE
COLUMBUS OH 43201-2693

JUNE 1989

FINAL REPORT

SEPTEMBER 1986 — DECEMBER 1987



AFESC

AIR FORCE ENGINEERING & SERVICES CENTER
ENGINEERING & SERVICES LABORATORY
TYNDALL AIR FORCE BASE, FLORIDA 32403

# NOTICE

PLEASE DO NOT REQUEST COPIES OF THIS REPORT FROM HQ AFESC/RD (ENGINEERING AND SERVICES LABORATORY). ADDITIONAL COPIES MAY BE PURCHASED FROM:

NATIONAL TECHNICAL INFORMATION SERVICE
5285 PORT ROYAL ROAD
SPRINGFIELD, VIRGINIA 22161

FEDERAL GOVERNMENT AGENCIES AND THEIR CONTRACTORS REGISTERED WITH DEFENSE TECHNICAL INFORMATION CENTER SHOULD DIRECT REQUESTS FOR COPIES OF THIS REPORT TO:

DEFENSE TECHNICAL INFORMATION CENTER
CAMERON STATION
ALEXANDRIA, VIRGINIA 22314

UNCLASSIFIED

SECURITY CLASSIFICATION OF THIS PAGE

# REPORT DOCUMENTATION PAGE

Form Approved
OMB No. 0704-0188

| | |
|---|---|
| 1a. REPORT SECURITY CLASSIFICATION | 1b. RESTRICTIVE MARKINGS |
| 2a. SECURITY CLASSIFICATION AUTHORITY | 3. DISTRIBUTION/AVAILABILITY OF REPORT: Approved for Public Release Distribution Unlimited |
| 2b. DECLASSIFICATION/DOWNGRADING SCHEDULE | |
| 4. PERFORMING ORGANIZATION REPORT NUMBER(S) | 5. MONITORING ORGANIZATION REPORT NUMBER(S): ESL-TR-88-50 |
| 6a. NAME OF PERFORMING ORGANIZATION: Battelle Columbus Division; 6b. OFFICE SYMBOL (If applicable) | 7a. NAME OF MONITORING ORGANIZATION: Air Force Engineering and Services Center |
| 6c. ADDRESS (City, State, and ZIP Code): 505 King Avenue, Columbus OH 43201-2693 | 7b. ADDRESS (City, State, and ZIP Code): HQ AFESC/RDVS, Tyndall AFB FL 32403 |
| 8a. NAME OF FUNDING/SPONSORING ORGANIZATION: HQ AFESC; 8b. OFFICE SYMBOL (If applicable): RDV | 9. PROCUREMENT INSTRUMENT IDENTIFICATION NUMBER: F08635-85-C-0122 |
| 8c. ADDRESS (City, State, and ZIP Code): HQ AFESC/RDVS, Tyndall AFB FL 32403-6001 | 10. SOURCE OF FUNDING NUMBERS: PROGRAM ELEMENT NO. 62206F; PROJECT NO. 1900; TASK NO 4C; WORK UNIT ACCESSION NO. 08 |

11. TITLE (Include Security Classification)

Characterization of Chemicals on Engine Exhaust Particles

12. PERSONAL AUTHOR(S)

M. R. Kuhlman and J. C. Chuang

| 13a. TYPE OF REPORT | 13b. TIME COVERED | 14. DATE OF REPORT (Year, Month, Day) | 15. PAGE COUNT |
|---|---|---|---|
| Final | FROM 9/86 TO 12/87 | June 1989 | 116 |

16. SUPPLEMENTARY NOTATION

Availability of this report is specified on reverse of the front cover

| 17. COSATI CODES | | | 18. SUBJECT TERMS (Continue on reverse if necessary and identify by block number) |
|---|---|---|---|
| FIELD | GROUP | SUB-GROUP | |
| 04 | 01 | | Turbine engine; Aircraft exhaust; Organic emissions |
| 07 | 04 | | Photochemistry chamber studies, Particle emissions |

19. ABSTRACT (Continue on reverse if necessary and identify by block number)

The objective of the work described in this report has been the characterization of particulate-bound chemicals emitted from military aircraft, both as they are emitted and as the exhaust ages. Three Air Force turbine engines (TF33-P3, TF33-P7, and J79C) were examined in this study, using engine test cells at Tinker AFB OK. Emissions were collected at power settings of idle, 30 percent, 75 percent, and injected into smog chambers for subsequent aging. Samples were collected from these chambers periodically during the photochemical experiments to permit measurements of the vapor phase and particle associated polycyclic aromatic hydrocarbon (PAH) and derivatives under experimental conditions. Throughout the course of the experiments, measurements of the concentrations of total hydrocarbons, NO, $NO_x$, and $O_3$ were made. The samples collected on filter and sorbent media were returned to the laboratory for extraction and analysis by gas chromatography/mass spectrometry (GC/MS) to determine masses of specific target compounds collected. The time profiles of these compounds are presented for the various engines, operating powers, sunlight levels, and photochemical reactivities examined.

| 20. DISTRIBUTION/AVAILABILITY OF ABSTRACT | 21. ABSTRACT SECURITY CLASSIFICATION | |
|---|---|---|
| ☒ UNCLASSIFIED/UNLIMITED ☐ SAME AS RPT. ☐ DTIC USERS | UNCLASSIFIED | |
| 22a. NAME OF RESPONSIBLE INDIVIDUAL: Surendra B. Joshi | 22b. TELEPHONE (Include Area Code): (904) 283-4234 | 22c. OFFICE SYMBOL: AFESC/RDVS |

DD Form 1473, JUN 86 *Previous editions are obsolete.* SECURITY CLASSIFICATION OF THIS PAGE

(The reverse of this page is blank.)

## PREFACE

This report was prepared by Battelle Columbus Division, Columbus OH 43201-2693, under Contract No. F08635-85-C-0122 for the Air Force Engineering and Services Center, Engineering and Services Laboratory (AFESC/ESL), Tyndall Air Force Base, Florida 32403-6001.

This final report describes the experimental methods and presents the results and interpretive analysis of the characterization of chemicals associated with particles in exhaust from three turbine engines. This work was performed between September 1986 and December 1987. The AFESC project officer was Mr Surendra Joshi.

Expert technical assistance in conducting the program was provided by L. W. Miga, C. Bridges, G. F. Ward, and S. W. Hannan. Engine testing at Tinker AFB was conducted with the cooperation and assistance of the Production Engine Test Section. We are especially grateful for the assistance provided by David Hughes and David Schley.

This report has been reviewed by the Public Affairs Office (PA) and is releasable to the National Technical Information Service (NTIS). At NTIS, it will be available to the general public including foreign nationals.

This technical report has been reviewed and is approved for publication.

Surendra B. Joshi

SURENDRA B. JOSHI, GS-12
Project Officer

Nils Akerlind, Jr.

NILS AKERLIND, Jr., Maj, USAF
Chief, Environics Division

Kenneth T. Denbleyker

KENNETH T. DENBLEYKER, Maj, USAF
Chief, Environmental Sciences Branch

Lawrence D. Hokanson

LAWRENCE D. HOKANSON, Colonel, USAF
Director, Engineering and Services Laboratory

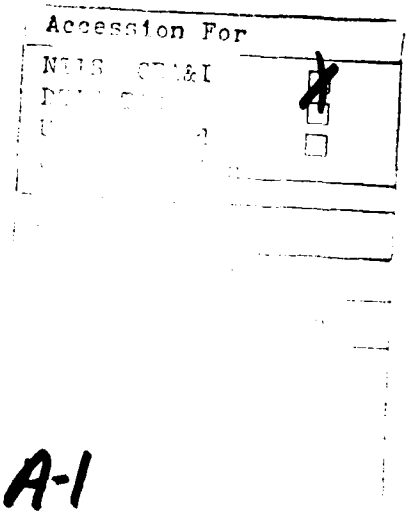


A-1



(The reverse of this page is blank.)

TABLE OF CONTENTS

TABLE OF CONTENTS
(CONCLUDED)

LIST OF FIGURES

LIST OF FIGURES
(Continued)

LIST OF FIGURES
(CONCLUDED)

LIST OF TABLES

# SECTION I

# INTRODUCTION

## A. OBJECTIVE

The Engineering and Services Center of the United States Air Force (AFESC) is conducting a joint program with the Naval Air Propulsion Center (NAPC) to update an engine emission catalogue last updated in 1978 (CEEDO-TR-78-33). Among the goals of the joint program are the identification of deficiencies in existing data and development of an engine emission data base. One gap identified in the existing data base is the lack of data about particulate-bound chemicals emitted from military aircraft. This study has as its objective, therefore, the characterization of these chemicals, both as they are emitted from the engine and as the emissions age in the environment.

## B. BACKGROUND

The visible plume of an aircraft jet engine is composed of $NO_2$ (a brown gas) and small particles. Both components depend strongly on engine type and engine operating power. The particles are, to a large degree, composed of unburned carbon which is black, relatively stable, and not a significant health threat. A more reactive component of the exhaust particulate matter is the hydrocarbons which are sorbed or condensed on the carbon particles. These compounds are a complex mixture of partially oxidized and reactive hydrocarbons with a variety of vapor pressures, reactivities, and physical properties. Although these particulate-bound compounds constitute only a very small fraction of the mass of emissions, they are very significant from an environmental and occupational health standpoint. Some of the compounds found in the exhaust from jet engines (and other combustion sources) have demonstrated mutagenic and/or carcinogenic properties in bioassay studies. These latter properties have guided our selection of compounds to be analyzed in the samples collected in this study.

## C. SCOPE

This report describes the results of a novel method for the study of the behavior of engine exhaust in the environment. In addition to sampling the

exhaust from jet engines operated in test facilities, aliquots of the exhaust gas were injected into specially constructed photochemical reaction chambers to undergo aging under the influence of ambient sunlight. Samples collected periodically during the course of a day are then used to track the decay/formation of potentially important polycyclic aromatic hydrocarbons (PAH) and their derivatives in the reactive exhaust gas mixture. Such aging experiments were performed in this study for three turbine engines (J79C, TF33-P3, TF33-P7) at different power settings, under light and dark conditions. This variation of test parameters provided a range of photochemical reactivity for the aging exhaust components.

## SECTION II

## EXPERIMENTAL METHODS

### A. TEST MATRIX

The exhaust aging experiments conducted include three engines, three power settings, and two light conditions. The matrix of tests was designed to permit assessment of the effects of engine type, power setting, and light on the PAH and $NO_2$-PAH behavior. The matrix of tests is presented in Table 1. The order of performance of the tests was selected to achieve the greatest efficiency of this subtask and for the comparison Subtask 1.06.

TABLE 1. MATRIX OF AGING EXPERIMENTS CONDUCTED FOR SUBTASK 1.05

| ENGINE | CHAMBER 1 | CHAMBER 3 | CHAMBER 2 | RUN NO. |
|---|---|---|---|---|
| J79C | 30%/Light | 30%/Dark | Ambient | 1 |
| | Idle/Light | Idle/Dark | Ambient | 2 |
| TF33-P3 | Idle/Light | Idle/Dark | EKMA/$NO_x$ | 3 |
| | 75%/Light | 30%/Light | Ambient | 4 |
| TF33-P7 | 30%/Light | Idle/Light | Ambient | 5 |
| | 30%/Light | 30% + EKMA/Light | EKMA/$NO_x$ | 6 |

For each day of the expermental program, two of the three chambers (Numbers 1 and 3) were loaded with engine exhaust to approximately 15 percent, by volume. The third chamber (Number 2) was used as a reference chamber and was run either with ambient air alone or with EKMA mix and $NO_x$ added to its

contents. One can see that the matrix of tests performed does not contain all possible combinations of the varied parameters, but it was selected as providing the maximum information possible within the available resources.

B. EMISSIONS SAMPLING/INJECTION

1. Engine Descriptions

The three engines studied include only two fundamentally different engine types. The J79C engine used in this study is a modified version of the somewhat older General Electric J79 turbojet engine. This particular version is referred to as "smokeless" as the modifications were effected to reduce the visible plume from this engine. Two such engines constitute the power plant of the F4 fighter, providing 17900 1 pound thrust each. The T B3-P3 and TF33-P7 are variants of the same basic design engine and differ principally in the amount of bypass air flow. Both are Pratt-Whitney turbofans, producing approximately 17000 1 pound thrust. Eight TF33-P3 engines power the B52H bomer.

2. Engine Test Facility

Engine emissions sampling was performed in an indoor test cell at Tinker Air Force Base, Oklahoma City, Oklahoma. The three engines examined in this study were operated in Test Cell 8. A diagram of a generic test cell is shown in Figure 1. The engine exhaust flows through a 75-foot long steel augmentor tube, the last 18 feet of which are perforated with numerous 1.25-inch holes. This portion of the tube runs into a separate "blast room" vented to the outside. The hot exhaust passes through these holes and out of the test cell through fifty-six 2.5-foot square vent tubes in the ceiling of the blast room. The test cell is instrumented to record numerous engine performance parameters.

3. Engine Exhaust Sampling and Chamber Injection

Sampling of the engine exhaust was performed for two purposes: injection of a measured volume of engine exhaust into the chambers for the aging experiments, and collection of exhaust components on filters and sorbent media for subsequent analysis. All sampling was performed by withdrawing exhaust from a point located near the exhaust plane of the engine, near the longitudinal axis of the engine. To permit engine exhaust characterization to be

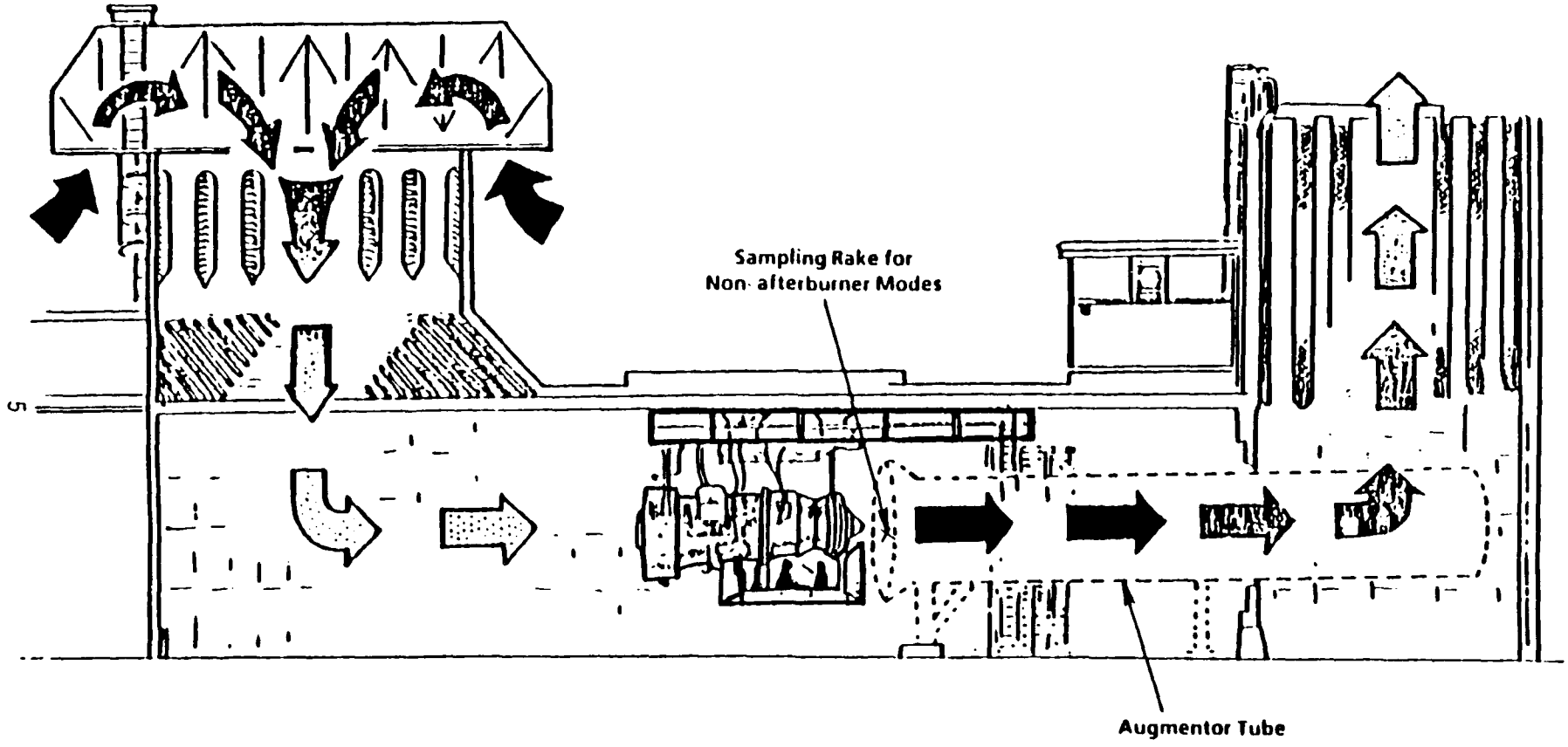


Figure 1. Test Cell Cross Section

performed at the same time as the chamber filling was performed, an auxiliary 3/8-inch I.D. stainless steel sampling probe was affixed to the cruciform sampling rake. The inlet for this probe was located in the same plane as the inlets for the rake. This probe was connected to a clean air purge line to prevent contamination from entering the probe until sampling was initiated. Also connected to the probe was a 50-foot length of 3/8-inch I.D., heat traced Teflon tubing which was maintained at 50°C. This Teflon$^{R}$ line conveyed the exhaust to a heated stainless steel metal bellows pump, which provided a flow rate of 3 scfm. This pump was used during both the exhaust sampling operation and during chamber filling.

The procedure used for the exhaust sampling and chamber injection was as follows. The flow rate at the pump outlet was measured using a calibrated rotameter prior to connecting the pump to the chamber. The short heated Teflon$^{R}$ line was then connected from the pump outlet to the chamber and the chamber's mixing fan and heated injection line were left on. Following stabilization of the engine at the desired power setting, the clean air purge of the sampling line was turned off and a timed injection of engine exhaust into the chamber was made, using the preheated sampling line and metal bellows pump. This injection period was typically about 30 minutes, during which the chamber hydrocarbon concentration was monitored using a Beckman 402 Total Hydrocarbon Analyzer. After the chamber was filled with the desired volume of exhaust, the metal bellows pump was disconnected from the chamber, but continued to draw engine exhaust through the heated sampling line. At this time, auxiliary pumps were turned on and withdrew a measured exhaust flow through a Millipore$^{R}$ filter for subsequent inorganic analysis, and through a quartz fiber filter and XAD-2 sorbent bed for organic analyses. Sufficient cooling of the sample gas stream was provided to obtain a 40°C temperature (or less) at the plane of the quartz fiber filter. This temperature was monitored to ensure that particle bound organic species would not evaporate and could be collected on the sorbent trap.

## C. CHAMBER OPERATIONS

### 1. Design Requirements

The chambers used in the photochemical aging experiments had to satisfy a number of requirements, some of which were unique to this project. It was required that the chambers be transparent, to permit actinic radiation to initiate photochemical processes and that they have chemically inert surfaces so as not to react significantly with the oxidizing species in the test atmospheres. The chambers also needed provision for mixing to insure uniformity of the atmosphere. The capacity of the chambers had to be 25 $m^3$ to insure that sufficient material would be present to exceed the detection limits of the GC/MS analytical method. It was also necessary to design the chambers in such a way as to minimize -- within practical limitations -- the surface to volume ratio. One of the chambers had to be equipped with a cover which could exclude sunlight. Finally, the chambers had to be movable, since the aging experiments were to be carried out several hundred meters from the engine exhaust sampling port.

### 2. Chamber Description

The three smog chambers were constructed as right circular cylinders having a diameter of 3.0 meters and a height of 3.4 meters, with a conical top of height 0.6 meters affixed to their top. The total volume enclosed by the chambers was 26.7 $m^3$. The materials used to construct the chambers consisted of an aluminum framework, stainless steel hardware, and Teflon$^R$ film. The Teflon$^R$ film which comprised nearly all of the surface of the chambers was heat-sealed from standard rolls of film into three separate pieces: a square floor upon which the aluminum frame rested, a cylinder which enclosed the cylindrical portion of the aluminum frame, and a cone which covered the top portion of the framework. The Teflon$^R$ film cylinder and cone were held in place using tensioning bands placed outside the chamber, and no structural problems were encountered when wind speeds remained below 45 mph. The chambers were made with a reflective (aluminum foil) floor beneath the Teflon$^R$ film of the floor to reduce the solar heating of the floor. One chamber was covered with an aluminized mylar film to exclude sunlight for those experiments which were to be performed in darkness.

The chambers were equipped with an axially positioned mixing fan, sampling/injection ports which entered through the chamber floor, an exhaust blower, and a trap door for entry through the floor. Since the chambers were required to be portable, they were fastened to wooden platforms, approximately 3.7 meters square. These platforms were equipped with wheels and a steering yoke which enabled them to be pulled by hand or towed with a vehicle at low speeds.

The framework of the chambers was made in segments so that the chambers could be taken apart for shipment and storage and reassembled for reuse. (It was anticipated at the start of this subtask that future studies would involve performance of jet exhaust aging experiments.)

3. Photochemistry Measurements

During the photochemical aging experiments, the concentrations of total hydrocarbons (THC), $O_3$, NO, $NO_x$, and $SF_6$ within each of the chambers was monitored. Heated Teflon$^R$ sampling lines were used to connect the three chambers to a switching station which directed air from one of the chambers or ambient air into the sampling manifold to which the instrumentation shown in Table 2 was connected. The data acquisition program cycled the sampling through each of the four sources so that each was monitored for 5 minutes in sequence. During the first 2 minutes the data were discarded to permit the sampling manifold to be completely flushed with air from the specified source. During the following 3 minutes, the continuous instruments were read every second and 1-minute averages were printed and stored on the computer disk. Finally, the 3-minute averaged data were stored and printed. With the three chambers and ambient air being sampled, this permitted a 3-minute average to be obtained from each source every 20 minutes. In addition to the gases mentioned above, the temperatures and dewpoints of the gas streams were continuously monitored as well as the incident ultraviolet radiation.

TABLE 2. INSTRUMENTATION USED FOR MONITORING DURING PHOTOCHEMICAL AGING EXPERIMENTS

| PARAMETER | INSTRUMENT |
|---|---|
| Total hydrocarbons | Beckman 402 |
| $O_3$ | Bendix Model 8002 |
| $NO_x$, NO | Monitor Labs Model 8440 |
| $SF_6$ | Varian Gas Chromatograph with Electron Capture Detector |
| Ultraviolet radiation | Eppley UV radiometer |
| Temperature/dewpoint | EG&G Model 911 |
| Chamber temperature | Type K thermocouples |

4. Run Procedure

Performance of the aging experiments required a number of operations, described here in order of occurrence. The objective was to complete the injection of exhaust into the chambers as early as possible. Ideally one would perform the exhaust injections into the chambers simultaneously, and before dawn so as to permit the clearest comparison between the chambers' atmospheres performance, but this was not a possibility. One test cell was used to run the engine whose exhaust was to be injected into the chambers, and the chambers were filled one after the other. The exhaust injections required approximately 30 minutes, and engine operations were not possible until about 0730. Within these constraints, everything possible was done to initiate the aging experiments early and with the two chambers filled as near in time to each other as possible.

Overnight, before performance of an aging experiment, the chambers were purged with house air which was filtered and run through an activated charcoal scrubbing apparatus. Upon arrival onsite the purge air was turned off and $SF_6$ injections were made into each chamber while the background

concentrations of all parameters were obtained. After the concentration of $SF_6$ was established, Chambers 1 and 3 were repositioned in preparation for engine exhaust injection. This process was described above. Following exhaust injection, each chamber was returned to the site for the aging experiment and immediately connected to the sampling system. The software-controlled switching of the manifold system was overridden by the operator during the run startup period to eliminate the 20-minute cycle time between readings on the chamber of interest. After both Chambers 1 and 3 were in their run location and their initial (post exhaust injection) atmosphere measured, the software was put in control of the sampling and data acquisition once again.

At several times during the aging experiments samples of the chambers were collected on filter and sorbent media for subsequent analysis as described above. At the conclusion of the aging experiment, a large volume sample (~5 $m^3$) of the chamber atmosphere was collected to assure collection of as much mass of the PAH and $NO_2$-PAH species as possible. Following the collection of these samples from the two exhaust-containing chambers, all three chambers were purged with ambient air at a high flow rate, then flushed with cleaned house air overnight for approximately 8 hours, in preparation for the following day's run.

5. Chamber Characterization

Before use of any smog chamber is appropriate, it is necessary to characterize the performance of the chamber with respect to leakage and reactivity. This is especially true when results obtained in different chambers are to be compared. Before the chamber characterization experiments, the three chambers were charged with high concentrations of $O_3$ (>10 ppm) to oxidize reactive surfaces present in the chambers initially. This was performed for two overnight periods before the performance of the characterization experiments and was not deemed necessary to repeat after the reactivity runs' results were assessed.

The chamber leakage rates were measured by following the concentration of $SF_6$ in each of the chambers over the course of 8 or more hours. Following an injection into each chamber, concentrations were repeatedly measured and the first order decay rate was calculated for this nonreactive species in each

chamber. The results for two sets of such measurements are presented here, expresssed as percent per hour.

| Date | Chamber 1 | 2 | 3 |
|---|---|---|---|
| 9/22-23 | 0.91 | 1.5 | 1.8 |
| 10/3-4 | 0.35 | 0.40 | 0.53 |

The September 22-23 run was performed with the chambers positioned out of doors, with the normal sampling scheme followed. The tensioning bands on all chambers were readjusted before the experiment performed on October 3-4. During this latter experiment the chambers were indoors overnight, and therefore not subject to the pumping action of the wind, and no sampling was performed during the storage period. The lower rates seen here -- calculated from the data obtained at the beginning and end of the 14-nour storage period -- indicate very low leakage rates. These values compare favorably with those obtained for fixed installations, and are, in fact, better than was expected.

The reactivity of a smog chamber is assessed in two respects. The rate of $O_3$ decay in a chamber is an indicator of the surface reactivity which would reduce the apparent photochemical activity of a system contained in the chamber. There is also the possibility that a chamber will contribute reactive contaminants to the contained atmosphere and so artificially enhance the apparent reactivity of the system under study. The decay of $O_3$ was measured in conjunction with the $SF_6$ leakage experiments discussed above, and the results are again presented in terms of percent decay per hour (corrected for dilution):

| Date | Chamber 1 | 2 | 3 |
|---|---|---|---|
| 9/22-23 | 5.9 | 8.3 | 9.9 |
| 10/3-4 | 2.6 | 3.3 | 2.5 |

The apparent reduction in $O_3$ decay rates between these two trials is likely attributable to the action of oxidant formed during shakedown photochemical

runs performed in the interim, and to the reduced leakage of potentially reactive species into the chambers. It would be desirable to have still lower $O_3$ decay rates, but given the schedule constraints and the limitations imposed by a field setting, further improvement was not possible. Chambers 1 and 3 were selected to receive the engine exhaust injections, partly because of the agreement in their measured decay rates.

Matched runs of EKMA/$NO_x$ mixtures were carried out in all three chambers, on October 5 and 6, to examine whether the three behaved similarly as photochemical reaction vessels. To perform such experiments, equal amounts of a reactive hydrocarbon mixture (EKMA) and NO and $NO_2$ are injected into each chamber. Measured parameters such as the maximum $NO_2$, and maximum $O_3$ concentrations and the times at which these maxima are achieved are examined as indicators of reaction chamber performance. Figures 2, 3, and 4 depict the time profiles of THC, $NO_x$, and $O_3$ for the three chambers. The EKMA injection into each chamber brought the indicated concentration from a background value of about 3.5 ppmC to nearly 12 ppmC for all three chambers. The instrumentation does not provide concentration data for specific hydrocarbons, but the THC data do indicate very similar behavior for the three chambers -- a gradual decrease of nearly 1 ppmC in the indicated THC concentration from 1000 to 1300, followed by a gradual apparent increase in the THC concentration such that the initial concentration values are nearly equalled at 1700. Examination of the NO and $NO_2$ data presented in Figure 3 indicates that the $NO_2$ concentrations for all three chambers peak at nearly the same time, which is also the time corresponding to the minimum in the THC curves. This may reflect the formation of reactive organo-nitrate compounds which are not detected by the hydrocarbon detector. In Figure 3 it is apparent that the initial $NO_2$ concentrations achieved in the three chambers differ because of variations in the injected amounts of $NO_2$. The initial differences are maintained up to the times of $NO_2$ maxima, which are slightly different -- with the chamber having the highest initial $NO_2$ concentration reaching its maximum first, as one would expect. This chamber (Number 3) exhibits an $NO_2$ decay a little greater than that observed for the other two chambers. The NO disappearance observed is essentially indistinguishable for the three chambers.

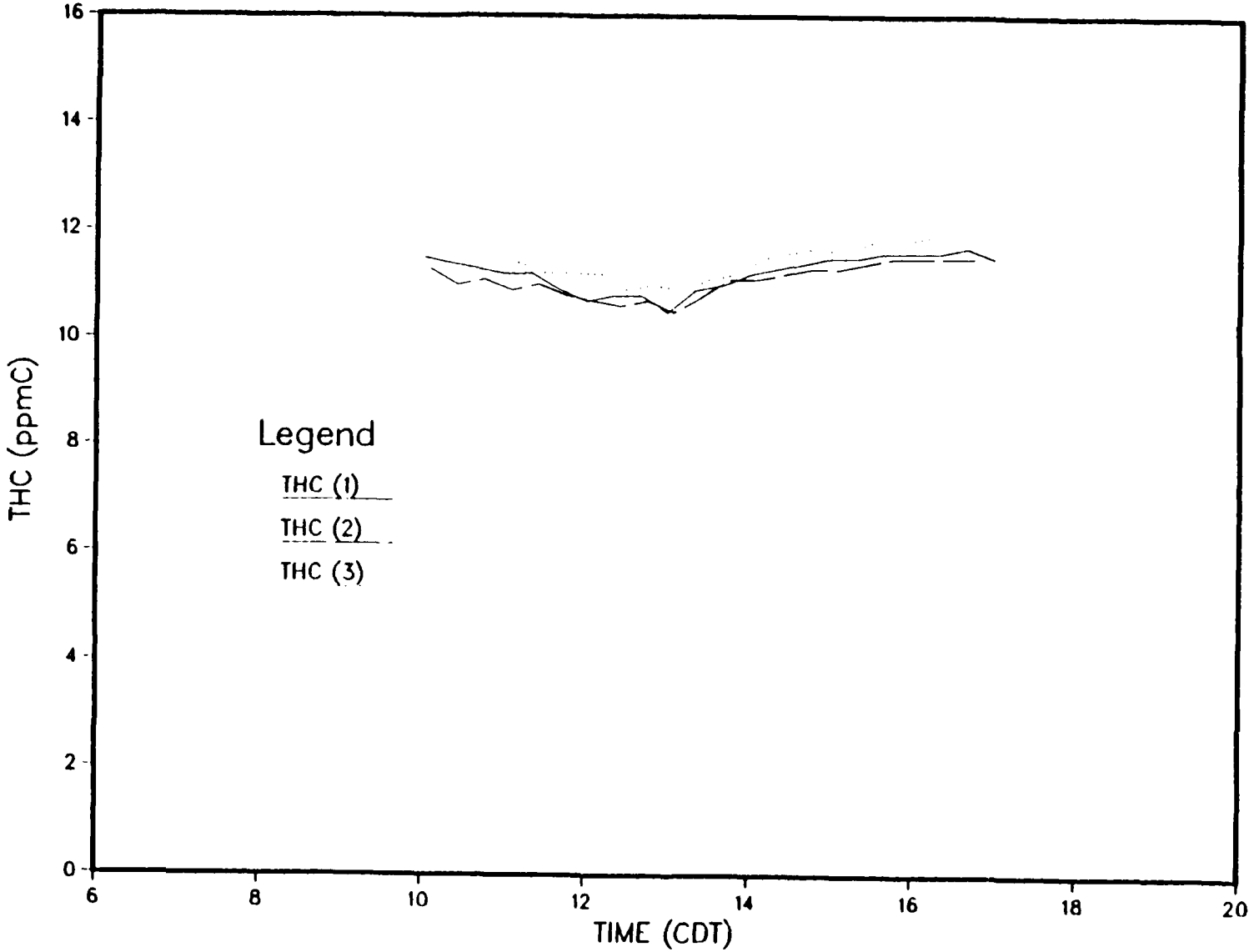


Figure 2. THC Profile for Each Chamber for Matched Run Performed 10/5

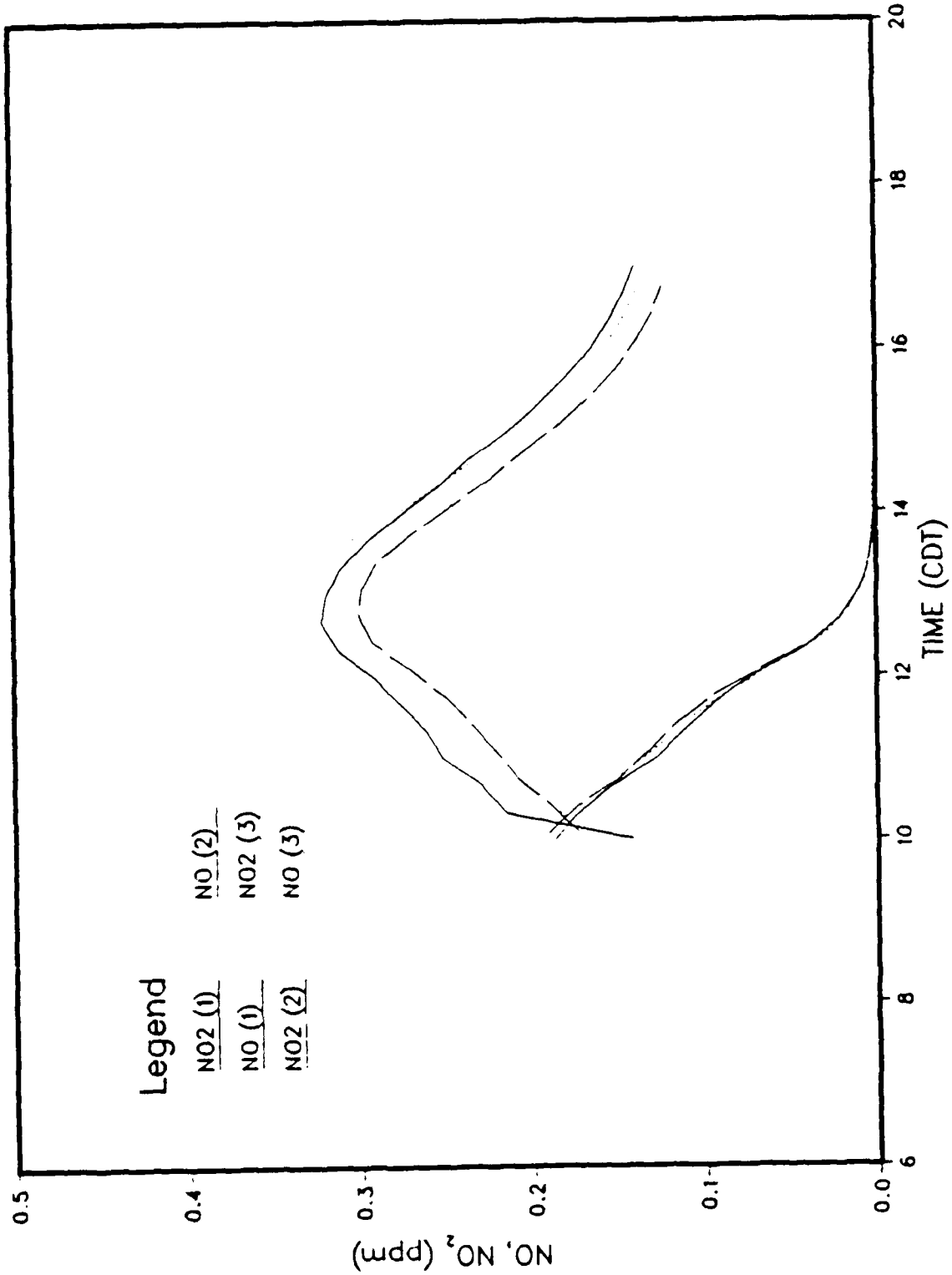


Figure 3. NO, $NO_2$ Profiles for Each Chamber for Matched Run Performed 10/5

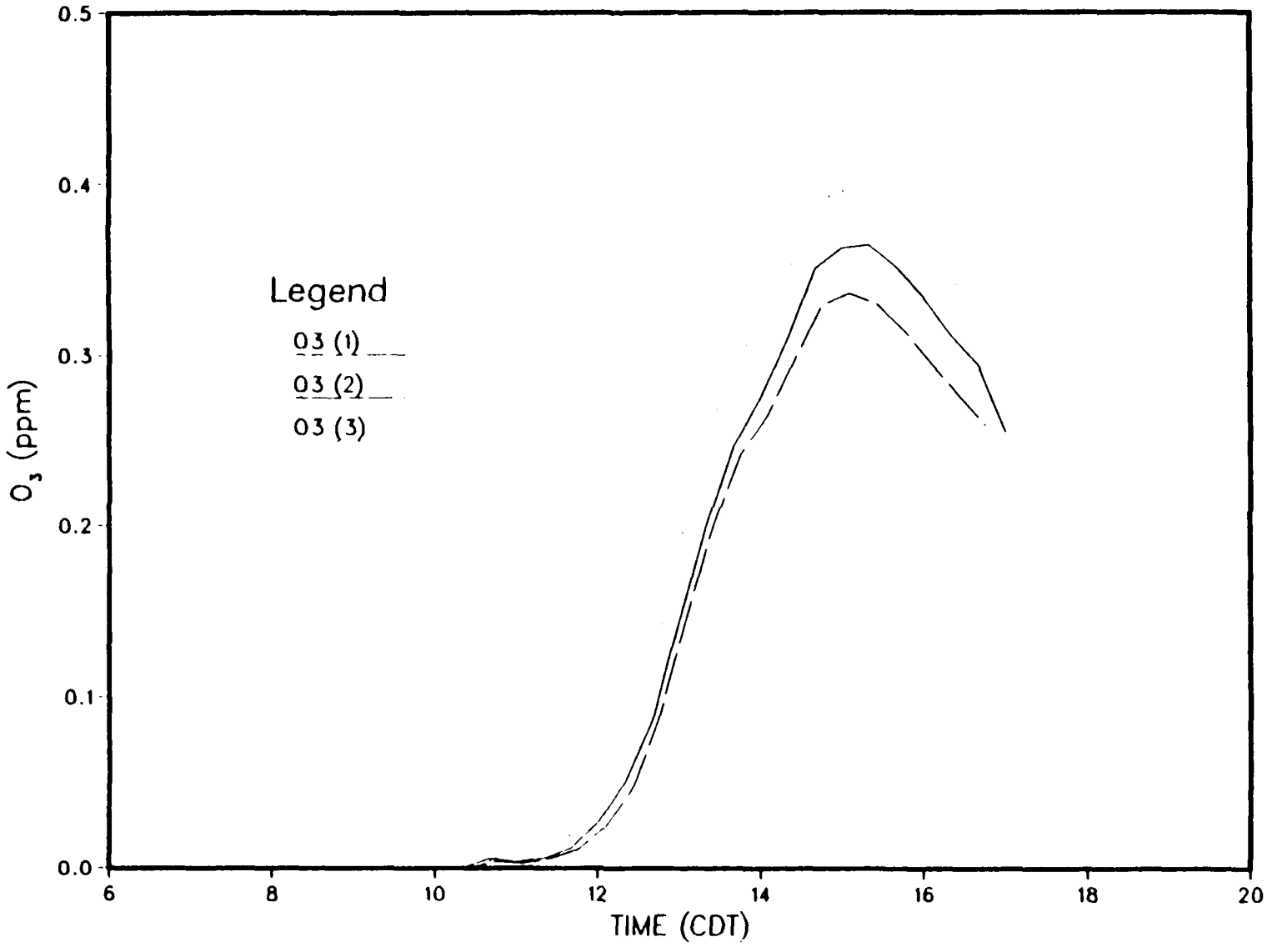


Figure 4. $O_3$ Profile for Each Chamber for Matched Run Performed 10/5

The $O_3$ productions observed for the three chambers track one another as well as one could expect, given the initial differences in the $NO_2$ injections. The chamber having the largest initial $NO_2$ concentration produces the greatest $O_3$ maximum. All three chambers initiate $O_3$ formation and achieve the $O_3$ maximum at nearly the same time. Following the maximum, the $O_3$ decay rate is nearly the same for all three chambers, as the $O_3$ decay runs presented above indicated.

After an overnight purge of the chambers, an additional EKMA/$NO_x$ photochemical run was performed. Again the intention was to have matched injections in all three chambers to examine how well the chambers duplicate one another. Figures 5, 6, and 7 present the measured concentrations for this run. While the $NO_2$ injections are well matched for all three chambers, Chamber 2 received higher NO and EKMA injections than did the other chambers, and this is reflected in the photochemistry observed during the run. Chambers 1 and 3 differ only very little throughout the course of the day. Chamber 2, however, with the excess initial NO, produces a greater maximum $NO_2$ concentration. The $O_3$ maximum produced in Chamber 2 is close to that found in the other two chambers. In the absence of photochemical modeling results, it is not clear whether this $O_3$ behavior would be expected in light of the differences in the chambers' initial conditions.

The results obtained in these "matched" EKMA/$NO_x$ runs demonstrated sufficiently similar performance of the chambers for use in the aging experiments. The final step in the chamber intercomparisons was the performance of background reactivity run to determine whether any significant differences would be expected when the chambers contained relatively nonreactive atmospheres. For this run, the performance of Chambers 2 and 3 were examined following overnight purging. An EKMA/$NO_x$ run was performed in Chamber 1, and Chamber 3 was covered during this run. The measurements obtained for Chambers 2 and 3 are shown in Figures 8, 9, and 10. The fluctuations in the apparent THC concentrations are believed to be caused by variations in instrument response. There appears to be a small amount of NO oxidation in both chambers, leading to formation of a small amount of $NO_2$. Chamber 2, exposed to sunlight does produce $O_3$, peaking at the same time as Chamber 1 with the EKMA/$NO_x$ mixture. Chamber 3, however, being covered, produces almost no $O_3$. The

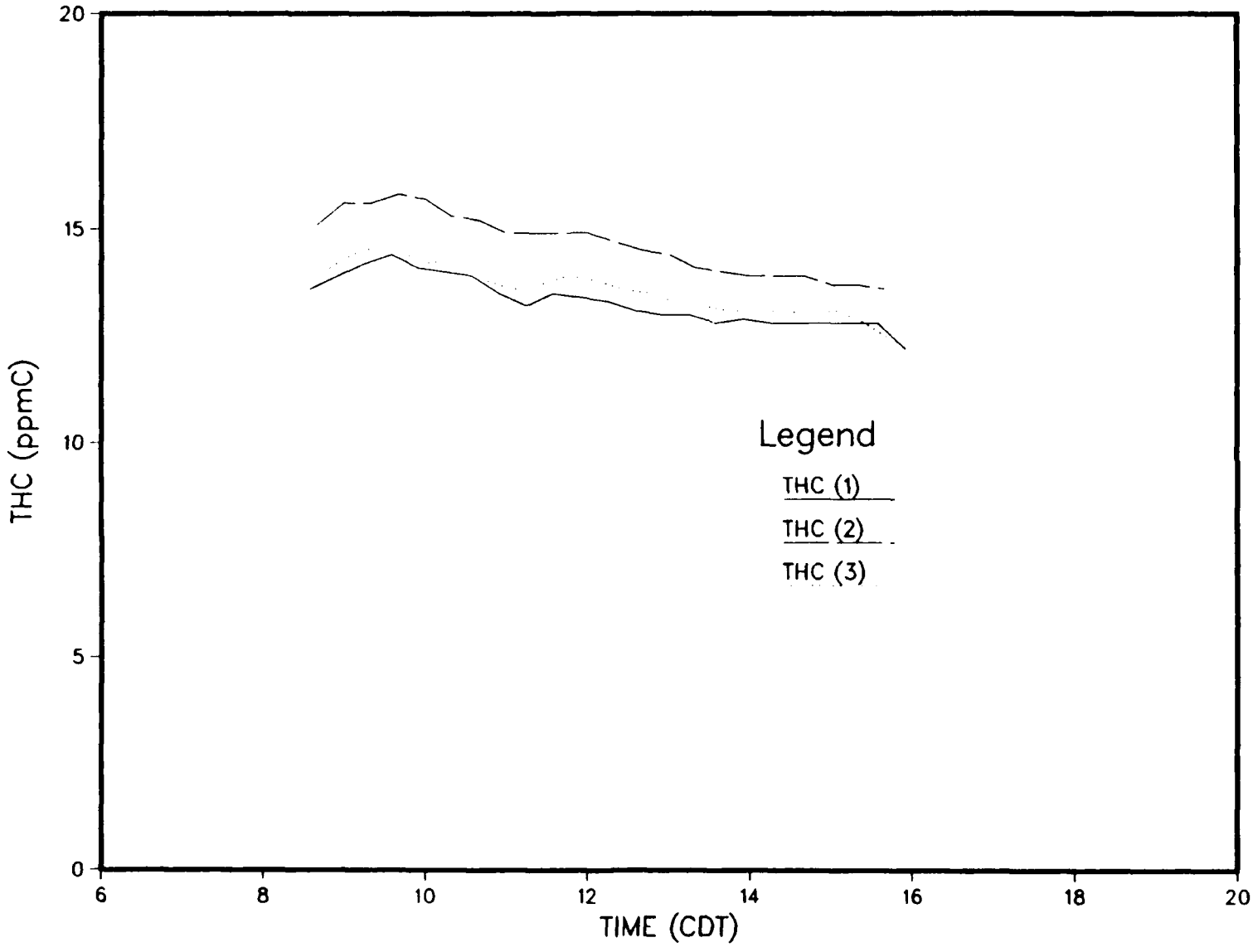


Figure 5. THC Concentration Profiles for Chambers 1, 2, and 3 During 10/6 Matched Run

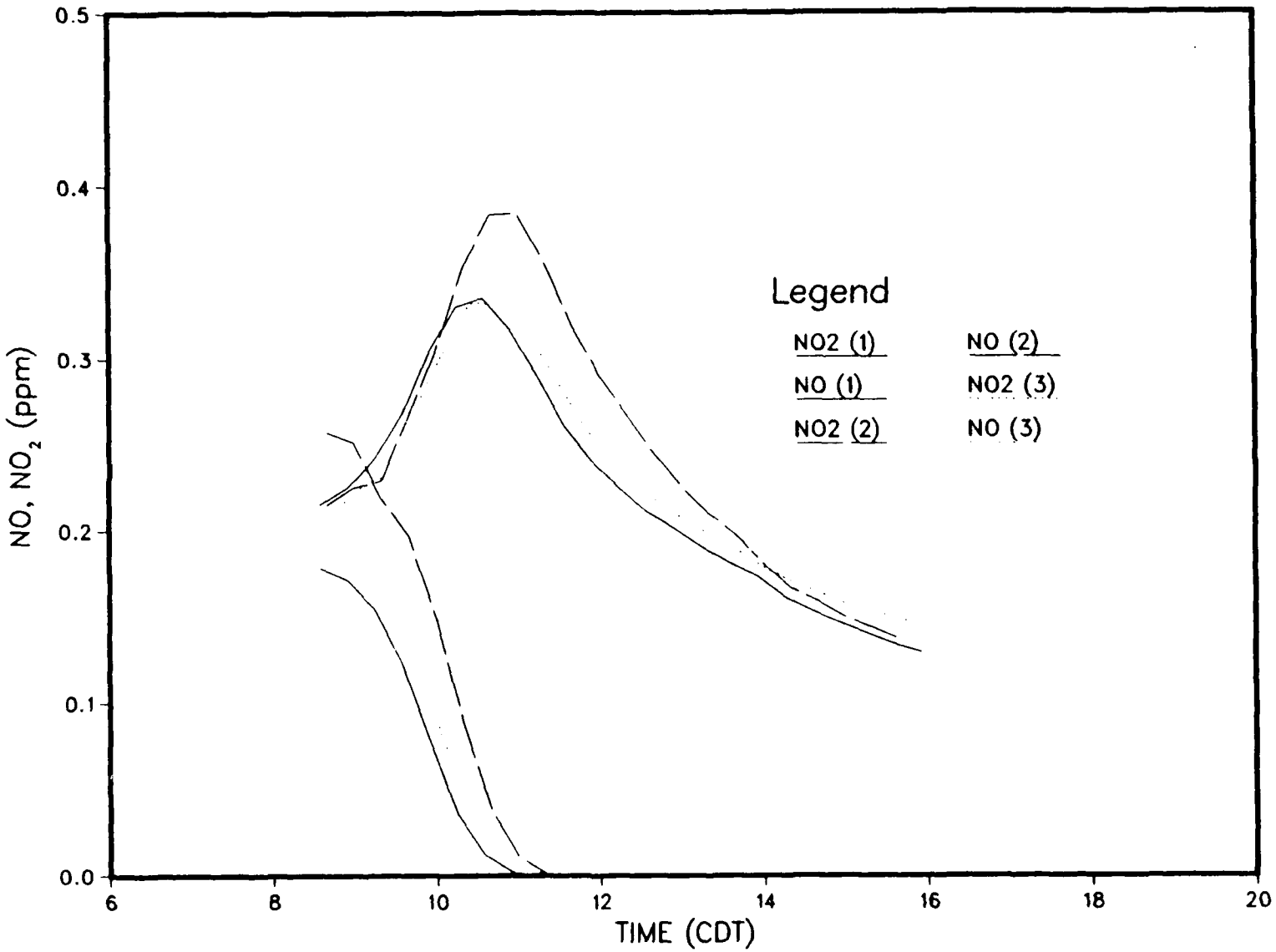


Figure 6. NO and $NO_2$ Concentration Profiles for Chambers 1, 2, and 3 During 10/6 Matched Run

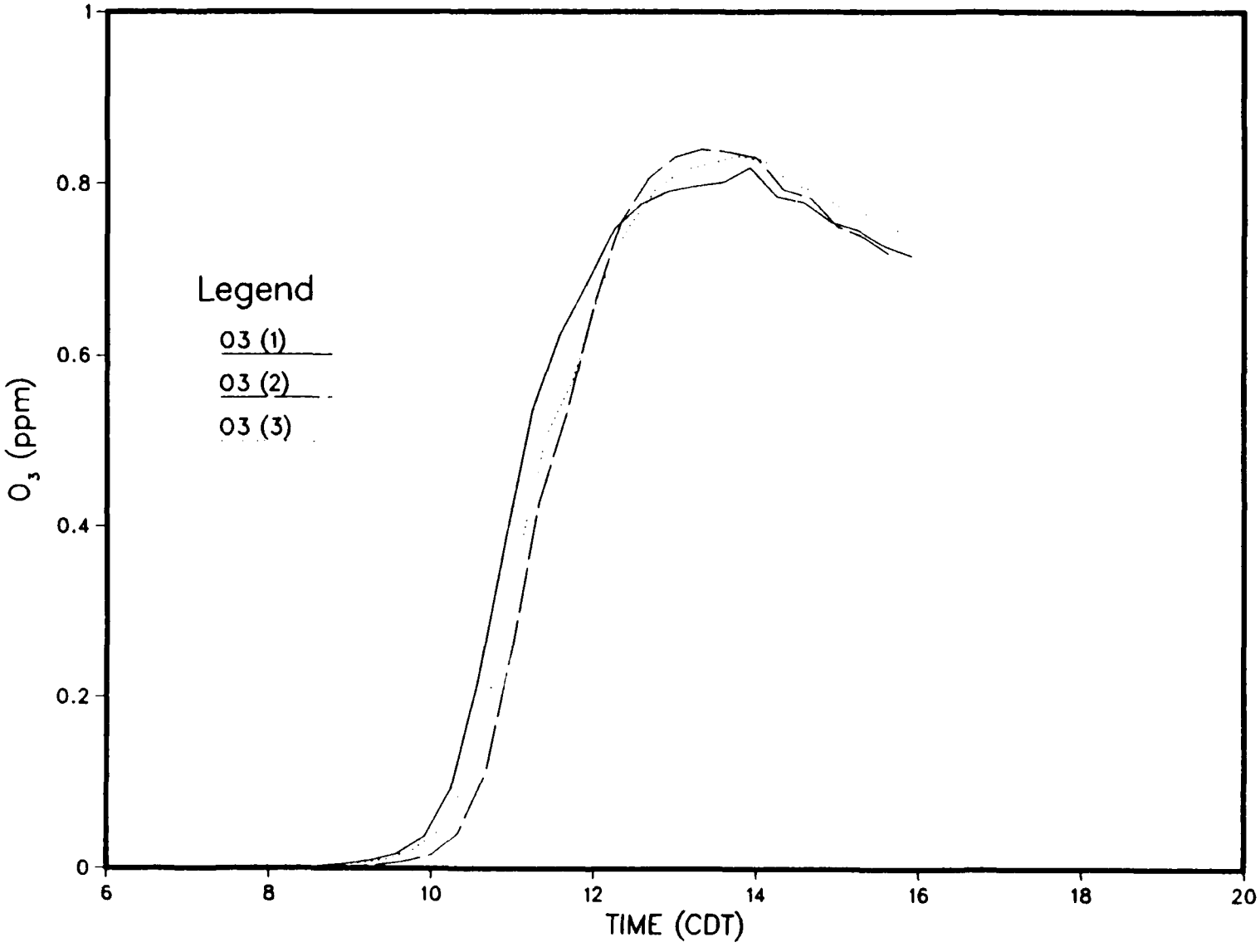


Figure 7. $O_3$ Concentration Profiles for Chambers 1, 2, and 3 During 10/6 Matched Run

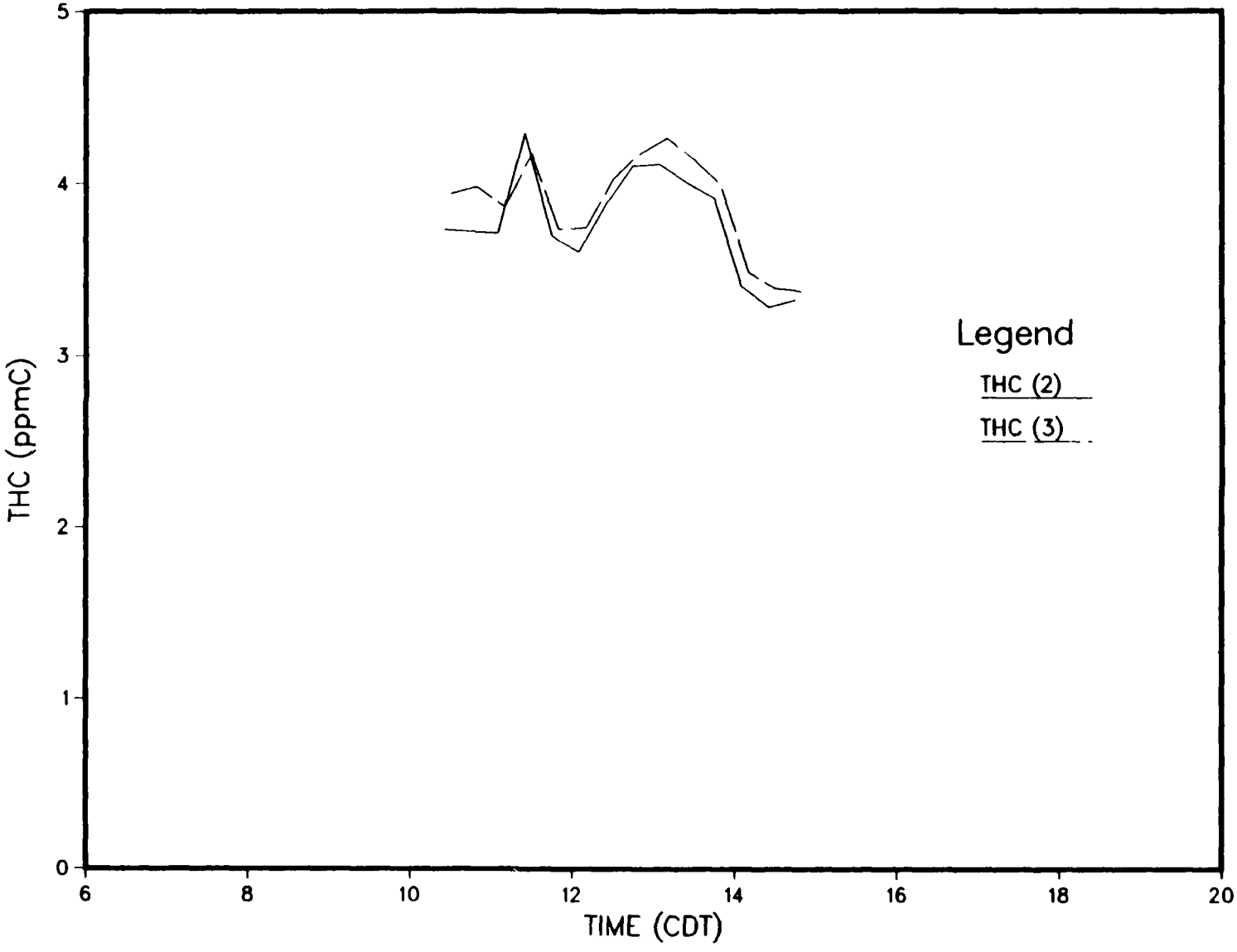


Figure 8. THC Concentration Profiles for Chambers 2 and 3 During Background Reactivity Run

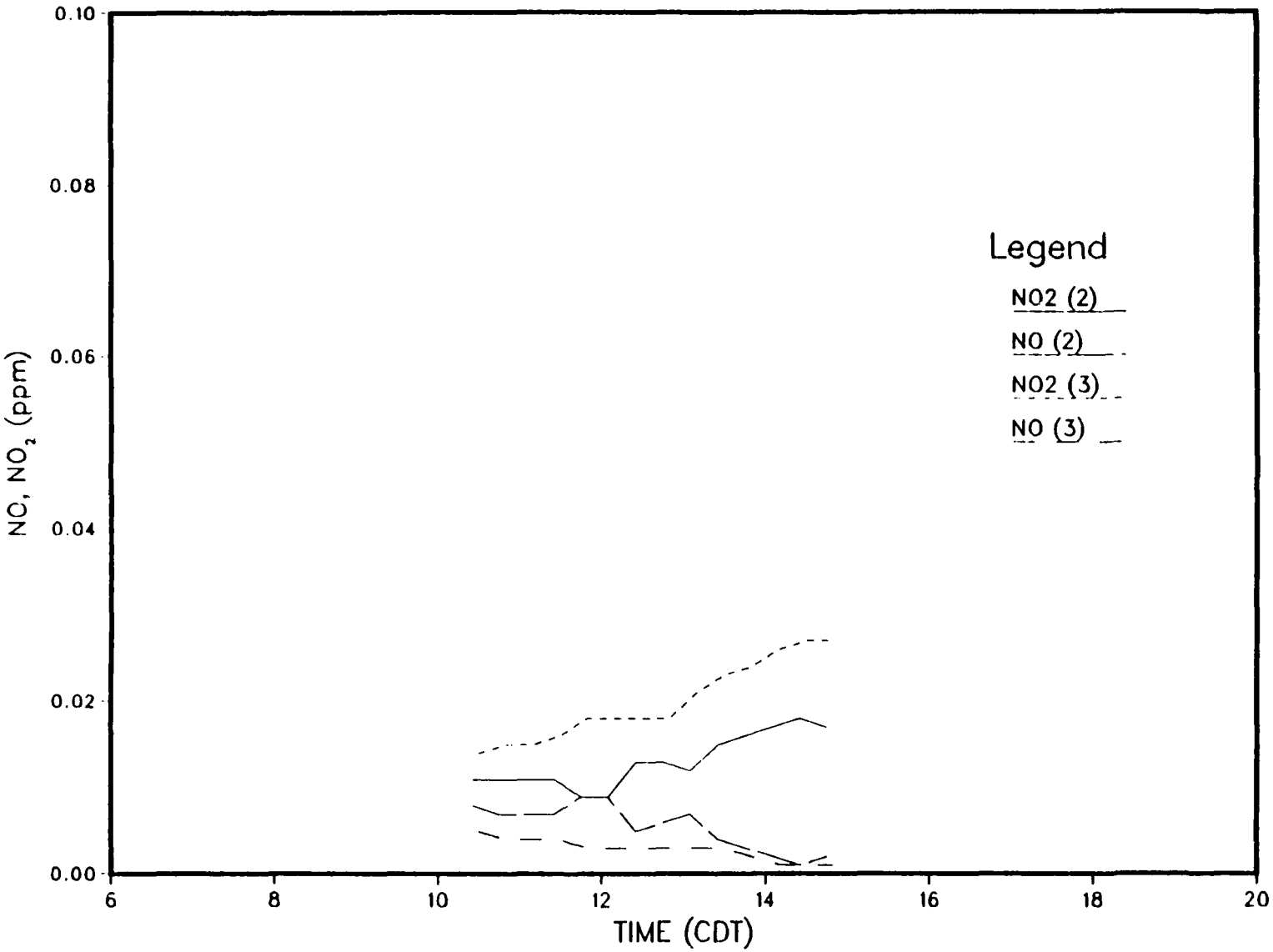


Figure 9. NO and $NO_2$ Concentration Profiles for Chambers 2 and 3 During Background Reactivity Run

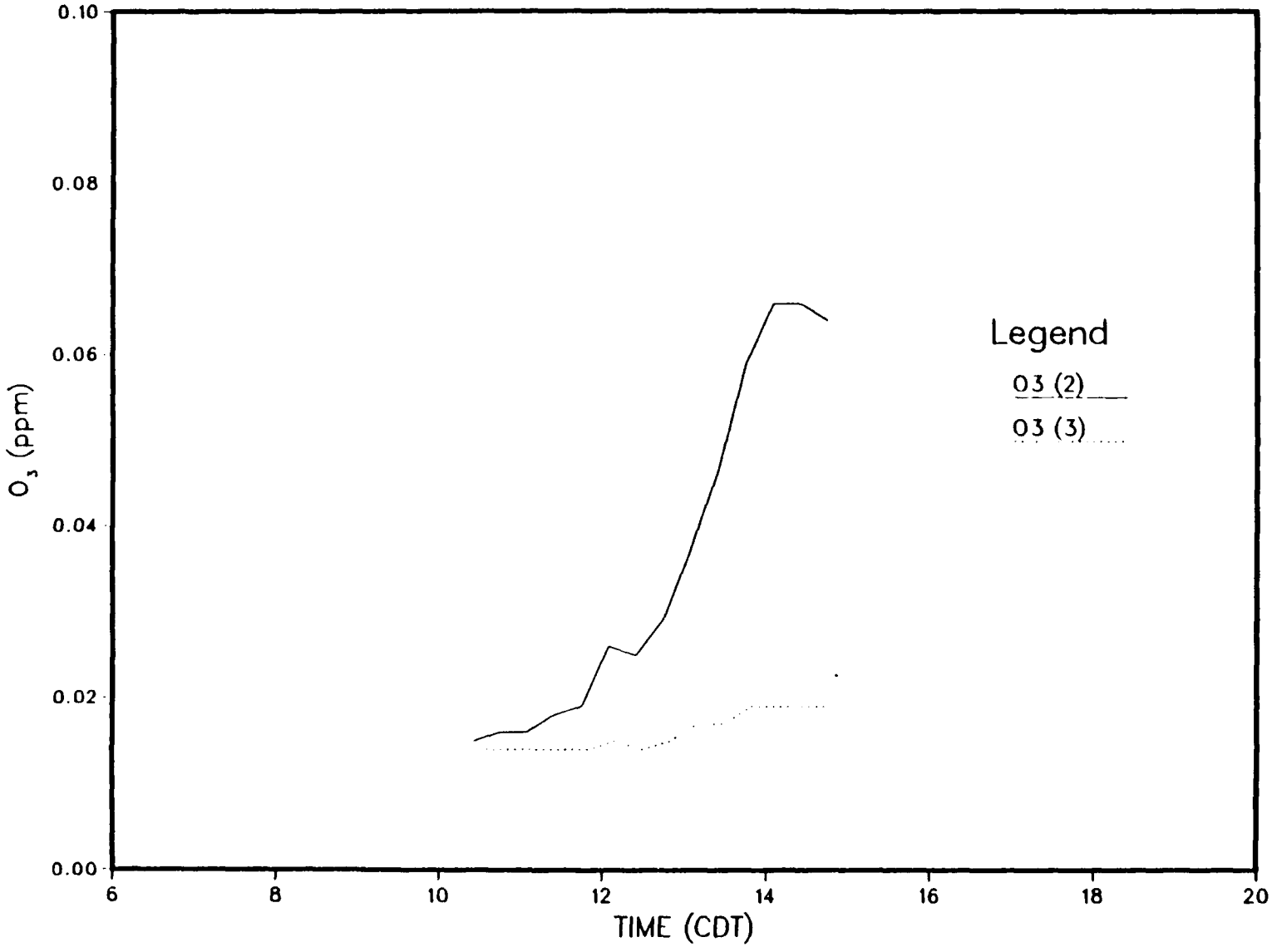


Figure 10. $O_3$ Concentration Profiles for Chambers 2 and 3 During Background Reactivity Run

results of this test and the other tests performed prior to engine testing indicate that the background air into which the engine exhaust would be injected is not completely unreactive when exposed to sunlight. The extent of reactivity exhibited in the chambers, however, did not appear to be great enough to have a significant impact on the results to be obtained. (This will be apparent when one examines the initial concentrations of $NO_x$ and THC found in the chambers during the photochemical aging experiments.)

## D. SAMPLE ANALYSES

The following subsections describe the sampling media used, their preparation and handling, quality control measures, the analytical methods used, and the data reduction techniques.

### 1. Sampling Media

Two types of filter media were used to collect particulate samples for subsequent analyses. For analysis of the inorganic material found in the particulate emissions, 47 mm Millipore$^R$ Type AA filters were used. These have been found to produce satisfactory results as they contain very low levels of inorganic contaminants. Quartz fiber filters (manufactured by Pallflex Corporation) were used to collect samples of the aerosol for subsequent organic analyses. These filters contain a relatively low amount of organic binder which is further reduced by heating the filters to 450°C in a muffle furnace for 16 hours. The XAD-2 sorbent media used to collect the organic vapor phase species is prepared for use by Soxhlet extraction with dichloromethane for 16 hours. After the resin has dried, it is loaded into precleaned Pyrex cartridges, wrapped with aluminum foil to exclude light, and placed in a labeled protective container.

### 2. Quality Control Measures

For quality control of the inorganic analysis of the Millipore filters, a carbon blank was analyzed as a reference and a blank filter from the same lot as the sample filters was analyzed to provide a background value.

The following quality control procedures were implemented for the GC/MS analyses of the quartz fiber filter and XAD-2 samples. For each set of samples generated at the field test site, there were an additional field blank filter

and XAD-2 trap, as well as one laboratory blank. These samples were analyzed concurrently with the field samples to determine whether there are any significant sources of contamination to the samples. In addition, the field blank XAD-2 and the laboratory method blank were spiked with the four perdeuterated PAH recovery standards in order to demonstrate PAH recovery in the absence of the matrix. The field blank XAD-2 was spiked with the $d_{12}$-benzo[e]pyrene and $d_{12}$-benzo[k]fluoranthene as soon as possible after sampling. The spiking solution containing $d_{12}$-chrysene and $d_{12}$-benzo[a]pyrene was spiked onto the XAD-2 resin just before extraction.

In the quantitative GC/MS analysis, the sample extracts or fractions were spiked with the internal standard, 9-phenylanthracene, immediately before GC/MS analysis. This PAH does not occur naturally, and thus does not pose a problem as an interferent. The use of an internal standard from the same compound class as the compounds to be quantified and having an average molecular weight and elution time of those compounds to be quantified enhances the analytical precision of the quantification. This is because an average correction factor for injection technique, chromatographic active site effects, and slight variations in the daily mass spectrometer tuning is applied to the quantification of all compounds.

The ordering of samples and standards for GC/MS analyses ensures that standard analyses bracket all of the sample analyses. In general, one set of standards over the calibration range is analyzed first to ensure linearity and range.

A three-point standard curve was generated for each of the target compounds. These standards were analyzed in triplicate along with a blank sample which tests the baseline. For each standard 2 μL were injected and the response was compared to that of the internal standard. The computer determined a calibration factor for each of the target compounds which minimized the differences in ionization efficiencies between the target compounds and the internal standard. The computer performed a least-squares analysis and provided a correlation coefficient and intercept. The correlation coefficient must be at least 0.990 for an acceptable calibration curve. After the calibration curve is established, the order of analyses was: standard, sample, sample, sample, standard until all analyses in a set were completed. In this way, the

calibration curve generated from the standard analyses accurately reflects the condition and operation of the mass spectrometer throughout a set of samples.

The validity of the calibration curve was monitored by analyzing successive calibration solutions using the curves, and comparing the value obtained with the known value. Quantification within 20 percent of the true value is considered acceptable and requires no reanalysis of the sample.

Mass spectral intensities for the calibration compound FC-43 were also recorded daily and these intensities were used to verify that the ion balance tuning of the mass spectrometer had not varied significantly during the analyses of the sample extracts.

Both the quartz fiber filters and the XAD-2 sorbent traps were enclosed in labeled airtight containers and stored at 0°C within 15 minutes of sample collection. The samples were then shipped to the laboratory at that temperature within 48 hours for storage prior to extraction. During storage and shipment the XAD-2 traps were enclosed in aluminum foil to exclude light.

3. Organic Extraction and Fractionation

The filter and XAD-2 samples were extracted with methylene chloride (distilled-in-glass) by Soxhlet extraction for at least 16 hours, or until the solvents in the top extraction chamber were clear. In previous studies (References 1 and 2) we have demonstrated that by using this extraction technique, the extraction efficiencies for most PAH, mono-nitro PAH, and dinitro PAH from diesel exhaust particulate matter are usually greater than 80 percent. A preliminary study was conducted to estimate the extraction efficiency of PAH and PAH derivatives in the exhaust particles using this procedure. A known amount of $D_8$-naphthalene, $D_{10}$-phenanthrene, $D_{10}$ -pyrene, $D_{12}$-chrysene, $D_{12}$-benzo[a]anthracene, $D_{12}$-benzo[a]pyrene and $D_{12}$-benzo[k]fluoranthene was spiked onto the filter and XAD-2 samples and carried through the extraction procedure. The recoveries of the spiked compounds were found to be greater than 80 percent in all cases.

A fractionation method has been developed by Battelle to separate complex organic extracts of diesel particulate matter, ambient air particulate matter and wood stove exhaust samples into different compound classes (References 1, 3, 4). The open column chromatographic techniques used in this

fractionation scheme are not sample size limited. Larger or smaller quantities of elution solvent are expected to produce the same compound class separation for a large range of sample amount. The method has previously been applied to extracts containing as little as 1 mg of mass up to extracts containing as much as 1 gram.

In the fractionation method, a silica gel column is slurry packed with 5 percent $H_2O$-deactivated silica gel (70-150 mesh, Woehlm-Pharma silica). Aliquots of known amounts of sample are solvent exchanged into hexane and placed onto the top of the silica gel column. Some of the polar compounds are insoluble in hexane. When the column elution solvent is changed, 1 mL of the new solvent is first added to the sample container to dissolve soluble residues. The aliquot is then placed onto the silica gel column before elution with the remainder of the solvent. This procedure is repeated for all the elution solvents. No material is left in the sample container after the last elution solvent. Four elution solvents with increasing polarity are applied to the column in the following sequence: hexane, hexane/benzene (1:1), methylene chloride, and methanol. Each fraction generated from the silica gel column is concentrated by K-D evaporation. An aliquot of 10-100 µL is used for a residue weight measurement, where this is practicable.

Aliphatic hydrocarbons elute in the hexane fraction. PAH and mononitro PAH are present in the hexane/benzene fraction. Polynitrated PAH, oxygenated 2- and 3-ring PAH, and other moderately polar compounds are found in the methylene chloride fraction. The methanol fraction contains PAH with more than one functional group and other highly polar compounds.

If the quantities of organics in the fractionated extracts are from 1 mg to 100 mg, the quantities of silica gel and eluting solvents used are adjusted accordingly, as listed in Table 3.

TABLE 3. QUANTITIES OF SILICA GEL AND REAGENTS USED IN THE FRACTIONATION PROCEDURES

| TOTAL MASS OF ORGANIC EXTRACT, mg | QUANTITY OF SILICA GEL USED, g | VOLUME OF ELUTING SOLVENT, mL | | | |
|---|---|---|---|---|---|
| | | $C_6H_{12}$ | $C_6H_{12}/C_6H_6$ | $CH_2Cl$ | MeOH |
| 1-5 | 1 | 2.5 | 4 | 4 | 4 |
| 50 | 10 | 50 | 150 | 150 | 150 |
| 100 | 20 | 80 | 250 | 250 | 250 |

4. GC/MS Analytical Method

In general, the selection of target compounds to be studied on the jet exhaust particles is mainly based on:(1) the mutagenicity and/or the carcinogenicity of the compounds, (2) identification of compounds from the exhaust particles from related studies, and (3) the availability of analytical standards. The selected target compounds are summarized in Table 4.

A standard Finnigan Model 4500 GC/MS equipped with a Carlo Erba on-column injector was used for the GC/MS analyses. An ultra Number 2 cross-linked 5 percent phenyl methyl silicone fused silica capillary column was used as both the GC column and the transfer line between the GC oven and the MS ionization source. Data collection and processing was performed by a Finnigan INCOS Model 2300 data system. Typical GC/MS operating conditions used in the analyses are given in Table 5.

Before analysis of standards or samples, the system is calibrated by introducing a standard substance, perfluorotributylamine (FC-43) and determining the mass assignment for principal fragment ions. The mass calibration table is stored and serves to calibrate the ion masses over the scanning range.

The filter and XAD-2 extracts from selected initial samples were analyzed by on-column injection, full scan EI GC/MS. The identification of sample components was conducted by comparison to reference spectra in the EPA/NIH mass spectral library which contains over 30,000 reference mass spectra. Based on these results, the target compounds for the future test samples were

TABLE 4. TARGET COMPOUNDS FOR GC/MS ANALYSES

| COMPOUND | EVIDENCE OF CARCINOGENICITY | REMARKS |
|---|---|---|
| Naphthalene | | |
| Acenaphthalene | | |
| Dibenzothiophene | | |
| Phenanthrene | No | Not active; marker for volatile PAH |
| Anthracene | No | Ditto |
| Fluoranthene | No | Not active; marker for total PAH; nitro-derivatives are mutagens |
| Pyrene | No | Nitro-derivatives are strong mutagens |
| Benz[a]anthracene | Yes | Also is precursor for DMBA, a potent carcinogen |
| Chrysene | Limited | Weak mutagen; some methyl derivatives are very active |
| Cyclopenta[c,d]pyrene | Limited | Active mutagen |
| Benzofluoranthenes | Yes | Active mutagens and carcinogens |
| Benzo[e]pyrene | Inadequate | Limited activity |
| Benzo[a]pyrene | Yes | Active mutagen and carcinogen |
| Indeno[1,2,3,-c,d] pyrene | Yes | Has been identified in mobile sources |
| Benzo[g,hi]perylene | Inadequate | Weak carcinogen |
| Dibenzo[a,h]anthracene | Yes | |
| 2-Nitro-1-naphthol | | |
| 4-Hydroxy-3-nitrobiphenyl | | |
| 1-Nitronaphthalene | | |
| Nitronaphthalene isomer | | |
| 9-Nitroanthracene | | |
| 9-Nitrophenanthrene | | |

TABLE 4. TARGET COMPOUNDS FOR GC/MS ANALYSES (CONCLUDED)

| COMPOUND | EVIDENCE OF CARCINOGENICITY | REMARKS |
|---|---|---|
| Nitroanthracene/ phenanthrene | | |
| 3-Nitrofluoranthene | | Mutagen |
| 1-Nitropyrene | | Strong mutagen |
| 6-Nitrochrysene | | |
| Dinitropyrene isomer | | Mutagen |

TABLE 5. GC/MS OPERATING CONDITIONS

| | |
|---|---|
| **GC PARAMETERS** | |
| Column | Ultra No. 2 fused silica, cross-linked 5% phenyl methylsilicone, 50 m x 0.31 mm I.D., 0.52 μm film (Hewlett-Packard) |
| Carrier | $CH_4$, velocity 50 cm/sec at 250°C |
| Sample injection | 1-2 μL, on-column mode or splitless mode |
| Program | 45°C; 1 min; ballistically to 150°C, 3 min; 150°C to 320°C at 6°C/min; hold for 20 min. |
| **MS PARAMETERS** | |
| Interface | 320°C; fused silica column directly introduced into ion source |
| Typical full mass scan range | 45 to 450 amu at 1 sec/scan in EI mode 100 to 450 amu at 1 sec/scan in PCI and NCI modes |
| Multiple-ion detection | Selected target molecular ion monitored |
| Filament Emission Current | 0.3 ma |
| Signal Amplifications | $10^{-7}$ amp/volt with $10^5$ electron multiplier gain |
| Electron Energy | 70 eV |
| PCI Reagent Gas | $CH_4$ at 1.0 torr; 150 eV |
| NCI Reagent Gas | $CH_4$ at 1.0 torr; 200 eV |
| Ionizer Temperature | 180°C |

chosen. A quantitative multiple-ion detection (MID) GC/MS analysis was then used for the remaining samples. Typically, the sensitivity for the analysis of PAH increases approximately 100 times in the MID mode as compared to the full scan mode. A three-point standard curve is generated for each of the target compounds. The standards are analyzed in triplicate, along with a blank sample to determine the baseline. The internal standard, 9-phenylanthracene, was added to the standards and the samples at a fixed concentration level. The response factor for each compound is generated from the calibration curve. The identification of the target compounds in the extracts is based on the correct molecular ion and the correct retention time relative to the internal standard as determined from the standard analyses. The quantification of each target compound is based on the following equation:

$$C_S = \frac{A_S\ C_{is}}{A_{is}\ R_f}$$

where:

$C_S$ = Concentration of a target compound, ng/μL
$A_S$ = Molecular ion area of a target compound
$C_{is}$ = Concentration of the internal standard, ng/μL
$A_{is}$ = Molecular ion area of the internal standard
$R_f$ = Response factor of a target compound.

a. Negative Chemical Ionization, Gas Chromatography/Mass Spectrometry (NCI GC/MS).

The NCI on-column injection GC/MS method provides significant benefits for the analysis of nitro-aromatic compounds over the conventional, EI GC/MS method. The on-column injection at a lower temperature avoids degradation of the thermally labile nitro-PAH. The chemical ionization technique is more gentle than electron impact and therefore, enhances sensitivity for detection of a molecular ion by decreasing the amount of fragmentation. The NCI GC/MS method is especially sensitive and selective for the detection of nitro-PAH. This is due to the electro-negative nature of the nitro substitution which is highly susceptible to attachment of a thermal electron from the reagent gas

plasma. Therefore, the NCI GC/MS method was used for the selected samples to determine nitro-PAH.

b. Positive Chemical Ionization, Gas Chromatography/Mass Spectrometry (PCI GC/MS).

With the positive chemical ionization (PCI) method, there is also minimal fragmentation associated with the ionization process. When methane is used as the reagent gas, the most abundant ions in the reaction plasma, $CH_5^+$ and $C_2H_5^+$, are approximately 90 percent of the ionic content. The $CH_5^+$ and $C_2H_5^+$ ions act as Bronsted acids and protonate the sample molecule. Therefore, the predominant ions formed are protonated molecular ions $(M+H)^+$. The nitrogen heterocyclic compounds (N-PAH) are good proton acceptors and exhibit high sensitivity. In addition, by adjusting the ionization conditions, it may increase the selectivity for the N-PAH. The PCI, GC/MS method is used for N-PAH in selected samples.

5. Data Calculational Method

In order to determine the concentration of a species in a chamber, the mass collected, $M_s[\mu g]$, was divided by the volume sampled. The volume sampled was dependent upon the operating conditions when the sample was collected such as temperature and pressure which could vary during collection. So, a series of readings was taken during sampling and the average values were used in the calculations. The mass was determined by GC/MS as described above.

The indicated sampling flow rate, $Q_{ind}$ (l/min), is determined from the average vacuum pump rotameter reading and a rotameter versus flow rate calibration curve. This calibration is for a specific temperature and pressure and the indicated flow rate must be corrected for deviations in temperature and pressure to give the actual sampling flow rate, $Q_{act}$ (l/min). The correction is as follows:

$$Q_{act} = Q_{ind}\left[\frac{P_2\ T_1}{T_2\ P_1}\right]^{1/2}$$

where P denotes pressure ("Hg), and T absolute temperature (K). The subscripts 1 and 2 refer to calibration conditions and sampling conditions, respectively.

The volume sampled, $V_s$, was then calculated from the actual sampling flow rate:

$$V_s = Q_{act}\ t_s$$

where $t_s$ = Sampling time (min).

The concentration determined by $C_I = \frac{M_s}{V_s}$ is an intermediate concentration which has to be corrected due to dilution of the chamber contents. The corrections for dilution depends on when the sample was taken in the chamber. There are three cases: initial, intermediate, and final sampling. An explanation of each case follows.

a. Case I. Initial Sampling.

In this case the sample was collected directly from the engine exhaust. The assumption was made that the chamber was being filled with exhaust of the same composition. The concentration of the exhaust comes directly from the mass sampled divided by the volume sampled:

$$C_{ex} = \frac{M_s}{V_s}\ .$$

To determine the initial chamber concentration, correction must be made for the dilution taking place in the chamber during charging. This correction is termed the exhaust injection factor. The exhaust injection factor, $E_f$, is calculated from the initial $SF_6$ concentration, $[SF_6]_o$, and the $SF_6$ concentration after filling the chambers; $[SF_6]_f$:

$$E_f = \frac{[SF_6]_o - [SF_6]_f}{[SF_6]_o}$$

Finally, the initial chamber concentration, $C_o$, is calculated by multiplying $C_{ex}$ by $E_f$:

$$C_o = E_f\ C_{ex}.$$

b. Case II. Intermediate Sampling.

In intermediate sampling, the samples were taken directly from the chamber while the chamber was being diluted with clean air. So, the concentration determined from the mass and the sampled volume must be corrected for the dilution that had occurred up to and through the time the sample was taken. This correction, a dilution factor, $D_f$ was also determined from the $SF_6$ concentration and was given by the formula

$$D_f = \frac{[SF_6]_o}{[SF_6]_s}$$

where $[SF_6]_o$ was the initial $SF_6$ concentration before dilution and $[SF_6]_s$ was the $SF_6$ concentration when the sample had been half collected.

c. Case III. Final Sampling.

For final chamber sampling, dilution caused by sampling was taken into consideration since the sampled volume was a considerable percentage of the chamber volume (~20 percent). The concentration present in the chamber at the beginning of this sampling was calculated from the equation:

$$C_I^* = \frac{M_s}{V_T}\left(1 - e^{\frac{-Q_{act}}{V_T} t_s}\right)^{-1}$$

where

$Q_{act}$ = Sampling rate [$m^3$/min]
$t_s$ = Sampling duration [min]
$V_T$ = Volume of the chamber [$m^3$]
$M_s$ = Mass of species in sample [μg] or [ng].

To correct for the dilution that has occurred up to the time that sampling begins, the $SF_6$ data were used. The $SF_6$ concentration at the beginning of the sampling $[SF_6]_i$ is divided by the original $SF_6$ concentration $[SF_6]_o$ after the chamber has been charged with engine exhaust. Thus, the dilution factor becomes

$$D_f = \frac{[SF_6]_o}{[SF_6]_i}$$

and the corrected concentration was calculated from $C_o = C_I^* D_f$.

# SECTION III

# RESULTS

The experimental results are subdivided into sections concerning the engine exhaust composition, the exhaust aging experiments' photochemistry, and the changes of various PAH and $NO_2$-PAH compounds during the aging experiments.

## A. ENGINE EXHAUST COMPOSITION

The data presented in this section are taken from measurements performed on the samples collected from the engine exhaust sampling line. These data represent the starting material for the aging experiments and also permit comparison between engine types and power settings. Such comparisons appear in the Discussion section of this document.

### 1. Inorganic Constituents of Exhaust

The data obtained from the inorganic analysis of engine exhaust filter samples are presented in Table 6. The volume of exhaust sampled in each case was approximately 0.35 $m^3$, so it is clear that the mass of these elements found is quite small. The two columns of data for the TF33-P7 engine operated at 30 percent power were obtained on separate days, so that factors other than the imprecision of the spark source mass spectrometer may play a role in the observed differences in the measured values. The column of "Blank" values presents the equivalent "concentration" of the elements found in the filter material prior to exposure to engine exhaust.

### 2. Exhaust Gas Composition

The characterization of the exhaust of the engines during this study was the principal objective of the companion task for this work and is reported elsewhere in detail (Reference 5). The data in Table 7 represent a summary of a portion of that work and are presented here for the sake of completeness.

The total extractable organic mass was measured in the exhaust filter and XAD-2 samples. These measurements are expressed as the concentration of extractable mass present in the exhaust gas in Table 8. These data were also

TABLE 6. CONCENTRATIONS ($\mu g/m^3$) OF ELEMENTS FOUND ON ENGINE EXHAUST FILTER SAMPLES USING SSMS FOR THREE ENGINES AT DIFFERENT POWER SETTINGS

| | J-79 | | TF33-3 | | | TF33-7 | | | BLANK[a] |
|---|---|---|---|---|---|---|---|---|---|
| | IDLE | 30% | IDLE | 30% | 75% | IDLE | 30% | 30% | |
| B | .23 | .07 | .01 | .01 | .05 | .01 | .02 | .01 | .01 |
| Na | 9.8 | 6.6 | 4.5 | 6.8 | 45 | 4.1 | 8.1 | 3.3 | .51 |
| Mg | .13 | .05 | .005 | .01 | .06 | .11 | .04 | .004 | .003 |
| Al | 9.8 | 3.3 | .09 | .09 | 1.8 | .83 | .27 | .13 | .15 |
| Si | 98 | 20 | 14 | 3.4 | 1.8 | 16 | 8.1 | 6.6 | .15 |
| P | .66 | .20 | .05 | .16 | .21 | .02 | .04 | .04 | .02 |
| S | 4.9 | 2.0 | .91 | .45 | 1.2 | .41 | .27 | .33 | .15 |
| Cl | 2.3 | .50 | .45 | 3.4 | 2.1 | 1.1 | .54 | .33 | .10 |
| K | 3.3 | .33 | .11 | .11 | 1.5 | .28 | .27 | .22 | .08 |
| Ca | 16 | 66 | 1.1 | .45 | 6.1 | .28 | .13 | .66 | .26 |
| Ti | .07 | 1.0 | .01 | .07 | .01 | .01 | .01 | .01 | .01 |
| V | .002 | .002 | ND | .001 | .002 | .001 | ND | ND | ND |
| Cr | .03 | .002 | .001 | .07 | .002 | ND | ND | .001 | .001 |
| Mn | .33 | .02 | .01 | .01 | .03 | .002 | ND | .01 | .002 |
| Fe | 1.3 | .33 | .09 | .23 | .12 | .17 | .16 | .13 | .02 |
| Ni | .33 | .07 | .002 | .005 | .01 | .01 | .003 | ND | .01 |
| Cu | 33 | 1.0 | .07 | .05 | .61 | .06 | .08 | .04 | .01 |
| Zn | 16 | .33 | .45 | .34 | 1.8 | .17 | .11 | .13 | .10 |
| Br | .005 | .23 | .01 | .003 | .12 | ND | ND | .01 | ND |
| Sr | .01 | .02 | .001 | .001 | .01 | .001 | ND | .001 | ND |
| Zr | 4.9 | .07 | .01 | .01 | .005 | .003 | ND | ND | ND |
| Ag | .02 | .07 | ND | ND | .001 | ND | ND | ND | ND |
| Sn | .49 | .02 | .01 | .01 | ND | .01 | ND | ND | ND |
| Cs | .02 | .001 | ND | ND | ND | .001 | ND | ND | ND |
| Ba | .02 | .66 | .002 | .09 | .01 | .01 | .003 | .01 | ND |
| Pb | .13 | .01 | .01 | .01 | .01 | .01 | ND | .004 | ND |

(a) Blank values converted to equivalent concentration using average sampled volume.

TABLE 7. EXHAUST GAS COMPOSITION SUMMARY

| ENGINE | POWER SETTING | THC, ppmC | NO, ppm | $NO_2$, ppm |
|---|---|---|---|---|
| J79 | Idle | 362 | 4.6 | 4.9 |
| J79 | 30% | 23.4 | 7.5 | 10.5 |
| J79 | 75%(a) | 2.18 | 44.5 | 8.0 |
| J79 | 100%(a) | 0.79 | 76.6 | 7.4 |
| TF33-P3 | Idle | 1260 | 3.5 | 7.5 |
| TF33-P3 | 30% | 77.8 | 10.7 | 13.8 |
| TF33-P3 | 75% | 6.01 | 47.0 | 9.0 |
| TF33-P3 | 100%(a) | 3.18 | 68.0 | 5.5 |
| TF33-P7 | Idle | 1348 | 5.5 | 5.7 |
| TF33-P7 | 30% | 54.3 | 10.0 | 13.0 |
| TF33-P7 | 75%(a) | 2.86 | 57.0 | 5.8 |
| TF33-P7 | 100%(a) | 2.94 | 93.0 | 2.5 |

(a) This power setting of this engine was not examined as part of the exhaust photochemical aging study; the results are presented here to illustrate trends.

TABLE 8. TOTAL EXTRACTABLE ORGANIC MASS IN ENGINE EXHAUST SAMPLES

| ENGINE | POWER | TOTAL EXTRACTABLE ORGANIC, $mg/m^3$ | | | PARTICULATE FRACTION |
|---|---|---|---|---|---|
| | | XAD-2 | FILTER | SUM | |
| J79 | Idle | 113 | 1.4 | 114 | 0.01 |
| J79 | 30% | 3.3 | 1.2 | 4.4 | 0.26 |
| TF33-3 | Idle | 237 | 4.7 | 242 | 0.02 |
| TF33-3 | 30% | 10.8 | 1.5 | 12.3 | 0.12 |
| TF33-3 | 75% | 2.6 | 1.3 | 3.9 | 0.33 |
| TF33-7 | Idle | 335 | 1.9 | 337 | 0.01 |
| TF33-7 | 30% | 8.0 | 0.7 | 8.7 | 0.08 |
| TF33-7 | 30% | 7.5 | 0.8 | 8.3 | 0.10 |

used to calculate the fraction of total extractable organic mass associated with the particulate phase of the collected material.

Because of the small masses collected, only selected samples were fractionated using the silica gel chromatrography method described above. The data obtained for the fractionation of engine exhaust samples are presented in Table 9. Only the idle power setting is reflected in this table because at 30 or 75 percent, the total mass of extractable organic matter is reduced by more than an order of magnitude from the mass found at idle, and the fractionation technique becomes much less reliable due to the very small mass present in the fractions.

TABLE 9. DISTRIBUTION OF ORGANIC MASS IN THE SILICA GEL FRACTIONS FOR IDLE EXHAUST SAMPLES (Fraction of Recovered Mass)

| FRACTION | J79 | TF33-P3 | | TF33-P7 | |
|---|---|---|---|---|---|
| | XAD | XAD | FILTER | XAD | FILTER |
| Hexane | 0.56 | 0.78 | 0.05 | 0.80 | <0.1 |
| Hexane/benzene | 0.14 | 0.02 | 0.30 | 0.02 | 0.33 |
| Methylene chloride | 0.09 | 0.03 | 0.20 | 0.02 | 0.11 |
| Methanol | 0.21 | 0.17 | 0.45 | 0.16 | 0.56 |

3. PAH Found in Exhaust Samples

The concentrations of the target PAH and $NO_2$-PAH compounds found in all the engine exhaust samples collected are presented in Table 10. It is clear that a number of these compounds are present at concentrations near or below the analytical method's detection limit.

B. PHOTOCHEMISTRY EXPERIMENTAL RESULTS

Chamber 2 was used as a control chamber during each day's experiment in which the remaining chambers were changed with engine exhaust. For three of the six runs (Runs 1, 2, and 4) this chamber was run containing only background air which was the starting contents for the other chambers prior to exhaust injection. For the remaining three runs, EKMA mixture and $NO_x$ were injected to provide a more photochemically reactive atmosphere. The measured concentrations of $NO_x$, $O_3$, and THC for this chamber are depicted in Figures 11 through 16. One can see, for Runs 1 and 4, that the $O_3$ level reaches 0.2 ppm in the mid-afternoon. This is probably because of reactive hydrocarbons contained in the background air, which was about 5 ppmC total hydrocarbon. One must keep in mind that these experiments were conducted on an airbase, in fairly close proximity to ground operation of aircraft and fuel handling.

TABLE 10. EXHAUST CONCENTRATIONS OF PAH AND $NO_2$-PAH FOR THE THREE ENGINES TESTED UNDER VARIOUS POWER SETTINGS

| | J79 30% | J79 Idle | TF33-3 Idle | TF33-3 75% | TF33-3 30% | TF33-7 Idle | TF33-7 30% | TF33-7 30% |
|---|---|---|---|---|---|---|---|---|
| | ug/m3 | | | | | | | |
| NAPHTHALENE | 98.4 | 988 | 2560 | 17.7 | 196 | 3350 | 52.0 | 141 |
| ACENAPHTHYLENE | 1.31 | 39.5 | 25.6 | 0.65 | 6.78 | 239 | 3.07 | 5.50 |
| DIBENZOTHIOPHENE | 0.22 | 3.81 | 2.12 | 0.31 | 1.35 | 2.07 | 0.74 | 0.53 |
| PHENANTHRENE | 1.53 | 13.9 | 21.2 | 4.99 | 10.8 | 43.7 | 7.46 | 13.6 |
| ANTHRACENE | 0.07 | 1.22 | 2.44 | 0.29 | 0.45 | 5.43 | 0.57 | 0.26 |
| FLUORANTHENE | 0.35 | 2.67 | 2.62 | 0.81 | 2.46 | 2.46 | 2.55 | 2.44 |
| PYRENE | 0.28 | 2.31 | 3.29 | 0.81 | 3.11 | 2.56 | 3.07 | 2.53 |
| BENZ[A]ANTHRACENE | <0.02 | <0.05 | 0.45 | <0.04 | <0.17 | <0.12 | <0.21 | <0.13 |
| CHRYSENE | <0.03 | 0.12 | 0.55 | <0.04 | <0.26 | <0.16 | 0.31 | 0.18 |
| CYCLOPENTA[C,D]PYRENE | <0.02 | <0.02 | <0.32 | <0.03 | 0.50 | <0.21 | 0.22 | <0.22 |
| BENZOFLUORANTHRENES | <0.02 | <0.06 | <0.65 | <0.04 | <0.27 | <0.69 | <0.20 | <0.18 |
| BENZO[E]PYRENE | <0.02 | <0.04 | <0.28 | <0.04 | <0.13 | <0.31 | <0.09 | <0.08 |
| BENZO[A]PYRENE | 0.00 | 0.01 | 0.24 | 0.00 | 0.09 | 0.31 | <0.10 | 0.06 |
| INDENO[1,2,3,-C,D]PERYLENE | 0.00 | 0.02 | 0.35 | 0.00 | 0.05 | 0.55 | <0.05 | 0.08 |
| BENZO[G,H,I]PERYLENE | 0.00 | 0.04 | 0.49 | 0.00 | 0.11 | 0.84 | 0.05 | 0.09 |
| DIBENZO[A,H]ANTHRACENE | 0.00 | 0.00 | 0.01 | 0.00 | 0.00 | 0.05 | 0.06 | 0.04 |
| | ng/m3 | | | | | | | |
| 2-NITRO-1-NAPHTHOL | 6970 | 20000 | 12800 | 1810 | 16000 | 12800 | 4300 | 6480 |
| 4-HYDROXY-3-NITROBIPHENYL | 479 | 78.0 | 106 | 121 | 168 | 80.8 | 241 | 124 |
| 1-NITRONAPHTHALENE | 108 | 181 | 42.3 | 59.9 | 178 | 42.1 | 95.4 | 100 |
| NITRONAPHTHALENE ISOMER | 124 | 142 | 80.6 | 37.9 | 129 | 46.8 | 80.5 | 73.7 |
| 9-NITROANTHRACENE | 8.77 | 12.2 | 8.91 | 22.0 | 208 | 6.43 | 116 | 214 |
| 9-NITROPHENANTHRENE | 2.08 | 4.54 | 3.66 | 1.20 | 7.31 | 1.94 | 5.95 | 22.2 |
| NITROANTHRACENE/PHENANTHRENE | 1.29 | 4.54 | 2.93 | 1.04 | 4.64 | 3.39 | 2.57 | 4.13 |
| 3-NITROFLUORANTHRENE | 0.00 | 1.01 | 1.89 | 0.00 | 5.77 | 0.76 | 0.59 | 1.63 |
| 1-NITROPYRENE | 1.37 | 5.53 | 0.92 | 0.91 | 1.98 | 1.24 | 8.74 | 7.47 |
| 6-NITROCHRYSENE | 0.42 | 0.57 | 0.00 | 0.00 | 0.00 | 0.31 | 0.97 | 0.59 |
| DI-NITROPYRENE ISOMER | 0.00 | 0.00 | 0.00 | 0.00 | 0.00 | 0.00 | 0.00 | 0.00 |

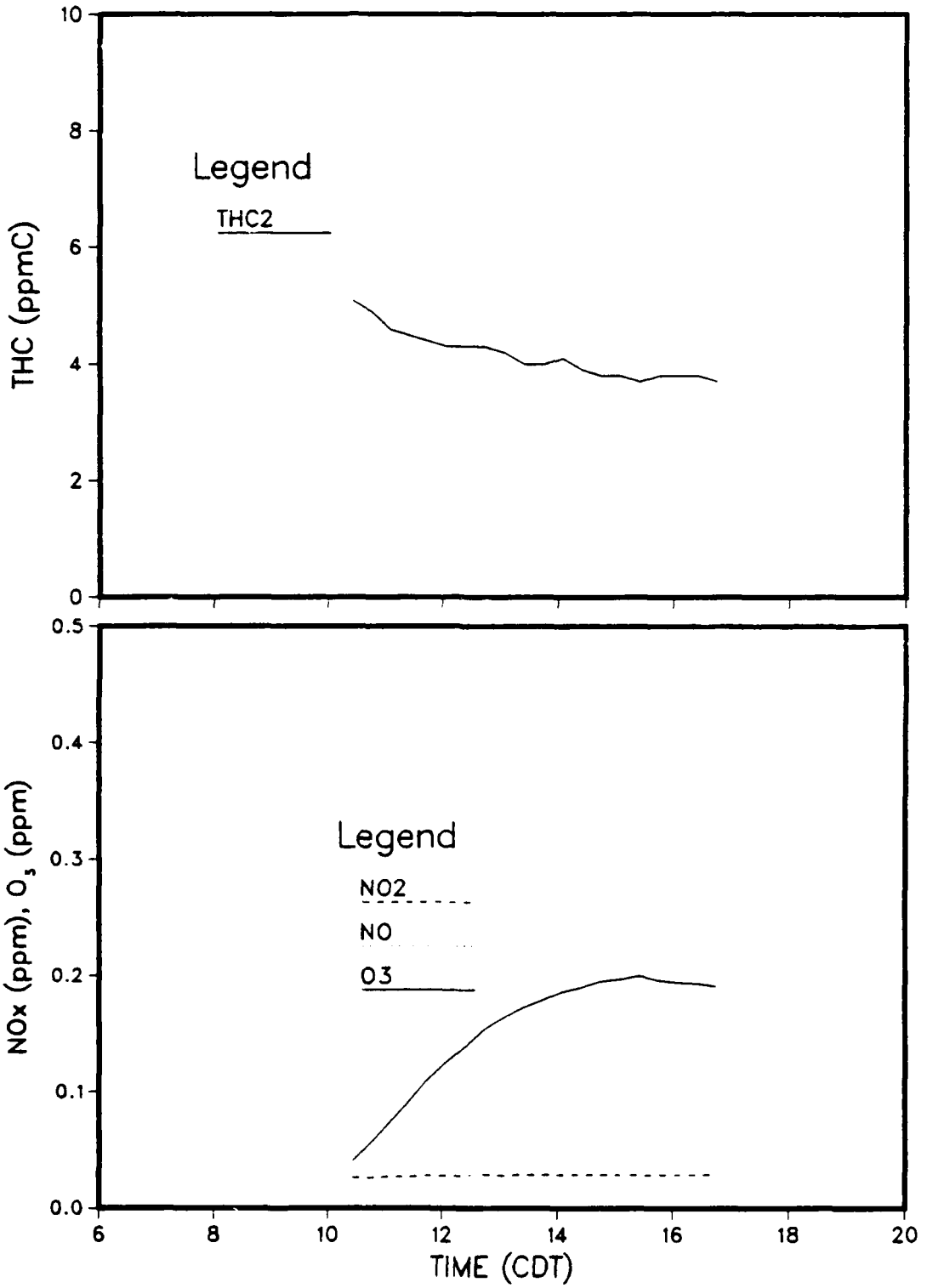


Figure 11. Total Hydrocarbon Concentration Profile and $O_3$ and $NO_x$ Profiles for Control Chamber During Run 1 (Background Atmosphere)

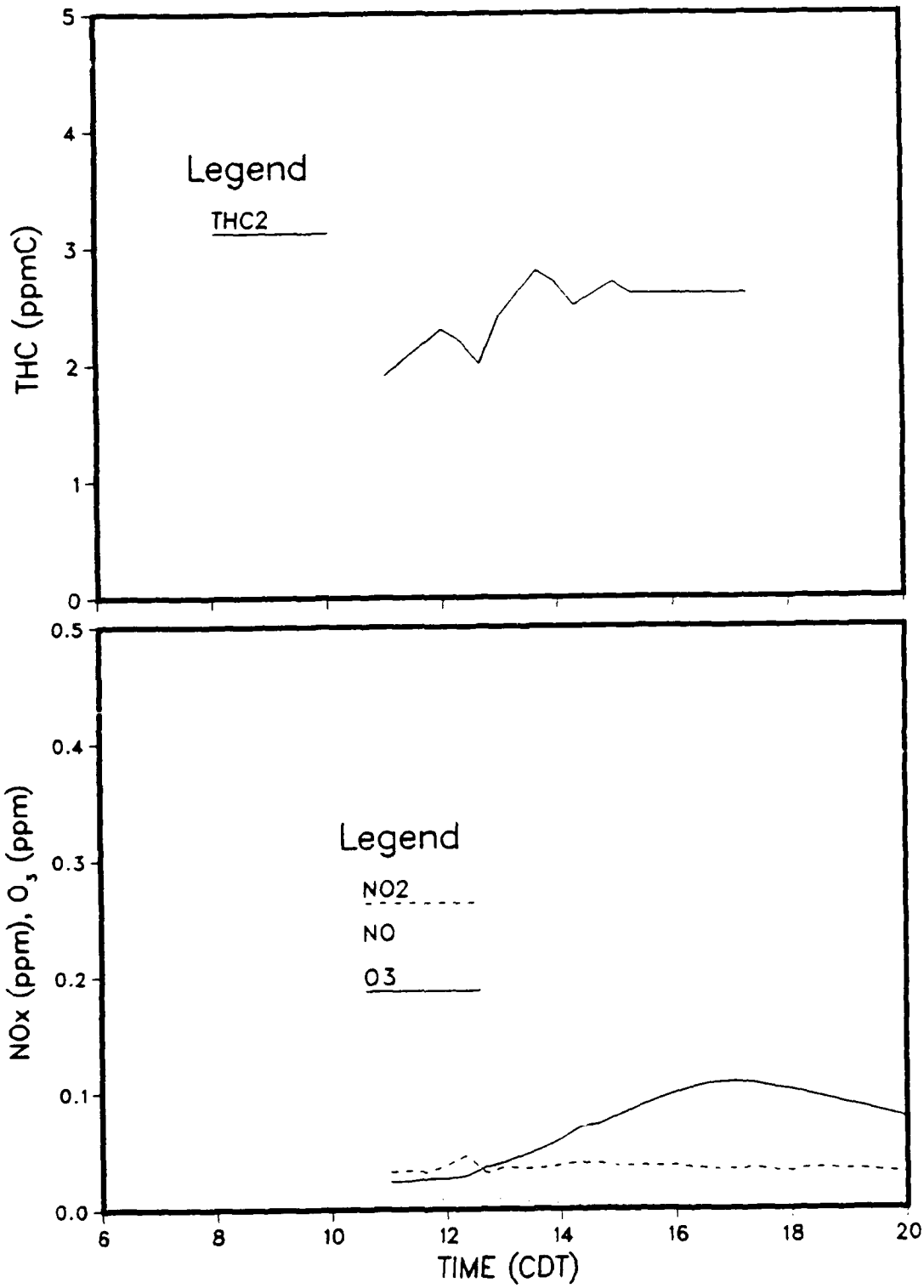


Figure 12. Total Hydrocarbon Concentration Profile and $O_3$ and $NO_x$ Profiles for Control Chambers During Run 2 (Background Atmosphere)

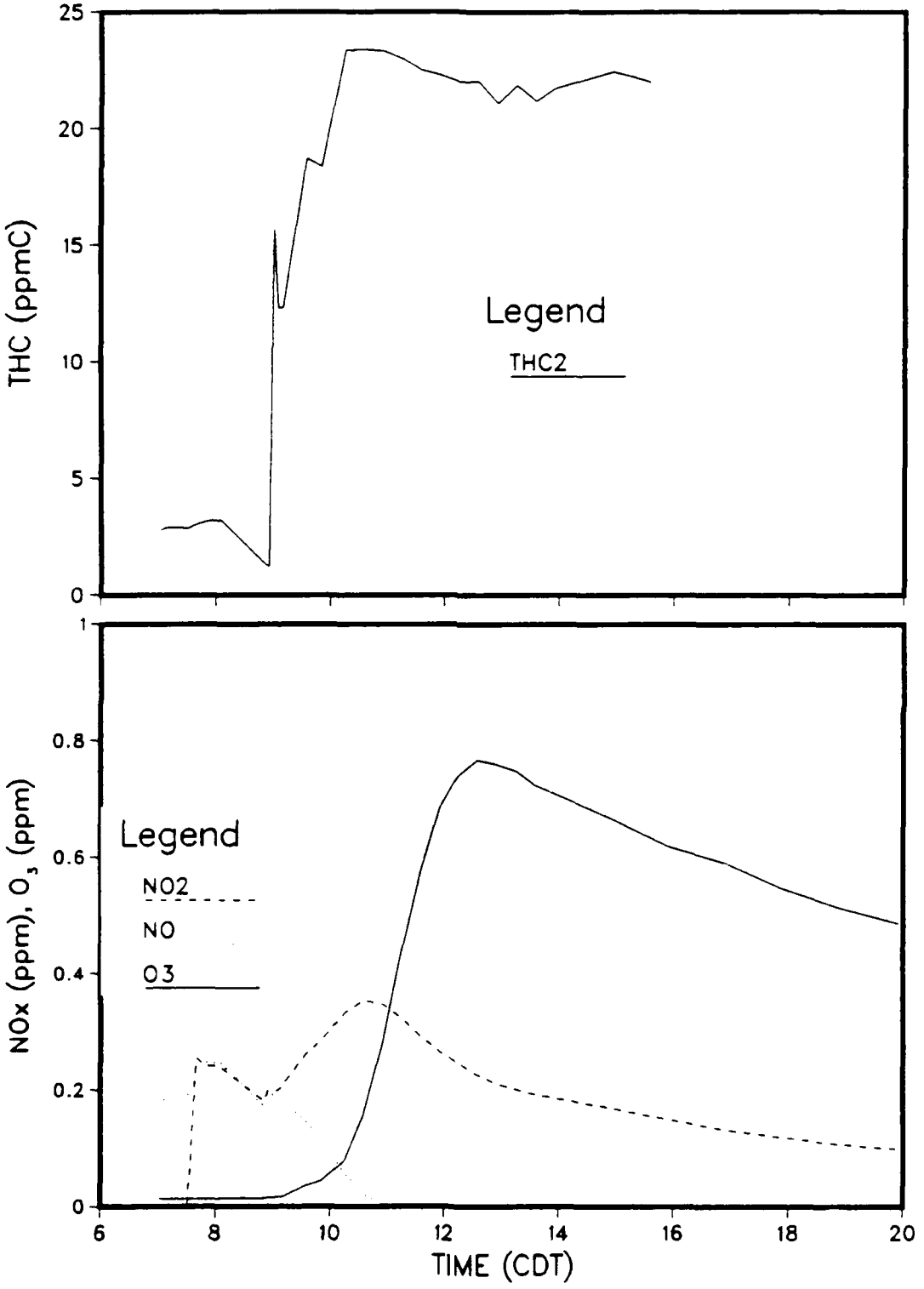


Figure 13. Total Hydrocarbon Concentration Profile and $O_3$ and $NO_x$ Profiles for Control Chamber During Run 3 (EKMA/$NO_x$)

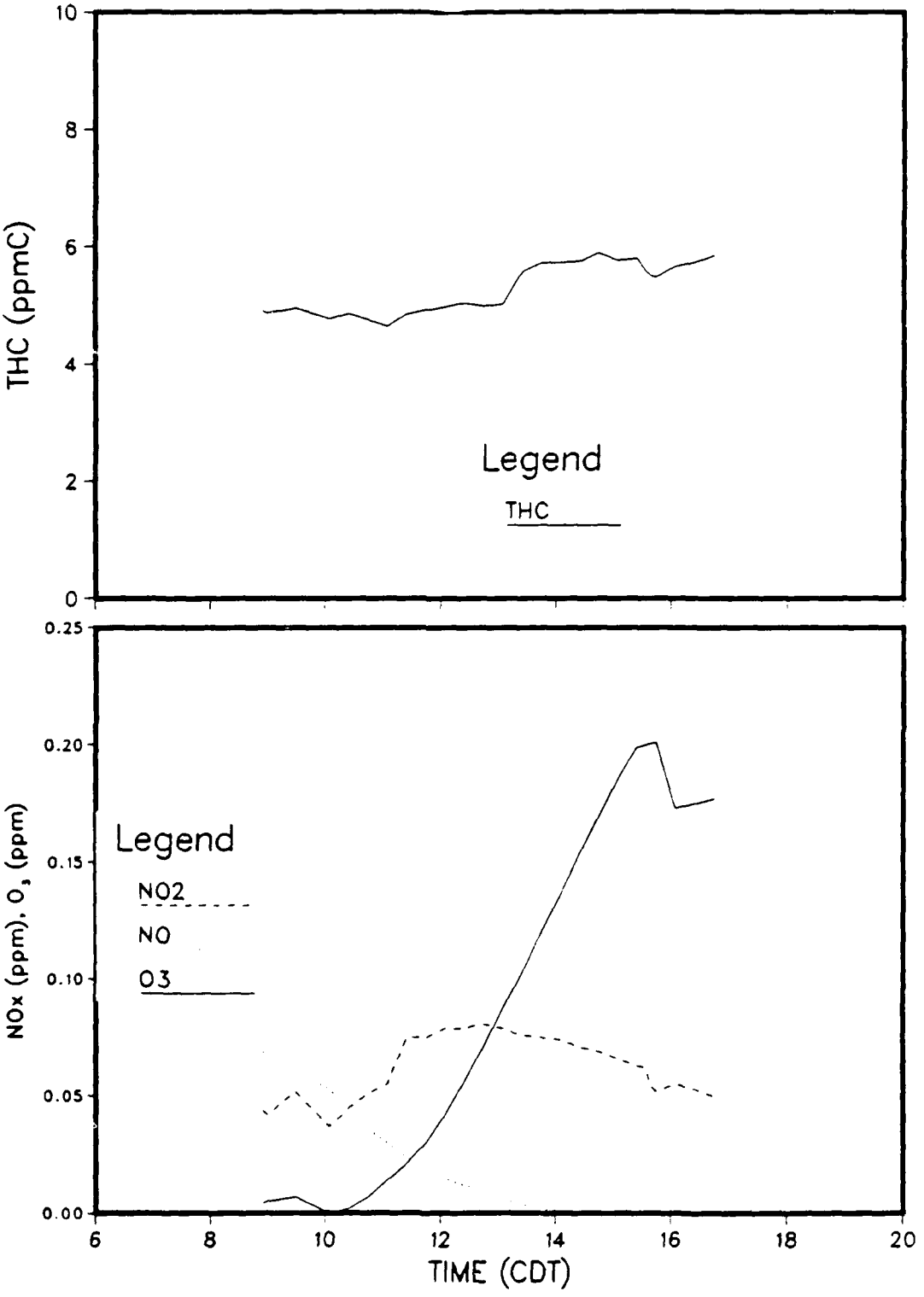


Figure 14. Total Hydrocarbon Concentration Profile and $O_3$ and $NO_x$ Profiles for Control Chamber During Run 4 (Background Atmosphere)

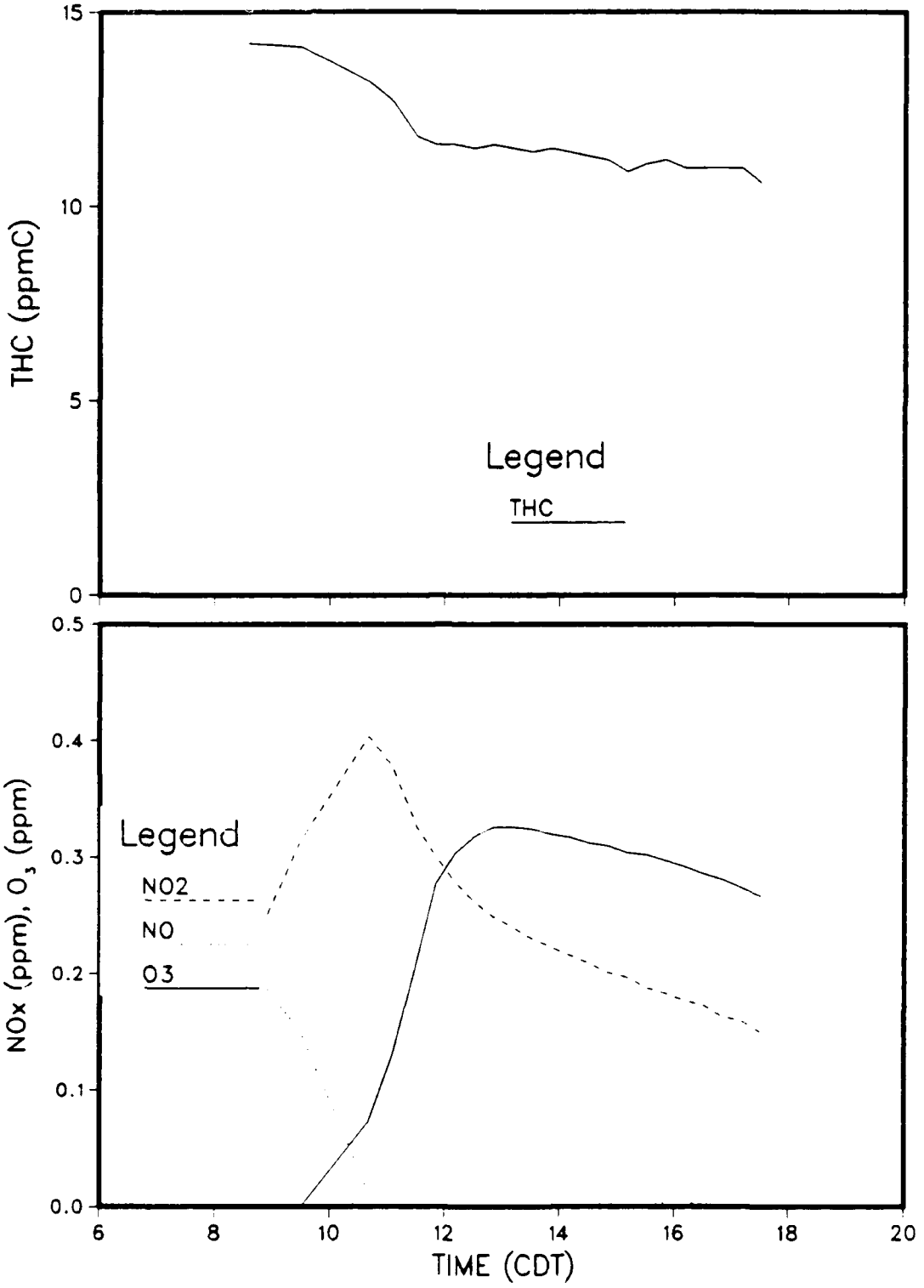


Figure 15. Total Hydrocarbon Concentration Profile and $O_3$ and $NO_x$ Profiles for Control Chamber During Run 5 (EKMA/$NO_x$)

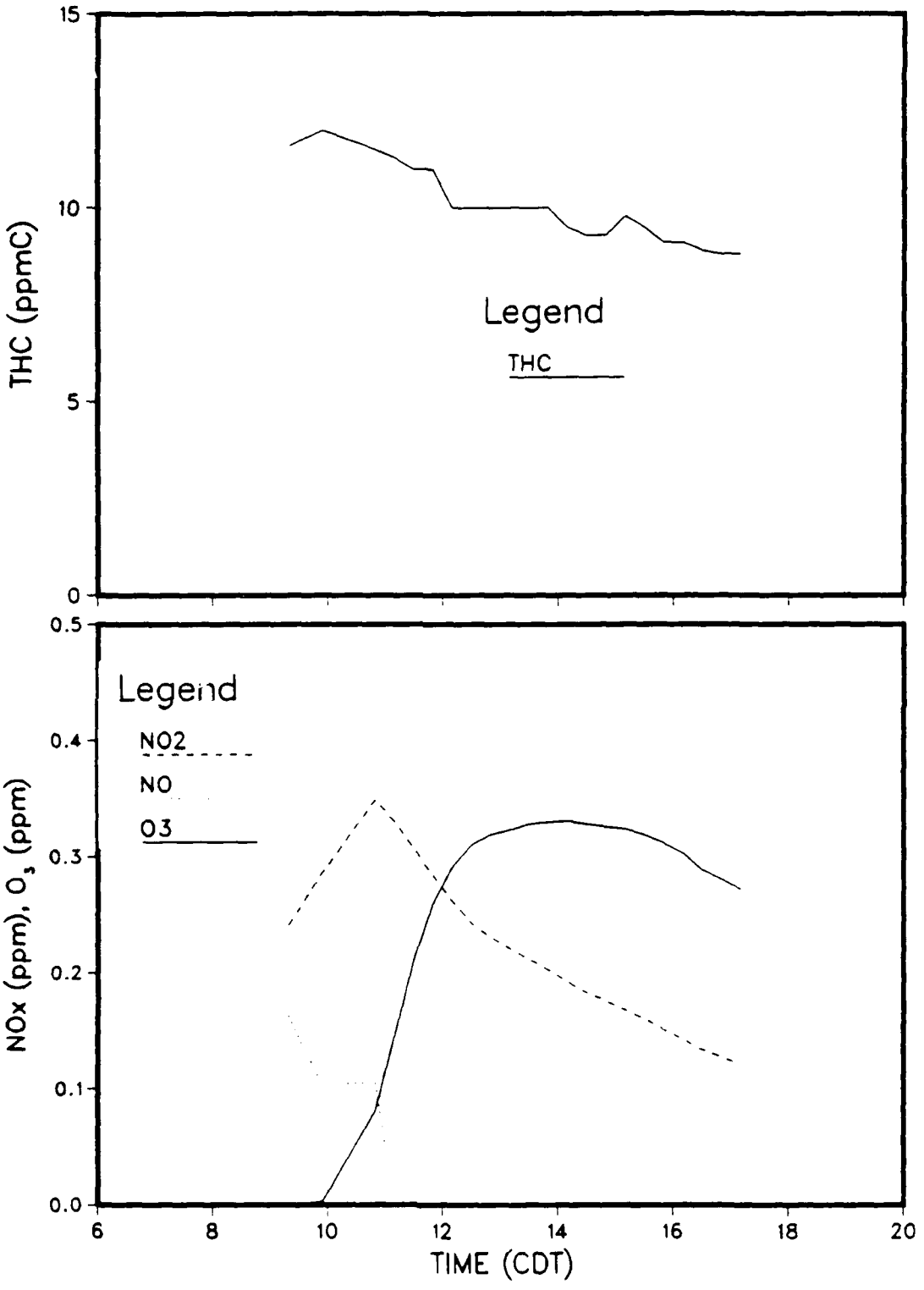


Figure 16. Total Hydrocarbon Concentration Profile and $O_3$ and $NO_x$ Profiles for Control Chamber During Run 6 (EKMA/$NO_x$)

Similar data for Chambers 1 and 3 are depicted in Figures 17 through 28. These figures are arranged in pairs to permit comparison between the two chambers for each day's run. These figures are all presented on a common abscissa, and the scale of the ordinate has been selected to facilitate comparisons between different test conditions. The reader is referred to Table 1 for a description of the test conditions corresponding to each of the figures.

## C. PAH AND $NO_2$-PAH CONCENTRATIONS

During the six exhaust aging experiments, 61 samples were collected for subsequent analysis by GC/MS for target PAH and $NO_2$-PAH compounds. That total includes field blanks and the engine exhaust samples collected at the start of the aging experiments. All results obtained in the aging experiment samples are presented in tabular form in Appendix A. Concentration-time profiles for selected species are presented in the Discussion section of this report. Appendix B presents the total ion chromatograms obtained in the GC/MS full-scan mode, and the attempted identification of the major peaks for each of the fractions of one selected exhaust sample. Because of the small mass of extractable material in the samples and the complex mixture of compounds present, only a selected few are quantified and reported. The results of the measurements of these compounds and other results from the aging experiments are presented below.

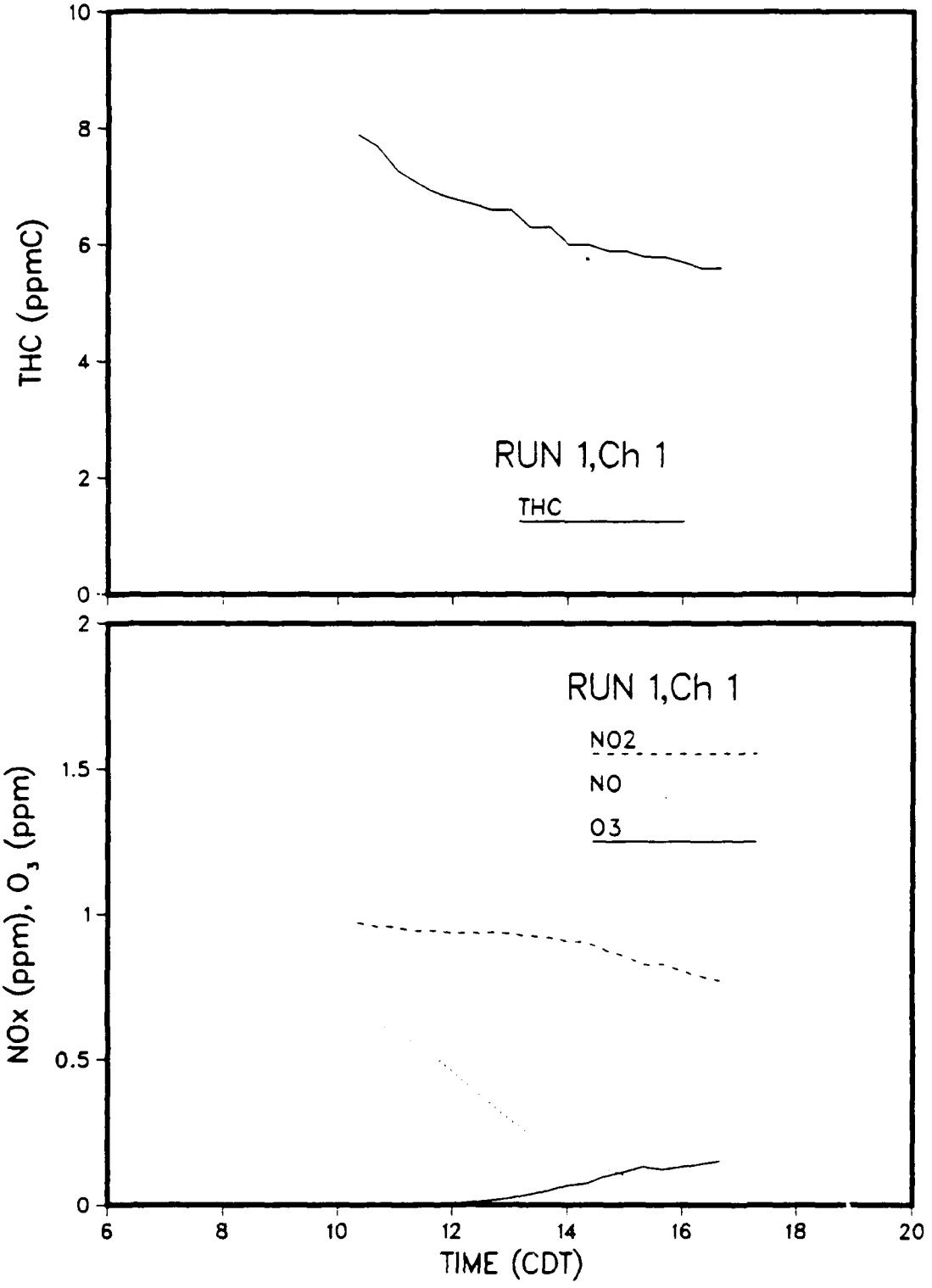


Figure 17. Total Hydrocarbon Concentration Profile and $O_3$ and $NO_x$ Profiles for Chamber 1 During Run 1 (J79, 30 Percent Power, Sunlit)

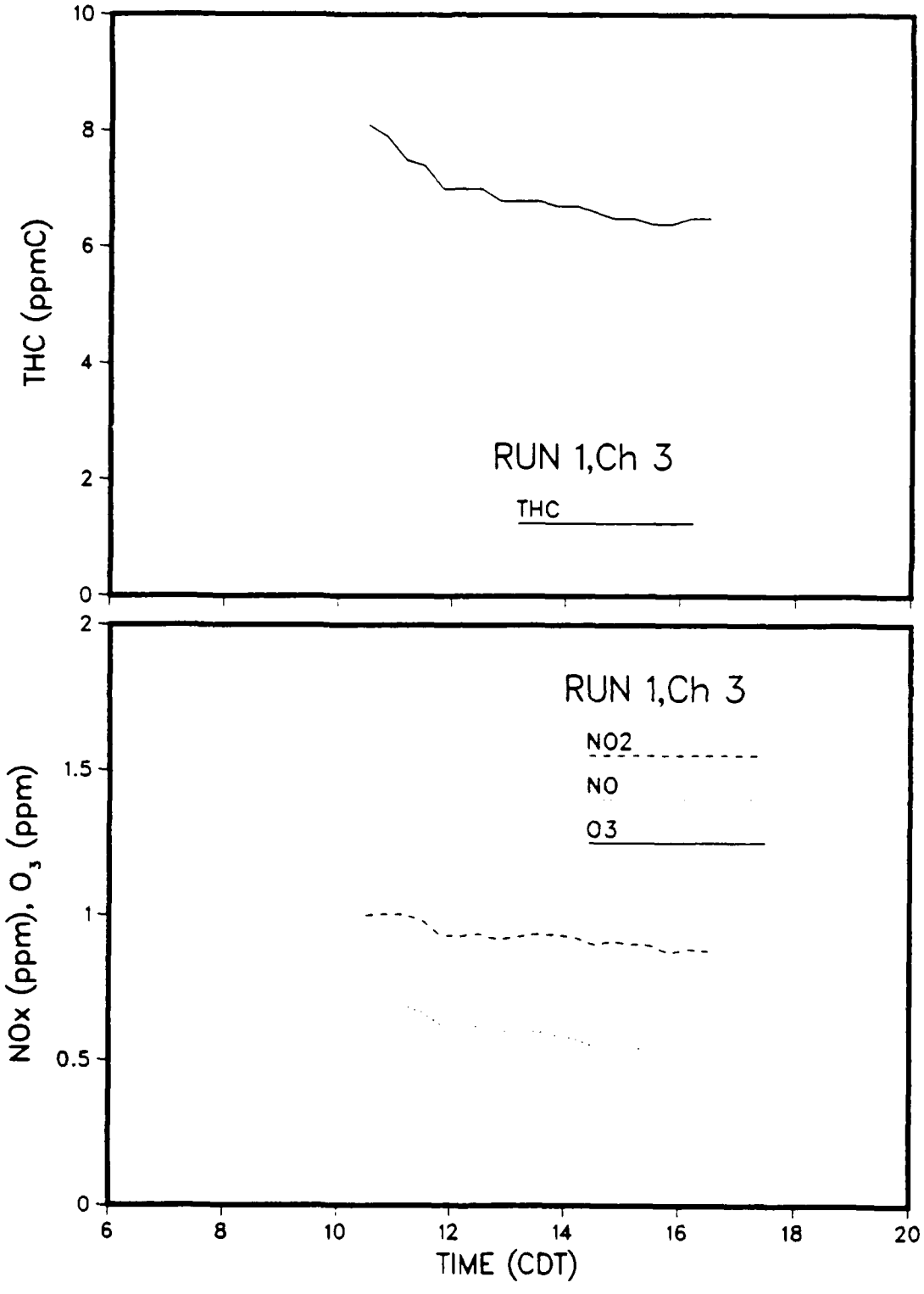


Figure 18. Total Hydrocarbon Concentration Profile and $O_3$ and $NO_x$ Profiles for Chamber 3 During Run 1 (J79, 30 Percent Power, Dark)

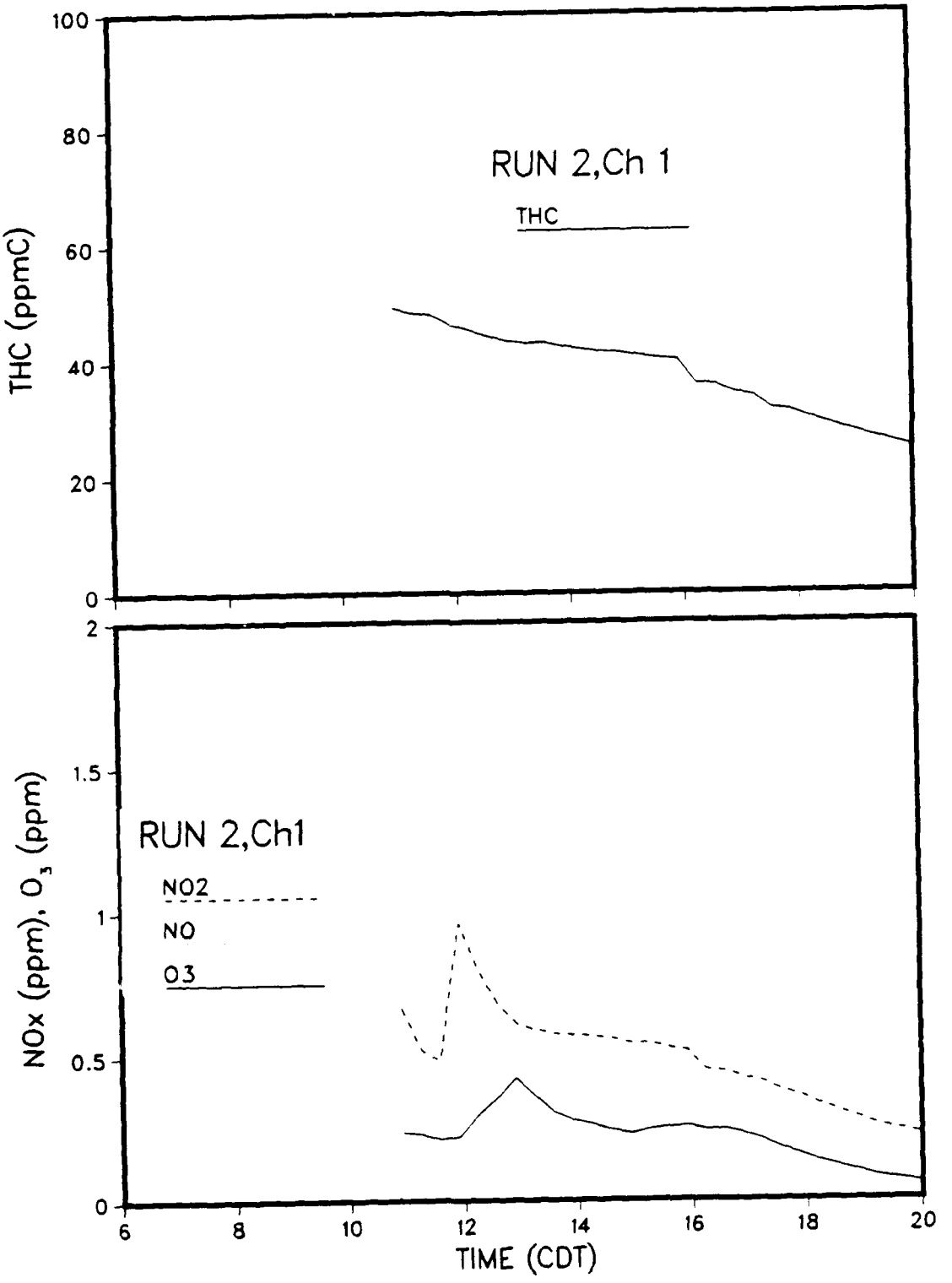


Figure 19. Total Hydrocarbon Concentration Profile and $O_3$ and $NO_x$ Profiles for Chamber 1 During Run 2 (J79, Idle, Sunlit)

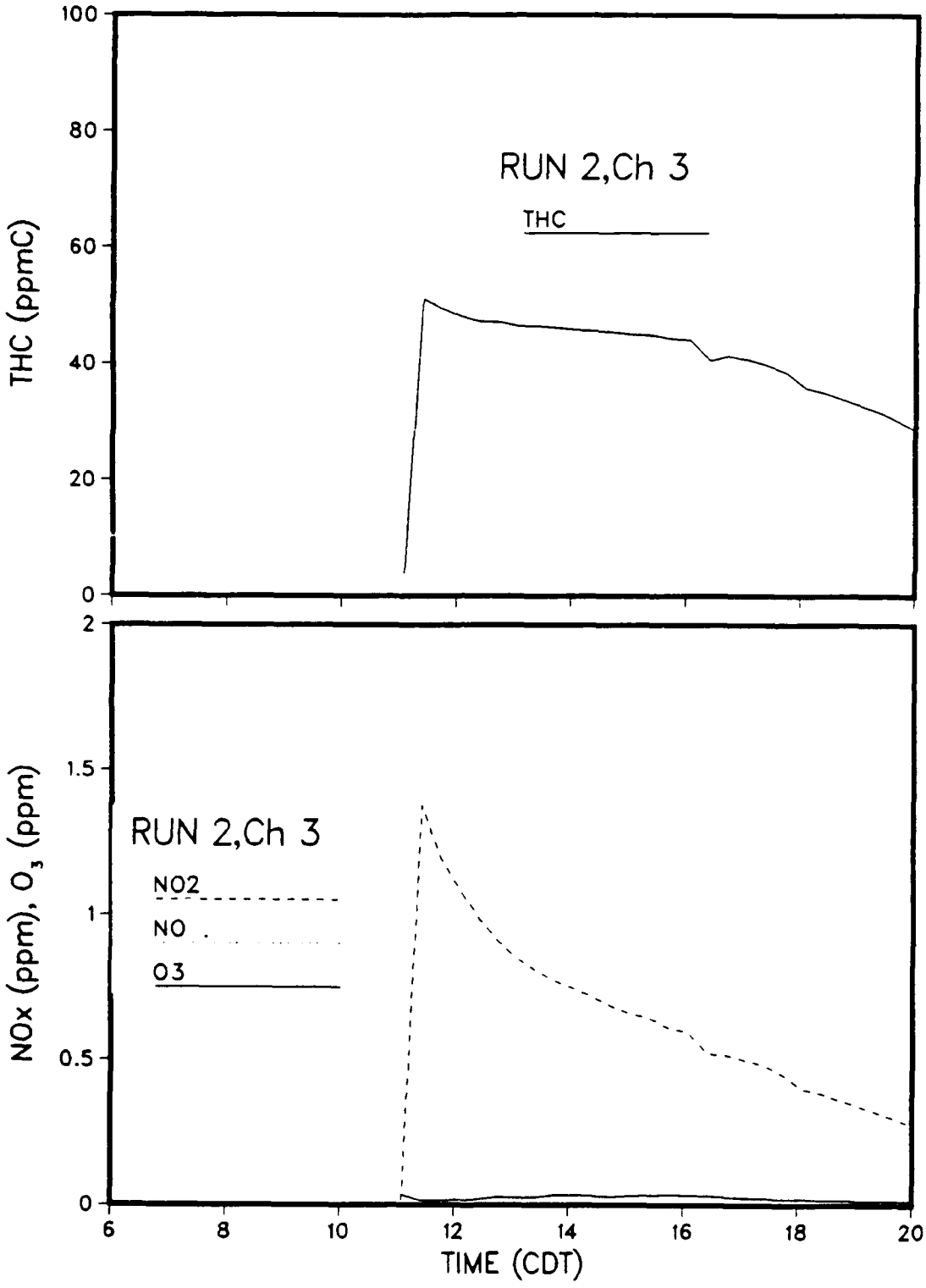


Figure 20. Total Hydrocarbon Concentration Profile and $O_3$ and $NO_x$ Profiles for Chamber 3 During Run 2 (J79, Idle, Dark)

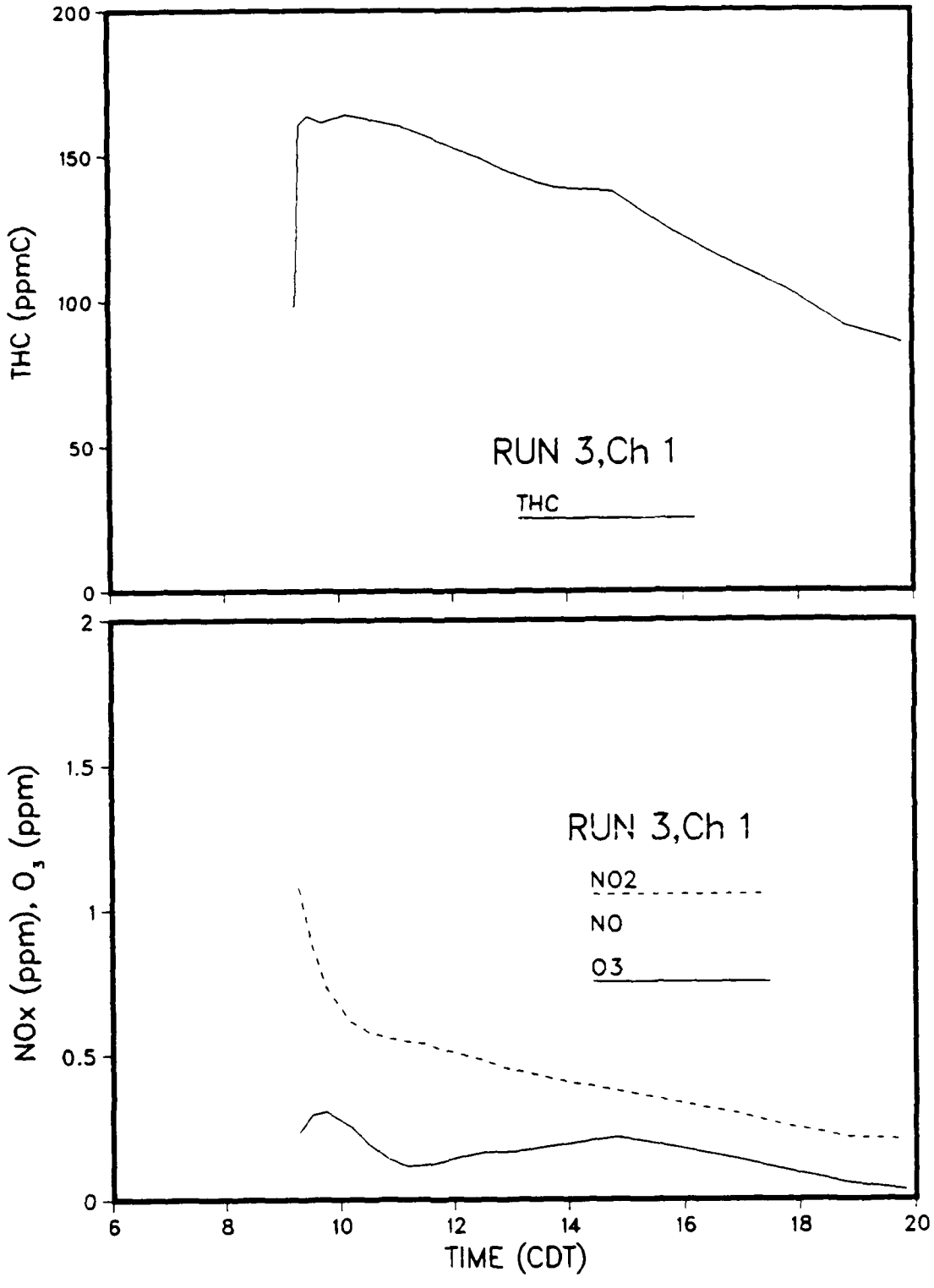


Figure 21. Total Hydrocarbon Concentration Profile and $O_3$ and $NO_x$ Profiles for Chamber 1 During Run 3 (TF33-P3, Idle, Sunlit)

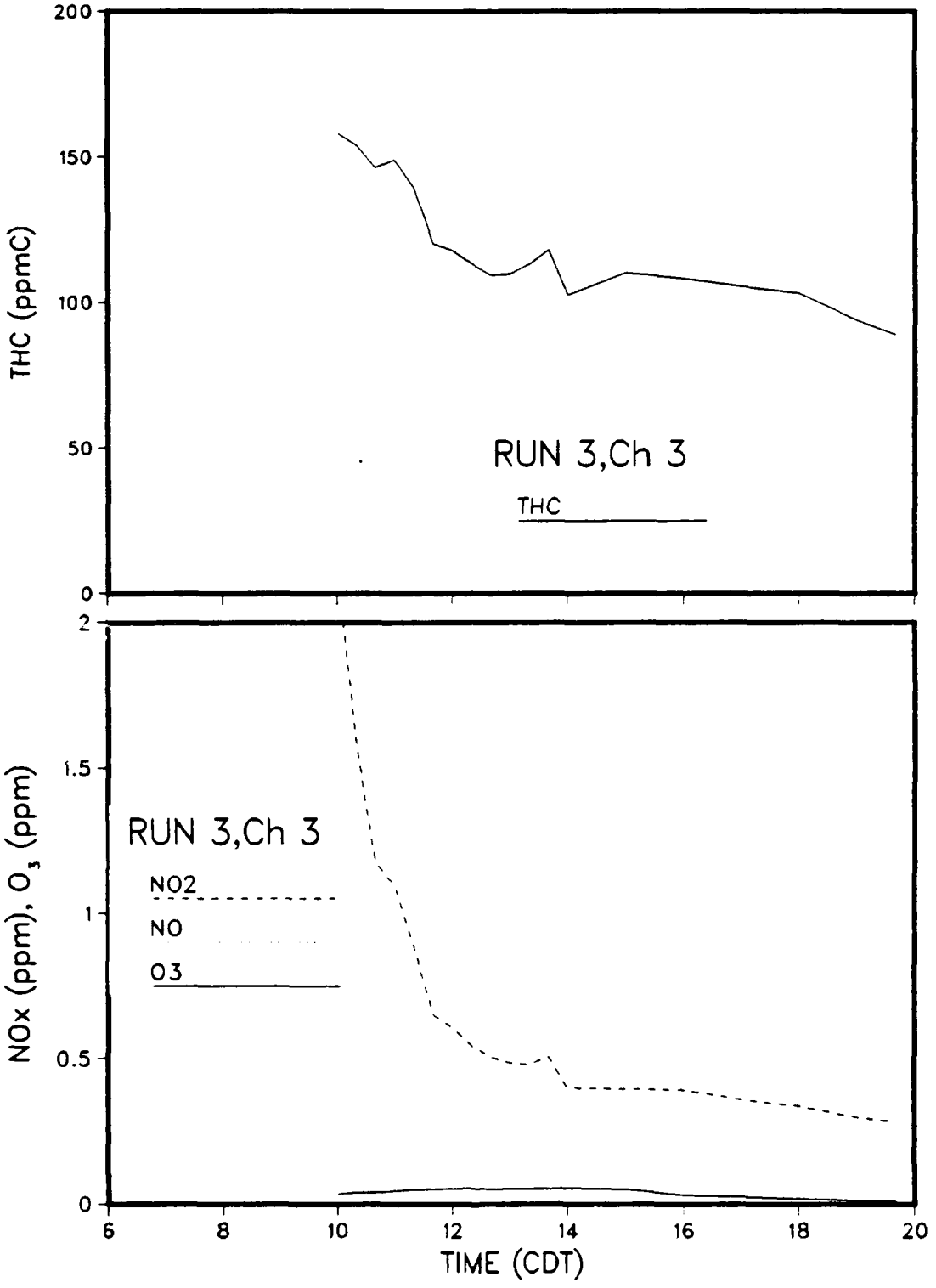


Figure 22. Total Hydrocarbon Concentration Profile and $O_3$ and $NO_x$ Profiles for Chamber 3 During Run 3 (TF33-P3, Idle, Dark)

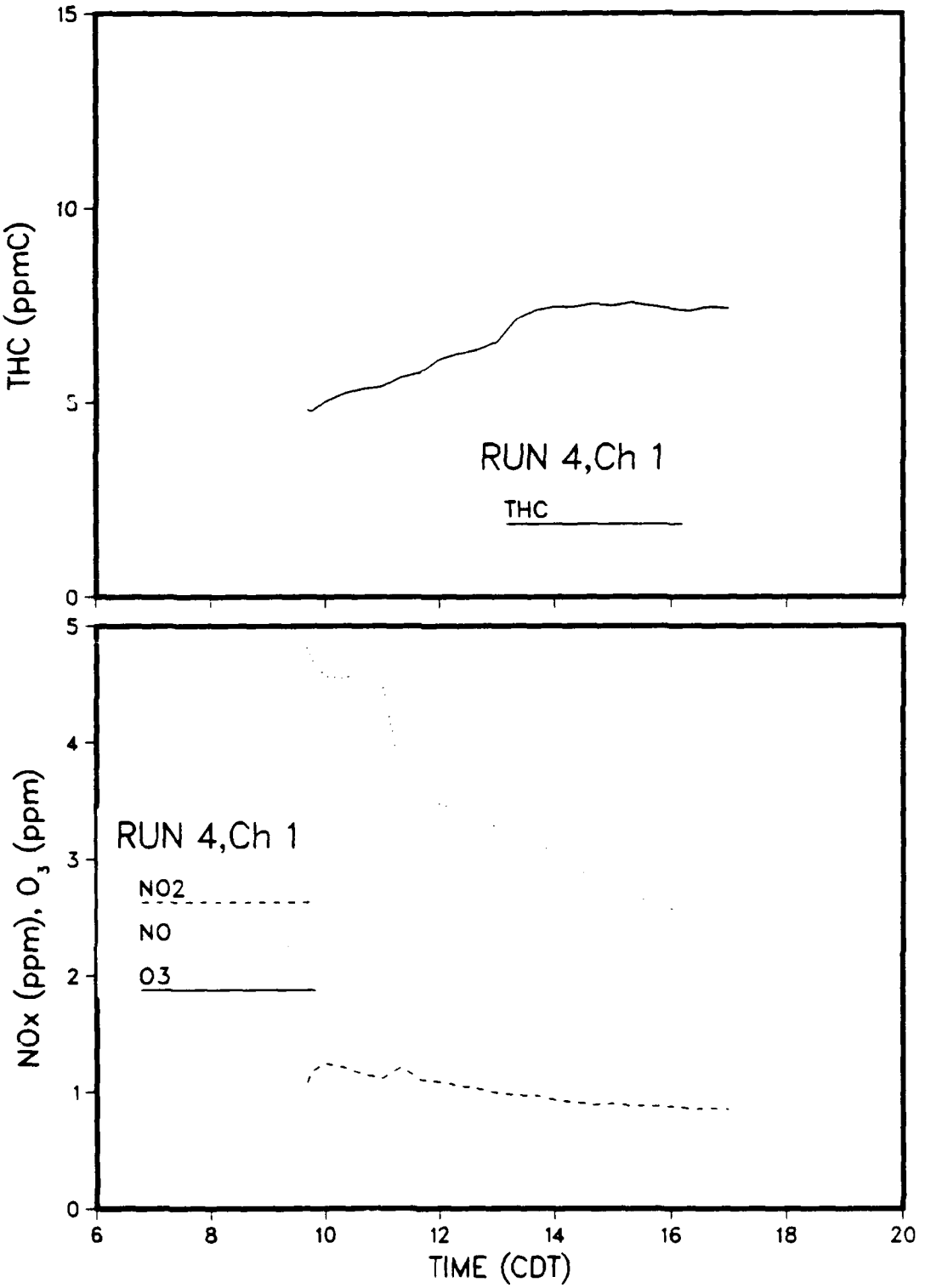


Figure 23. Total Hydrocarbon Concentration Profile and $O_3$ and $NO_x$ Profiles for Chamber 1 During Run 4 (TF33-P3, 75 Percent, Sunlit)

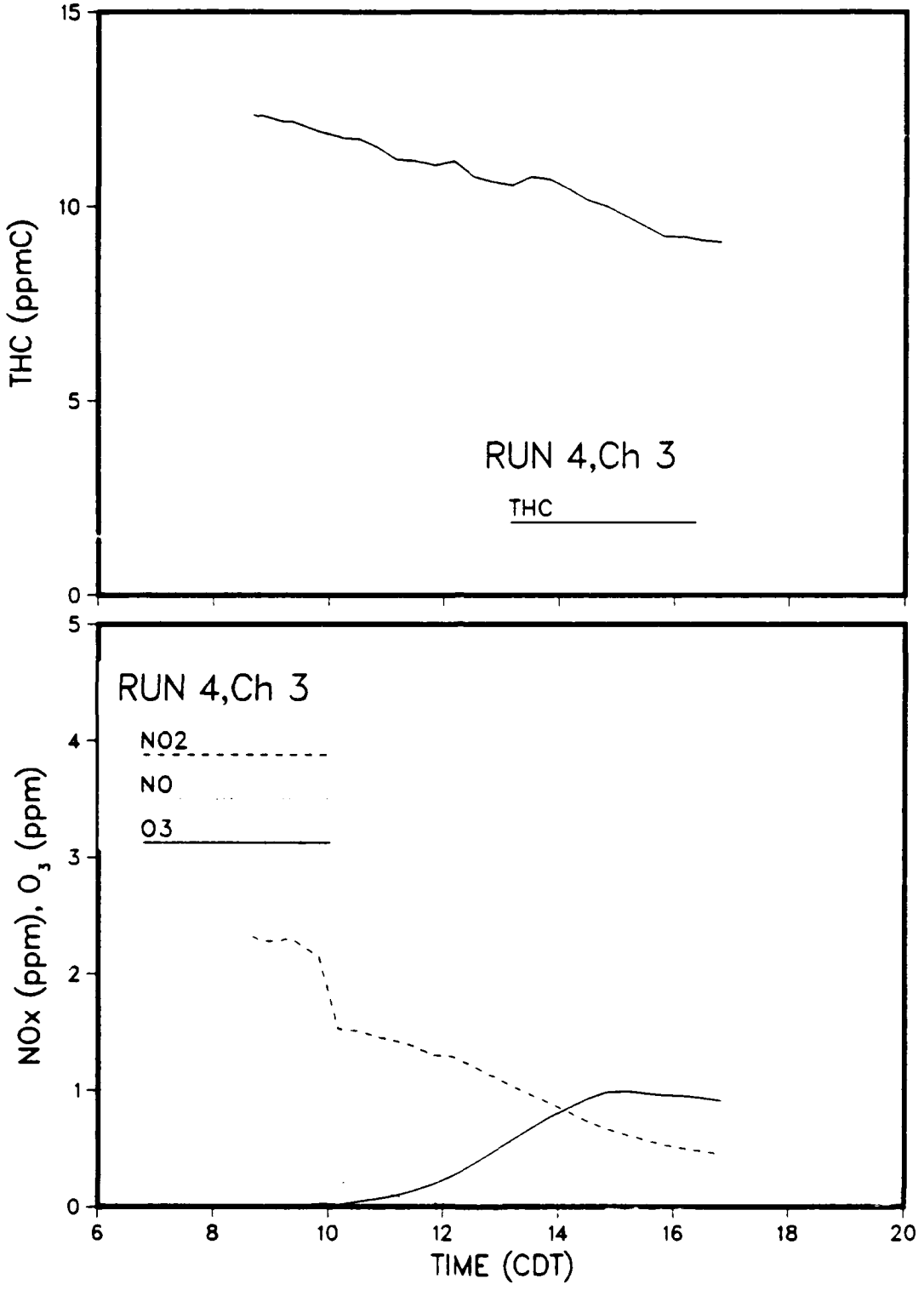


Figure 24. Total Hydrocarbon Concentration Profile and $O_3$ and $NO_x$ Profiles for Chamber 3 During Run 4 (TF33-P3, 30 Percent, Sunlit)

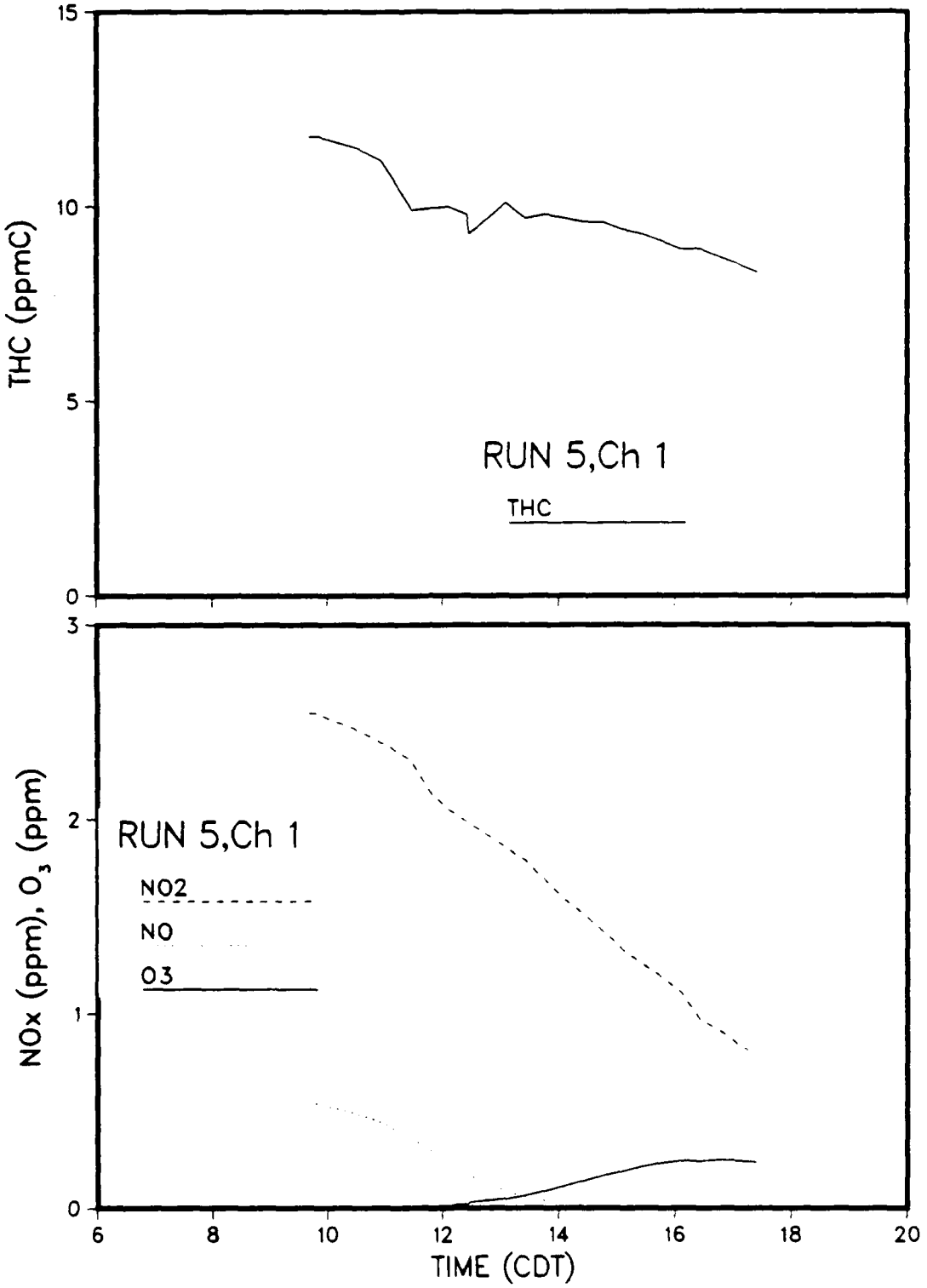


Figure 25. Total Hydrocarbon Concentration Profile and $O_3$ and $NO_x$ Profiles for Chamber 1 During Run 5 (TF33-P3, 30 Percent, Sunlit)

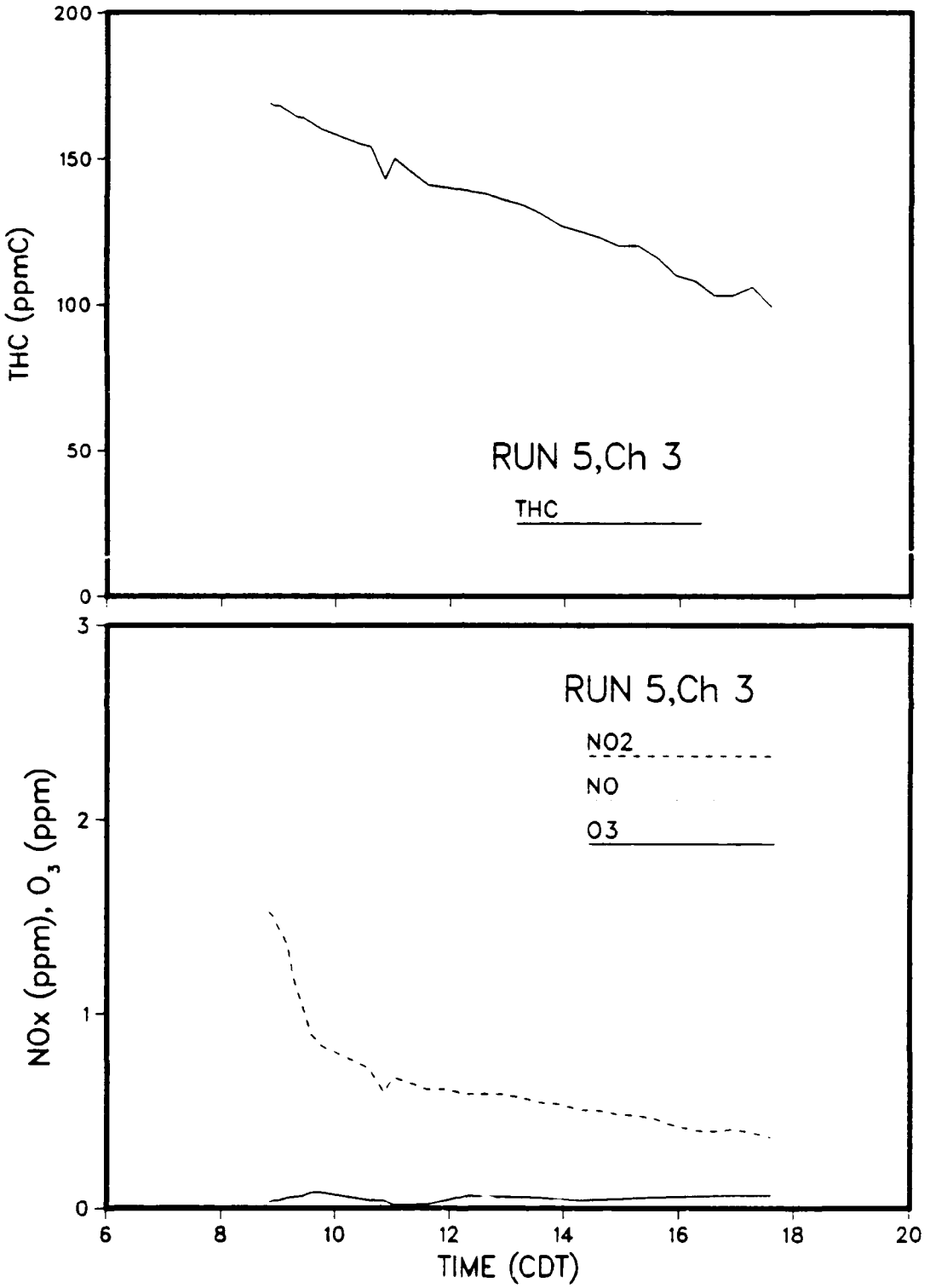


Figure 26. Total Hydrocarbon Concentration Profile and $O_3$ and $NO_x$ Profiles for Chamber 3 During Run 5 (TF33-P7, Idle, Sunlit)

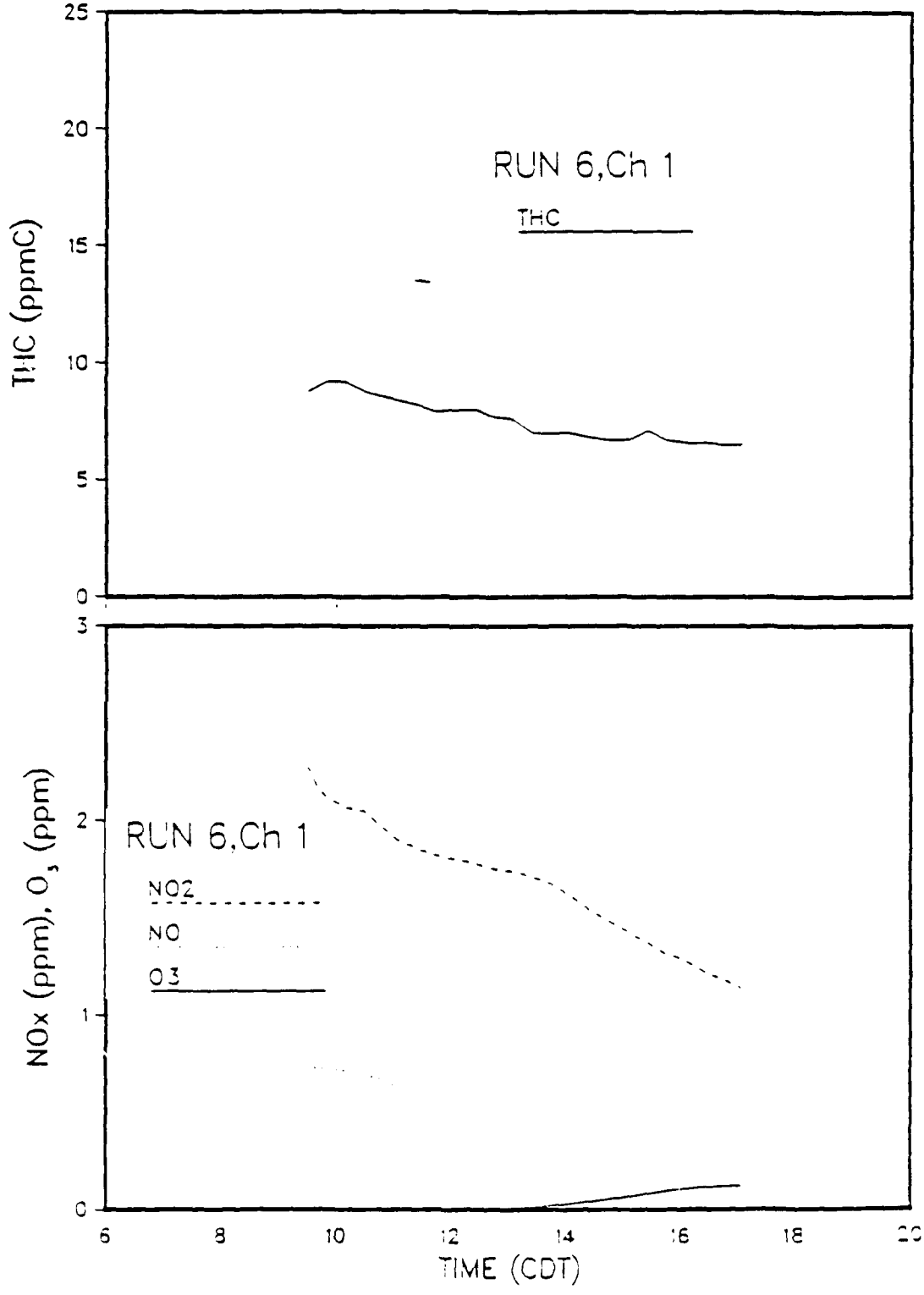


Figure 27. Total Hydrocarbon Concentration Profile and $O_3$ and $NO_x$ Profiles for Chamber 1 During Run 6 (TF33-P7, 30 Percent, Sunlit)

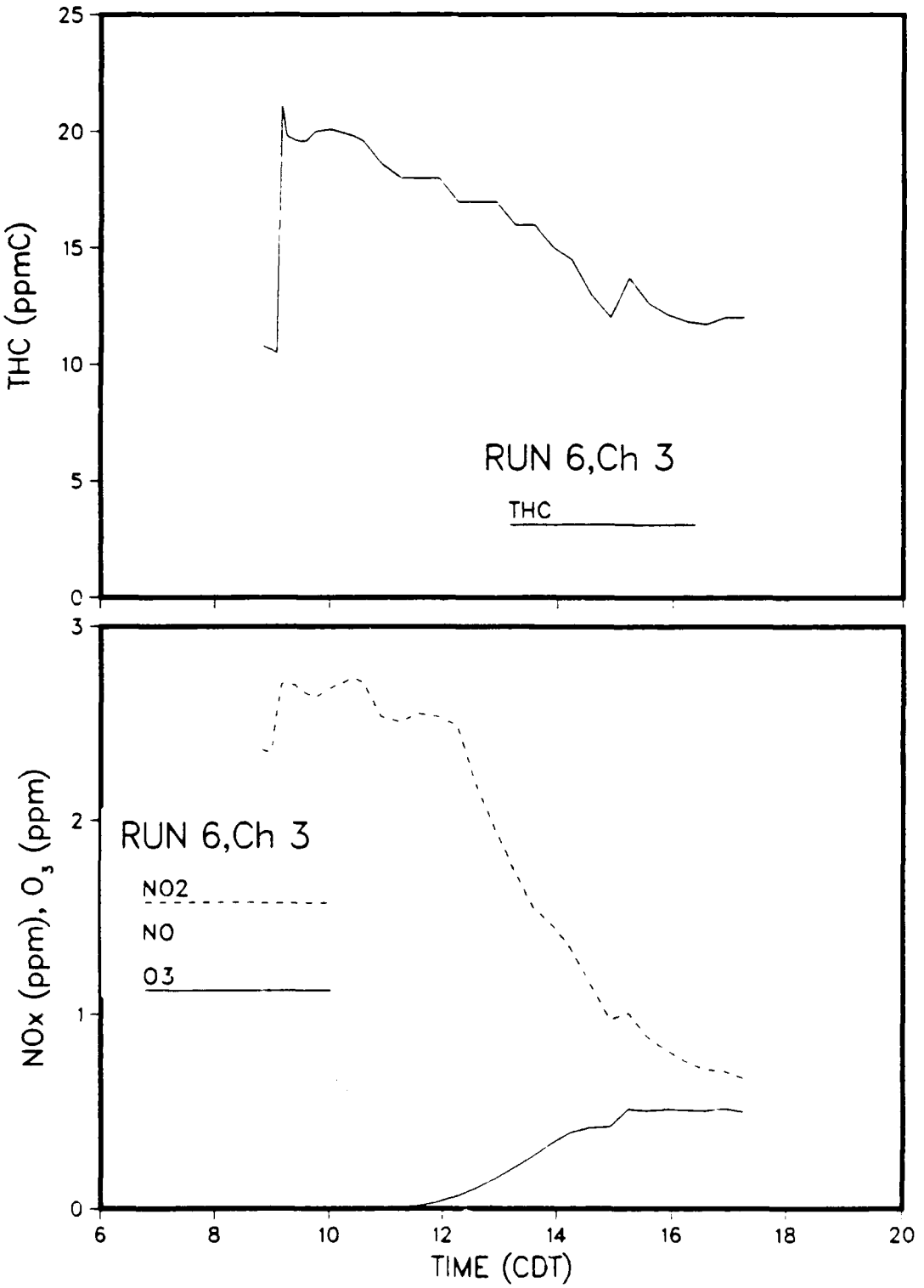


Figure 28. Total Hydrocarbon Concentration Profile and $O_3$ and $NO_x$ Profiles for Chamber 3 During Run 6 (TF33-P7, 30 Percent, Sunlit, Added EKMA/$NO_x$)

# SECTION IV

# DISCUSSION

## A. COMPARISON OF ENGINE EXHAUST COMPOSITIONS

This section provides discussion of the inorganic particulate material found in the engine exhaust samples, the total hydrocarbon and oxides of nitrogen content of the exhaust, and the PAH and $NO_2$-PAH concentrations measured in the exhaust samples.

### 1. Inorganic Particulate Matter

The first observation to be made regarding the inorganic components of the exhaust presented in Table 6 is that all of the materials detected are present at very low concentrations. The elements, Si, Al, and Ca, generally indicate the presence of soil in air samples due to wind-blown dust. Ordinarily, the masses of these compounds detected will track one another because of their common source. In these samples, however, there may be the influence of a source of Al in the exhaust which can change the amount of Al relative to the Si, which is certainly of crustal origin. The Ca and Zn found in these samples may result from wear of any brass which might be present (anywhere from the fuel handling system to the engine exhaust plane). These elements and the Zr are almost certainly not associated with wind blown soil. While somewhat higher concentrations of several of these elements are found in the 75 percent power condition for the TF33-P3, it is not understood why the greatest concentrations of many of these elements are found in the idle emissions from the J79 engine tested.

It is clear that the small concentration of inorganics in the engine exhaust require sensitive techniques and contaminant-free sampling media for their analysis. SSMS appears to have been a good choice of analytical method within the limitations imposed on this study. Additional samples would be desirable to permit further examination of the J79 engine at idle in order to resolve the anomalous results for the sample obtained.

2. Total Hydrocarbon and Oxides of Nitrogen

It is not intended to discuss in detail the composition of the engine exhaust gas, since that is done elsewhere (Reference 5). Only the salient features of the data from Table 7 are discussed here as they relate to the PAH concentrations measured. Comparing the two variants of the TF33 engine shows only minor differences in the exhaust composition as indicated by these measurements. For all but the 30 percent power setting, the -P7 version of this engine produces slightly (~10 percent) more $NO_x$ than does the -P3, at a lower ratio of $NO_2$:$NO_x$. The $NO_x$ data for the J79 engine indicate the same trend of increasing $NO_x$ concentration and decreasing $NO_2$:$NO_x$ ratio with increasing engine power, and the concentrations measured do not differ greatly between the engine types.

The engines differ considerably, however, in the concentration of total hydrocarbons found in their exhaust, with the J79 engine exhaust containing, typically, one-third the THC found in the TF33 exhausts. The data point for the TF33-P7 engine at 75 percent power seems low when compared with the remaining data obtained. With the exception of this data point, the THC measurements depict a consistent decrease with increased operating power, as one would anticipate. Clearly, the idle setting produces THC concentrations more than an order of magnitude above those found at 30 percent power. At 75 percent power, one finds near background levels of THC, and beyond this setting, the engine is consuming a portion of the background $CH_4$ and actually lowering the THC concentration of the air processes.

3. PAH and $NO_2$-PAH Concentrations

Before comparing the engines and power settings in Table 10, it is worthwhile to examine the final two columns of the table. These data were obtained from exhaust samples collected from an engine operated at the same nominal power setting on two consecutive days. The amount of data obtained in this study does not allow differentiation between variability which is attributable to the sampling and analysis, and that which is due to variations in the actual composition of the engine exhaust. The magnitude of the differences observed in the levels of these compounds found in replicate samples must be

kept in mind while attempting to interpret the apparent differences between engines and between power settings.

The PAH concentrations seen in Table 10 basically follow the trends seen in Table 7 for the THC concentrations in the exhaust under various conditions. At idle, most of the PAH concentrations are higher in the TF33 exhaust samples than in the J79. Benzo[a]pyrene and the perylenes are detectable in the TF33 idle exhausts but are barely detected in the J79 exhaust. Fluoranthene and pyrene are present at about the same concentration in the idle exhaust from all three engines and seems to persist at the 30 percent power setting for the TF33 engines. The compounds' concentrations are reduced at 75 percent power for the TF33 engine and at 30 percent power for the J79. In fact, at the 75 percent power setting for the TF33, naphthalene and phenanthrene are the only PAH remaining at concentrations in excess of 1 $\mu g/m^3$. While general statements regarding trends can be made, based on these data, there is too much variability between measured compounds to relate the whole set of PAH concentrations measured under one set of conditions to the set measured under other conditions. One cannot say, for example, that the TF33-P7 idle exhaust contains 10 times the PAH concentration at 30 percent power, although this is true for some of the compounds detected.

The $NO_2$-PAH data indicate very similar concentrations were found in the idle exhaust from the TF33 engines. The idle exhaust from the J79 contained more 2-nitro-1-naphthol, 1-nitronaphthalene, 9-nitroanthracene, and 1-nitropyrene. This is despite the fact that neither $NO_2$ nor the parent PAH compounds are present at higher concentrations in the J79 idle exhaust. For the J79 engine, the concentrations of all $NO_2$-PAH except 4-hydroxy-3-nitrobiphenyl decrease at the 30 percent power setting. For the TF33 engines, at 30 percent power the concentrations of 9-nitroanthracene greatly increase, and those of 1-nitropyrene and 1-nitronaphthalene also increase. This may be due to the increase in the $NO_2$ concentration in the engine exhaust at this power setting relative to the other power levels examined. An increase in those $NO_2$-PAH compounds is not observed at 30 percent power for the J79 engine. This appears to be because the concentrations of the parent PAH are much lower in this engine's exhaust than on the TF33 engines' exhausts at this power. This is another indication of the differences in the hydrocarbons found in the

different engine types' exhaust emissions. At 75 percent power, the concentrations of both the $NO_2$ and the parent PAH (and THC) decrease, as do the $NO_2$-PAH, but to a smaller degree.

The data contained in Table 8 indicate the phase with which the extractable organic mass is associated. At idle, nearly all the organic mass is associated with the vapor phase. For the TF33 engines, the extractable organic mass associated with the particulate phase decreases by just over a factor of two on going from idle to 30 percent power. The much larger reduction in the vapor phase components of this mass brings about an apparent increase in the aerosol fraction. So while both portions are decreasing at higher operating power, the gaseous compounds are undergoing a much more effective reduction in concentration. The report from the companion study (Reference 5) indicates that the particulate mass concentration increased for all three engines with increasing operating power and the smoke number of the exhaust increased for both TF33s with higher power settings. (This was not observed to occur for the J79C which is consistent with its designation "smokeless".) The increasing aerosol concentration at higher power settings may be partly responsible for the slower decrease in the extractable organic mass found on the filter samples, since increased surface area for adsorption is available.

## B. COMPARISON OF PHOTOCHEMISTRY RESULTS

Numerous comparisons can be drawn from the measurements performed in the smog chambers. The experimental matrix was designed to emphasize comparison between conditions in the Test Chambers 1 and 3 on a given day. This discussion is organized around comparisons between Chambers 1 and 3 for each day of testing, with less emphasis placed on comparisons across engine types. The reader is referred to Figures 10 through 28 for the following discussion.

For Run 1 (J79, 30 percent power), Chambers 1 and 3 were well matched initially for THC, NO, and $NO_2$ concentration. Figure 11 illustrates the NO decay and $O_3$ formation in the sunlit chamber, which can be characterized as a slow photochemical system. There is, of course, no $O_3$ formation in the darkened Chamber 3, and just the slow decay of NO and $NO_2$ is observed. There are no striking differences in the THC profiles, although the THC in Chamber 1

does display some consumption beginning near the start of $O_3$ accumulation. The background air chamber found more $O_3$ than did Chamber 1 and reached its maximum at about 1530. The low HC:$NO_x$ ratio and initial concentration of NO present the atmosphere in Chamber 1 from reaching $O_{3max}$ prior to the end of the experiment.

In Run 2 (J79, idle) the elevated hydrocarbon concentration in the injected exhaust is readily apparent in the initial THC values for Chambers 1 and 3. It is not immediately apparent that there are any differences in the THC decay rates in the light and dark chambers. This is due to the overabundance of hydrocarbons in the chambers for this run. The unusual shapes of the $O_3$ and $NO_x$ curves in Chamber 1 are explained by the following. Due to engine difficulties, the test chambers were not able to be charged with exhaust until about 0950. It was decided to fill the sunlit chamber first (Chamber 1) and then fill the covered Chamber 3. From the time Chamber 1 was filled to the time it was repositioned for measurements, approximately 10 minutes elapsed. When the contents of the covered chamber were measured, much of the injected $NO_x$ had been consumed in Chamber 1 before being measured. To bring the chambers to a more nearly equal concentration of $NO_2$, $NO_2$ was injected into Chamber 1 at about 1150. This injection is responsible for the spike observed in the $NO_2$ profile -- and for the resulting spike in the $O_3$ concentration immediately thereafter. It is interesting that the $NO_2$ and $O_3$ profiles appear to nearly recover their original conditions about 2 hours after the injection. It is also worth noting that the exhaust emissions were measured to contain nearly equal concentrations of NO and $NO_2$, but no NO was detected in either exhaust containing chamber, indicating that the NO injected was completely reacted within 10 minutes under the conditions of this run. Once again no $O_3$ is formed in the dark, and the surplus of hydrocarbons prevents the $O_3$ from exceeding 0.3 ppm for most of the run.

The control chamber for Run 3 (TF33-P3, idle) contained an EKMA/$NO_x$ mixture which yielded the typical $NO_x$ and $O_3$ profiles for this type atmosphere. Chambers 1 and 3 begin the run with more than 150 ppmC of THC, reflecting the high hydrocarbon content of the idle exhaust of the TF33 engines relative to that of the J79. Again, none of the NO presumably injected into the chambers is detected by the time the measurements are initiated. The $NO_2$ is also

rapidly reacting initially in both chambers and is likely converted to other species, some of which generate a response in the chemiluminescent $NO_x$ monitor. The double peak in the $O_3$ profile in Chamber 1 is indicative of a photochemical system capable of producing radicals initially, and then "storing" radicals in a reactive product which photolyzes later to produce the secondary $O_3$ peak. No such activity is observed in the dark chamber, although the $NO_2$ has obviously reacted to a large degree.

For Run 4 (TF33-P3, 75% = 1, 30% = 3) the control chamber was again injected with ambient air instead of the EKMA/$NO_x$ mixture. Note the very low scale used for the ordinate in the $NO_x$ and $O_3$ figure. Chamber 1 was charged with exhaust from the engine operating at 75 percent power. At this high power setting, the THC concentration differs but little from ambient. The gradual increase in THC seen in Figure 23 (and also seen this day in Figure 14) is believed to be due to a change in the instrument response rather than due to actual increases in THC in Chambers 1 and 2. As engine power setting is increased, the NO:$NO_x$ ratio increases, and this is reflected in Figures 23 and 24. There is initially about a ratio of 5:1 for NO:$NO_2$, which reflects the measured exhaust concentrations well. With such an excess of NO and nearly no hydrocarbons, one would not expect to see much photochemical reaction in this chamber, and this expectation is upheld. Chamber 3 contains exhaust from the engine at 30 percent power, and therefore contains emitted hydrocarbons and $NO_x$ at a much lower NO:$NO_x$ ratio and therefore a more photochemically reactive system. The NO is consumed by 1200, and $O_3$ formation begins slightly earlier, reaching 1 ppm at about 1500. This can be compared with Figure 11. The TF33-P3's greater hydrocarbon emissions, and to some extent, greater $NO_2$ emission at 30 percent power result in a more photochemically reactive system.

Run 5 (TF33-P7, 30% = 1, idle = 3) indicates some differences between the -P3 and -P7 emissions behavior; although the cause of the differences is not immediately apparent. Comparing Figures 25 and 24 shows that although the THC profiles do not differ greatly, and the initial concentrations of NO and $NO_2$ are reasonably close, the $O_3$ formed in the TF33-P7 exhaust system begins later and peaks at about one-third the value reached in the -P3 exhaust. It is not known how much the difference in starting time contributes to this observed different behavior. (It is recognized that photochemical experiments such as

these are best performed under identical conditions, with each test started before dawn. This was not compatible with the schedule of engine testing operations, however.) Chamber 3 received a charge of the idle exhaust, which results in the very high concentration of THC. The behavior of this system is similar to that observed for the other engines at idle, with apparent conversion of $NO_2$ to products, the absence of NO, and effective suppression of $O_3$ formation by the excess THC.

Run 6 (TF33-P7, 30% = 1, 30% + EKMA = 3) was performed to demonstrate the behavior of the engine exhaust when placed in a photochemically reactive atmosphere. Exhaust from the TF33-P7 engine operated at 30 percent power was injected into both chambers, with EKMA mix and $NO_x$ added to Chamber 3 to produce a more reactive atmosphere. The behavior seen in Figure 27 is similar to that seen under the conditions in Figure 25. For Chamber 3, however, one can observe consumption of the THC and earlier oxidation of the NO and formation of $O_3$. The effects of this greater photochemical reactivity will also be reflected in the subsequent discussion of the PAH data.

## C. DECAY/FORMATION OF PAH AND $NO_2$-PAH

### 1. PAH Formation/Decay

All PAH concentrations measured in the exhaust aging experiments are contained in Appendix A (Tables A-1 through A-6). If one examines first those among the target compounds which are biologically active (benzo[a]anthracene, cyclopenta[c,d]pyrene, benzofluoranthenes, benzo[a]pyrene, indeno[1,2,3,-c,d]pyrene, and dibenzo[a,h]anthracene), one finds that they are only present near or below detection limits in any of the samples obtained. In no instance is there any formation of these compounds during an aging experiment.

To accurately define the behavior of these compounds as they age in the test chambers, one would wish to have frequent data and to have atmospheres containing these compounds at concentrations well above the analytical detection limits. The frequency of the data obtained in this study is limited by the need to collect adequate mass for analysis and by the fairly intensive process required to extract and analyze the collected samples. The sampling and analysis scheme used in performance of this work is believed to represent a good balance between what would be desirable and what the program resources

permitted. The low concentration of most of the compounds of interest and the duration (30 min) of injection into the chambers placed the limits on the initial concentrations achieved in the tests.

As a rule, the PAH all appear to decay during the aging experiments, at a greater rate in sunlight than in the dark. The behavior of naphthalene, the most prevalent of the target PAH compounds in these measurements, seen in Figure 29, is typical of the class.

Phenanthrene concentration data are shown for selected runs in Figure 30. This compound is the only one of the PAH which exhibited an increase in concentration at any point in the runs performed. It is not apparent, however, what factors determine whether this compound forms a given system. For example, for Runs 5 and 6, Chamber 1 contains exhaust from the TF33-P7 engine operated 30 percent power. The differences in the photochemical data presented earlier are not great, yet there is apparent formation of phenanthrene in one case and not in the other.

While it will be seen below that the very active system sampled in Chamber 3 during Run 6 (TF33-P7 exhaust at 30% power, with added EKMA mix) led to formation of several of the $NO_2$-PAH compounds, the effect on the PAH compounds is not immediately evident, as both chambers exhibit similar decay profiles for the measured compounds.

The distribution of PAH between vapor and particulate matter is strongly dominated by the vapor phase. The most abundant compound, naphthalene, is found only in the vapor phase, as is true for acenaphthalene. The distribution of phenanthrene and pyrene at the beginning and end of several runs is shown in Table 11. While the pyrene is initially found associated with the filter sample, it is present mainly in the vapor phase at the end of the runs. It is not known how much of this shift is due to loss of aerosol from the chamber atmosphere and how much is due to chemical processes which may be occurring as the test atmosphere ages.

2. $NO_2$-PAH Formation/Decay

Before discussing the results of the measurements of this class of compounds, it must be noted that the concentrations observed are very low -- these are expressed in $ng/m^3$ in the tables, whereas the PAH concentrations are

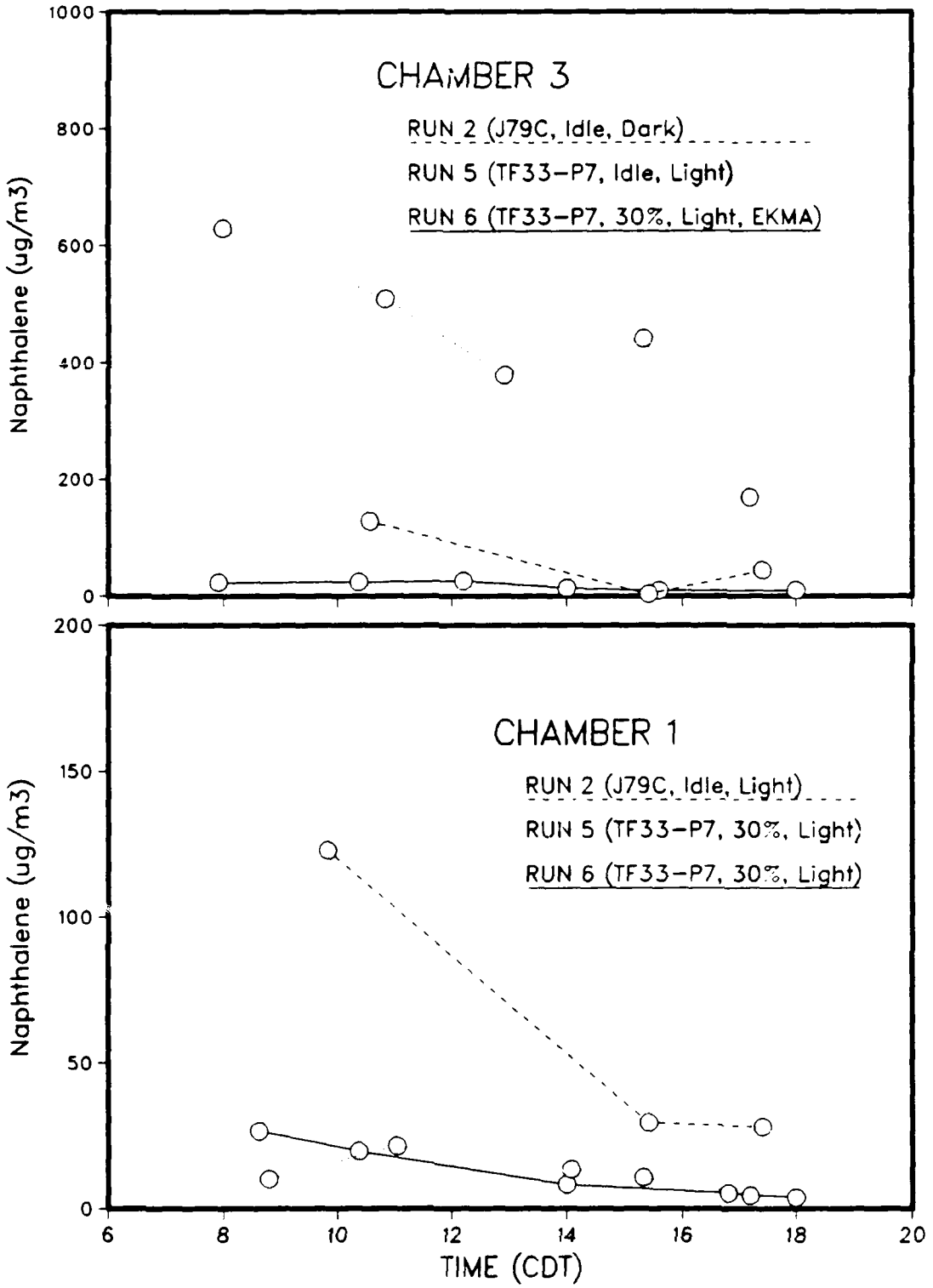


Figure 29. Naphthalene Concentration Profiles for Selected Runs

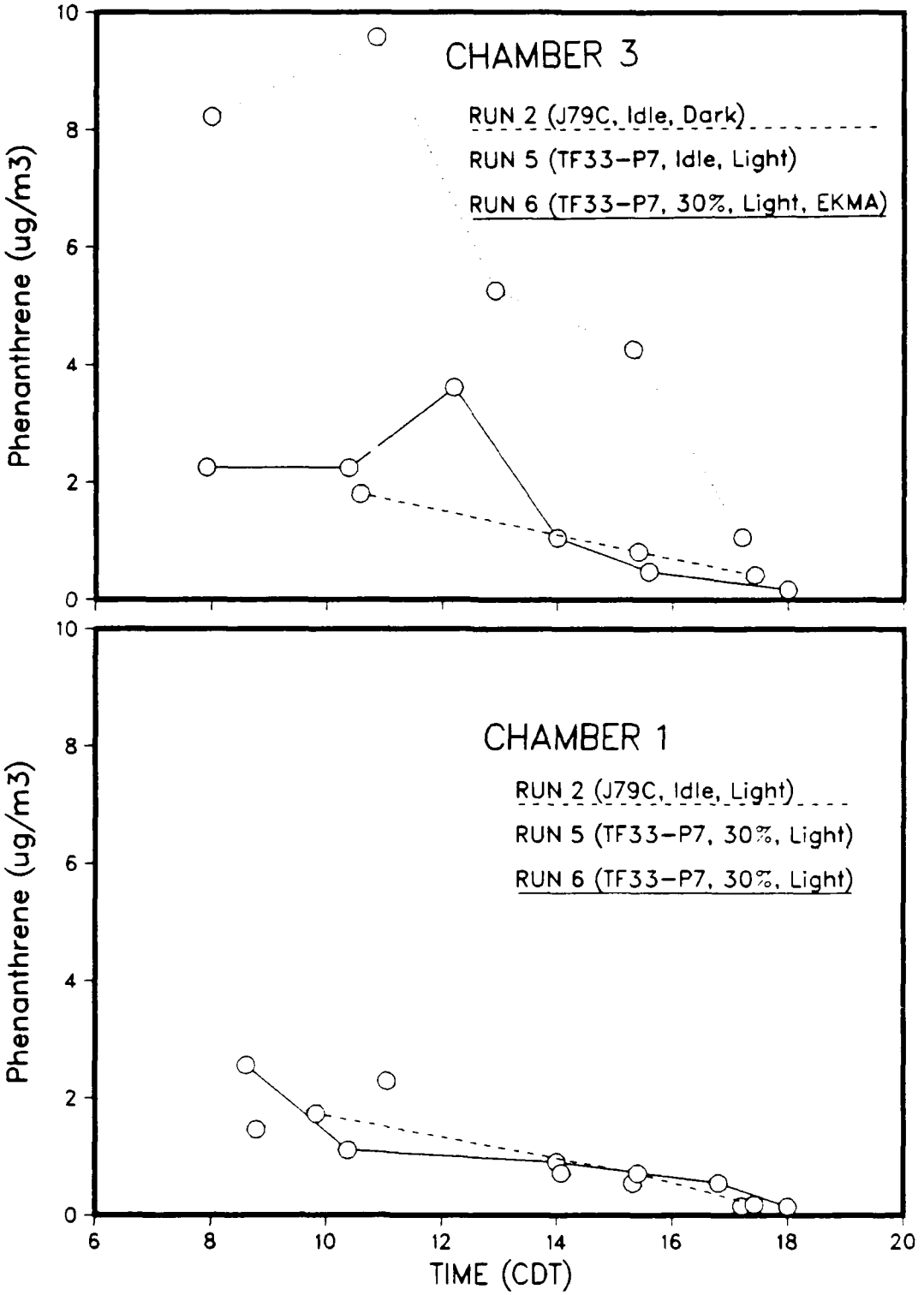


Figure 30. Phenanthrene Concentration Profiles for Selected Runs

TABLE 11. FRACTION OF SELECTED PAH COMPOUNDS FOUND IN VAPOR PHASE AT THE BEGINNING AND END OF AGING EXPERIMENTS

| Compound | Run 3, Ch 1 | | Run 3, Ch 3 | | Run 4, Ch 3 | | Run 6, Ch 1 | | Run 6, Ch 3 | |
|---|---|---|---|---|---|---|---|---|---|---|
| | Initial | Final | Initial | Final | Initial | Final | Initial | Final | Initial | Final |
| Phenanthrene | 0.78 | 0.98 | 0.78 | 0.96 | 0.70 | 0.89 | 0.88 | 0.92 | 0.88 | 0.94 |
| Pyrene | 0.22 | 0.92 | 0.22 | 0.93 | 0.03 | 0.73 | 0.07 | 0.84 | 0.07 | 0.73 |

expressed in $\mu g/m^3$. Because of this disparity in concentrations, one cannot observe any change in the PAH parent compound concentration which corresponds to the formation of the derived $NO_2$-PAH.

Examining the biologically active $NO_2$-PAH compounds first: 3-nitrofluoranthene (NF), 1-nitropyrene (NP), and dinitropyrene, we note that this last compound was detected in none of the samples collected. As was the case in the PAH discussion above, it is difficult to obtain a clear impression of the behavior of these compounds with such limited data for each set of conditions. While there is almost no NF found in the J79 runs and certainly no formation, the TF33 engines 30 and 75 percent power exhaust results information of this compound during the middle of the test run and to its subsequent decay. Figure 31 depicts NF concentrations in the TF33 exhaust. The Run 4, Chamber 1 curve corresponds to engine operation at 75 percent power, and the Run 6 data were obtained for 30 percent power exhaust. Recall that Chamber 3 contained the added EKMA mix in Run 6, resulting in enhanced NF formation. It is interesting that the idle exhaust from the TF33 does not result in formation of NF, in sunlight or in the dark (Run 3). Similar results are seen in Figure 32 for NP, in that formation (enhanced by the EKMA mix) and subsequent decay are observed, particularly for Run 6.

The compound 2-nitro-1-naphthol is seen to be present at the highest concentration of the $NO_2$-PAH in all cases. It is also seen to decay in nearly every run, doing so at a greater rate in sunlight than in the dark, suggesting possible photolysis. For the run using TF33-P3, 75 percent power, exhaust this compound does not appear to decay, but shows a slight increase throughout the run. This chamber contained the lowest initial concentration of this compound. In Run 6, the 30 percent power exhaust, with added EKMA resulted in a doubling of this compound's concentration, followed by a strong decay after noon.

In every case having sufficient data, 1-nitronaphthelene is formed during the mid-day period and then decays. Figure 33 illustrates this compound's behavior under several sets of conditions.

The phase distribution of the $NO_2$-PAH compounds is perhaps best illustrated by examining several of these compounds which were present at higher concentrations. Table 12 contains the fractions of the listed compounds which

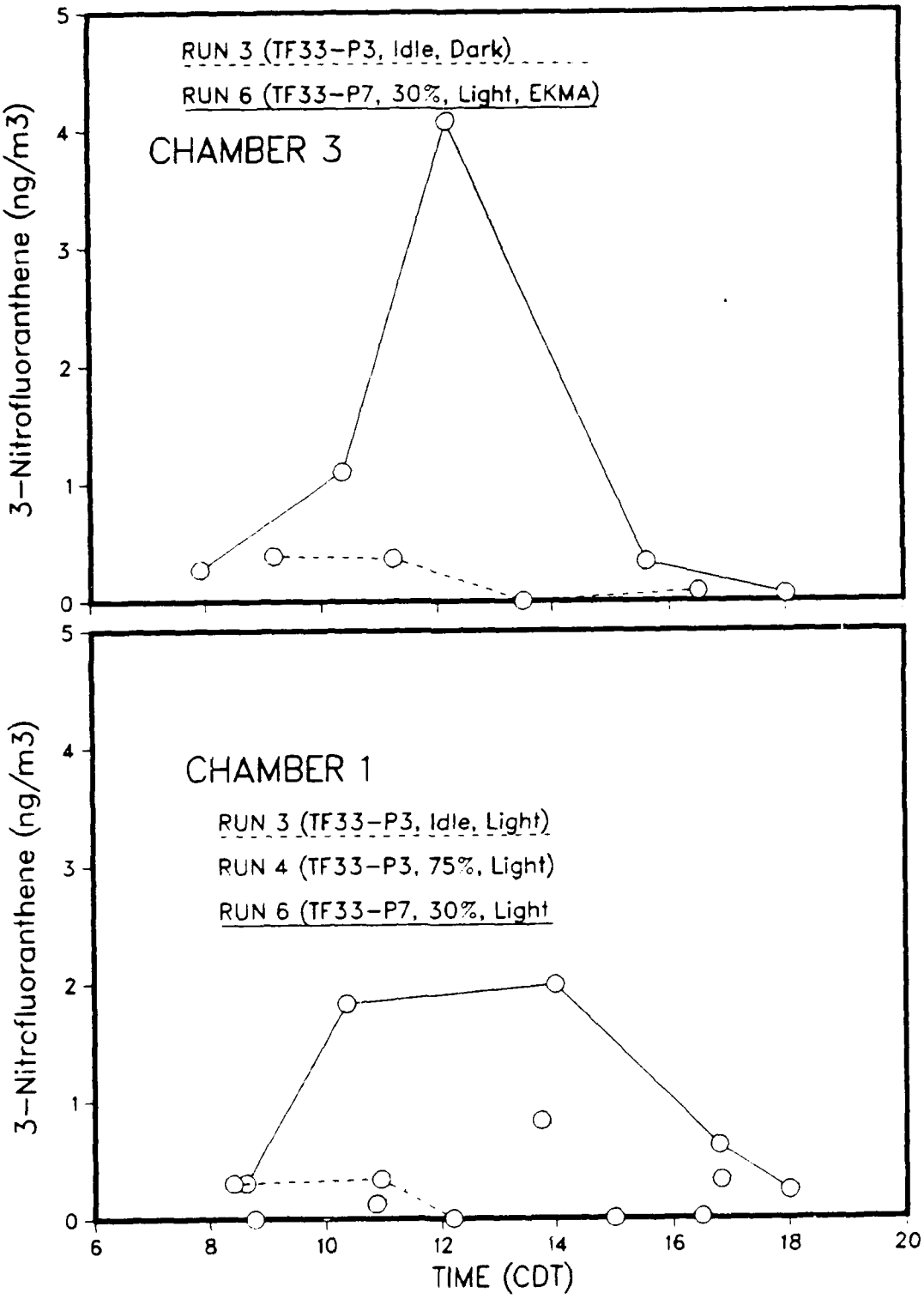


Figure 31. Concentration Profile of 3-Nitrofluoranthene for Selected Runs

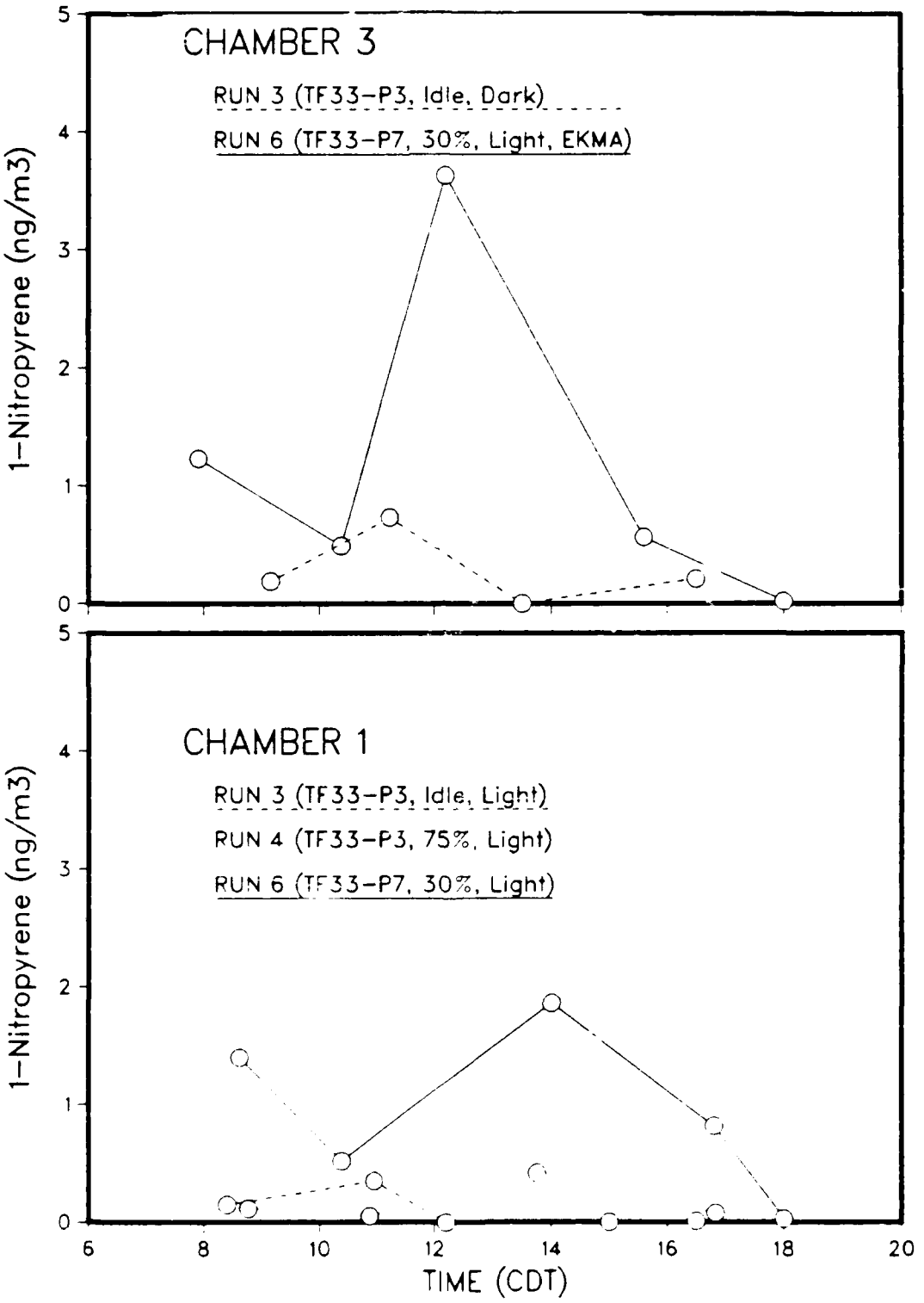


Figure 32. Concentration Profile of 1-Nitropyrene for Selected Runs

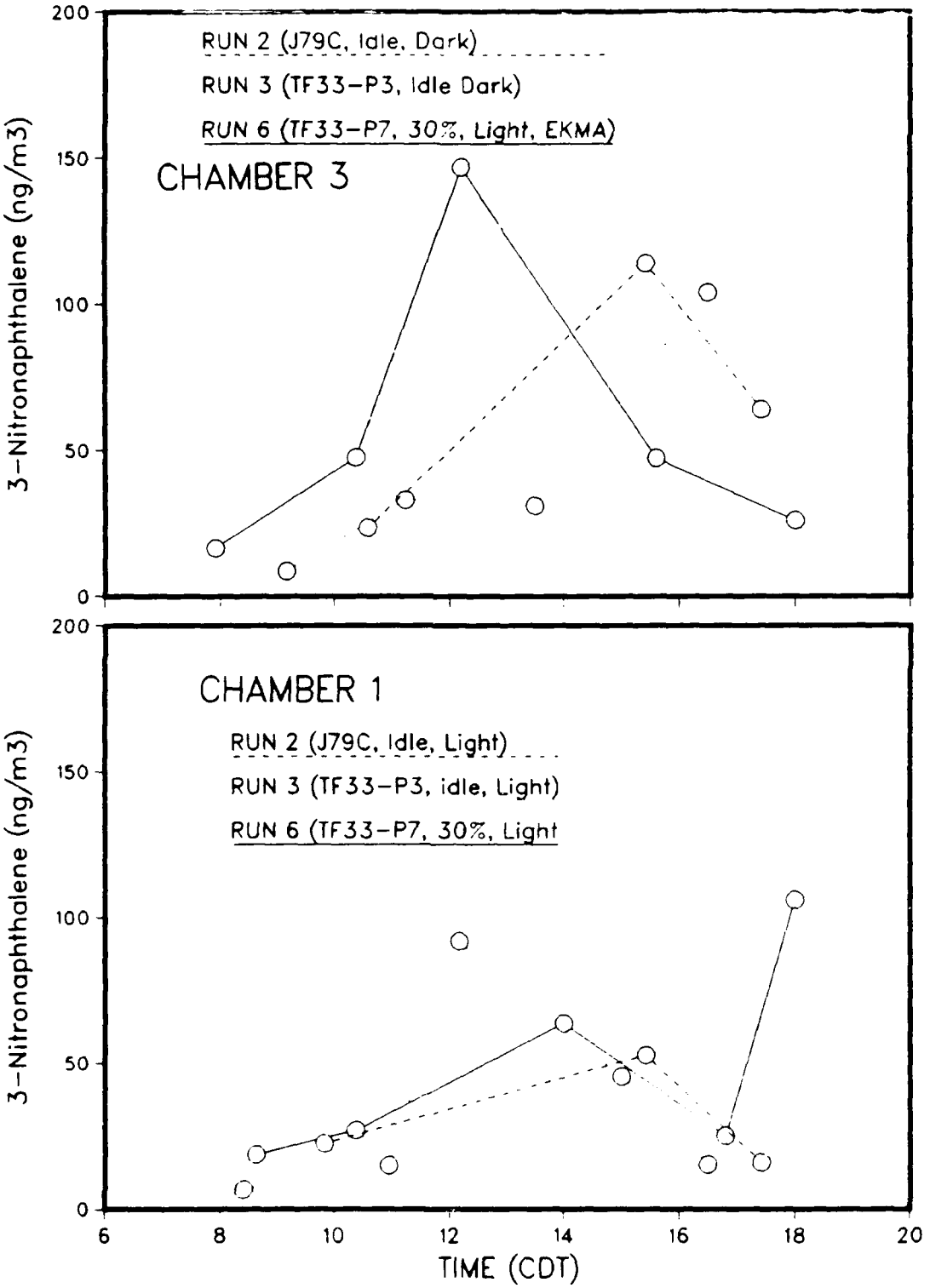


Figure 33. Concentration Profile of 1-Nitronaphthalene for Selected Runs

TABLE 12. FRACTION OF SELECTED $NO_2$-PAH COMPOUNDS FOUND IN VAPOR PHASE AT THE BEGINNING AND END OF AGING EXPERIMENTS

| Compound | Run 3, Ch 1 | | Run 3, Ch 3 | | Run 4, Ch 3 | | Run 6, Ch 1 | | Run 6, Ch 3 | |
|---|---|---|---|---|---|---|---|---|---|---|
| | Initial | Final | Initital | Final | Initial | Final | Initial | Final | Initial | Final |
| 2-Nitro-1-naphthol | 0.94 | 0.98 | 0.94 | 0.99 | 0.99 | 0.99 | 0.91 | 1.0 | 0.91 | 1.0 |
| 4-Hydroxy-3-nitrobiphenyl | 0.69 | 0.86 | 0.69 | 0.91 | 0.82 | 0.89 | 0.49 | 0.99 | 0.49 | 0.96 |
| 1-Nitronaphthalene | 0.70 | 0.98 | 0.70 | 0.98 | 0.86 | 0.97 | 0.80 | 1.0 | 0.80 | 0.99 |

were found on the XAD-2 sample (and were therefore present in the vapor phase) at the beginning and at the end of the runs. It is clear from these values that the $NO_2$-PAH compounds listed here are principally in the vapor state at the start of each run and completely so at the end.

The behavior of the remaining target $NO_2$-PAH compounds is not easily summarized, and the interested reader is referred to Appendix A for the tabulation of the data obtained.

To summarize the $NO_2$-PAH data, several comments can be made. In most instances, the relative concentrations of the major $NO_2$-PAH compounds measured do not vary by more than approximately a factor of five in the initial conditions for the chamber. The fact that some of these compounds are observed to form in the chambers while others do not changes their relative abundance. None of these compounds measured is stable through the course of the experiments, and the presence of sunlight increases the rate of decay of several of the compounds. In a number of cases, certain compounds' final and initial concentrations in the chamber were nearly the same, but when this occurred, it was due to formation and decay of the compound during the run.

# SECTION V

# CONCLUSIONS

The effects of engine type, power setting, sunlight, and photochemical activity of the atmosphere have been investigated in this study through use of matched reaction chambers which received injections of jet engine exhaust. Several conclusions can be drawn from the measurements made of the engine exhaust samples and from the measurements performed on the chambers as the exhaust containing atmosphere within them aged.

The following conclusions are based upon the measurements of the engine exhaust:

- The inorganic components of the exhaust particulate emissions are negligible under all conditions examined.
- The THC content of the exhaust decreases as engine operating power increases, such that at 75 percent power, the exhaust THC approximates the background air concentration.
- The $NO_x$ concentration and $NO:NO_x$ ratio increase with increasing power in a similar fashion for all three engines.
- Most PAH in the engine exhaust track the concentration of THC. As exceptions, the fluoranthene and pyrene persist in the TF33 exhaust at 30 percent power.
- The $NO_2$-PAH exhaust concentrations track the emitted THC less well, due to the role of $NO_2$ in their formation. Many of these compounds are present in the 30 percent exhaust at their greatest concentration.
- The exhaust from the engine operated at 75 percent power contains so little hydrocarbon it is probably not worth examining in future studies of this sort.

The following conclusions pertain to the operational aspects of this study:

- The portable smog chambers designed and constructed for this study served their function well in all respects.

- The low concentration of many of the compounds of interest in the exhaust requires that large sample volumes be handled. Any future studies of this sort should include sampling equipment capable of drawing larger flow rates (e.g., 1 $m^3$/min). This is especially true when sampling the exhaust at higher power settings.

The photochemical aging of the exhaust provided data from which the following conclusions can be drawn:

- Biologically active PAH are found at low levels in the exhaust from the TF33 engines at idle. Under all other conditions these compounds are at or below detection limits in the samples collected. No formation of these compounds was observed in the aging experiments.

- Biologically active $NO_2$-PAH compounds are found at low levels in each of the exhaust samples collected. Formation of two of these compounds was observed during the aging experiments.

- The PAH and $NO_2$-PAH measured are principally found in the vapor state.

- PAH are observed to decay under all conditions examined, the rate of decay being greater in sunlight than in the dark. No consistent PAH formation was observed.

- Several $NO_2$-PAH compounds were observed to form during the mid-day portion of the tests, especially in photochemically reactive atmospheres.

- For initial conditions of high THC:$NO_x$ ratio, such as idle exhaust injected into chambers, very rapid conversion of NO appears to have taken place in the chambers, without subsequent $O_3$ accumulation.

## REFERENCES


1. Petersen, B. A. and Chuang, J. C., "Methodology of Fractionation and Partition of Diesel Exhaust Particulate Sample" in Toxicological Effects of Emissions from Diesel Emissions, Joellen Lewtas (Editor), Elsevier Science Publishing Company, Inc., p 51-67, 1982.

2. Nishioka, M. G., Chuang, J. C., and Contos, D. A., "Screening, Identification, and Quantification of Mutagens and Potential Carcinogens in Ambient Air and Source Emissions," Final Report for the U.S. Environmental Protection Agency, EPA Contract No. 68-02-3169, 1984.

3. Chuang, J. C., Nishioka, M. G., and Petersen, B. A., "Fractionation and Analysis of Particulate Organic Matter from Ambient Air Samples," Final Report for the U.S. Environmental Protection Agency, Contract No. 68-02-3169, 1983.

4. Nishioka, M., Strup, P., Chuang, J. C., and Cooke, M., "Fractionation and Chemical Analysis of Wood Stove Samples," Final Report for the U.S. Environmental Protection Agency, Contract No. 68-02-2686, 1982.

5. Spicer, C. W., Holdren, M. W., Miller, S. E., Smith, D. L., Smith, R. N., and Hughes, D. P., "Aircraft Emissions Characterization: TF33-P3, TF33-P7, and J79 (Smokeless) Engines," Report ESL-TR-87-63, Tyndall AFB, Florida, March, 1988.




(The reverse of this page is blank.)

# APPENDIX A

## CONCENTRATIONS OF PAH AND $NO_2$-PAH COMPOUNDS MEASURED DURING EXHAUST AGING EXPERIMENTS

TABLE A-1. CONCENTRATIONS OF TARGET PAH COMPOUNDS ($\mu g/m^3$) MEASURED IN CHAMBERS 1 AND 3 AT INDICATED TIMES DURING RUN 1

J79 (30% power) CHAMBER #1

| | Sampling Time (CDT) | | | |
|---|---|---|---|---|
| Compound Name | 8.68 | 9.25 | 11.43 | 17.50 |
| Naphthalene | 6.06 | * | 6.30 | 16.7 |
| Acenaphthylene | .0824 | * | .0869 | .0051 |
| Dibenzothiophene | .0141 | * | .0435 | .0063 |
| Phenanthrene | .0963 | * | .348 | .0859 |
| Anthracene | .0046 | * | .217 | .0042 |
| Fluoranthene | .0219 | * | .174 | .0251 |
| Pyrene | .0173 | * | .0869 | .0136 |
| Benz[a]anthracene | <.0013 | * | <.0217 | <.0028 |
| Chrysene | <.0018 | * | <.0217 | .0059 |
| Cyclopenta[c,d]pyrene | <.0012 | * | 0 | <.0026 |
| Benzofluoranthenes | <.0013 | * | <.0217 | <.0028 |
| Benzo[e]pyrene | <.0013 | * | <.0217 | <.0028 |
| Benzo[a]pyrene | <.0001 | * | <.0217 | 0 |
| Indeno[1,2,3,-c,d]pyrene | 0 | * | <.0217 | 0 |
| Benzo[g,h,i,]perylene | 0 | * | 0 | 0 |
| Dibenzo[a,h]anthracene | 0 | * | 0 | 0 |

J79 (30% power) CHAMBER #3

| | | | | |
|---|---|---|---|---|
| Naphthalene | * | 8.62 | 9.26 | 8.00 |
| Acenaphthylene | * | .0900 | .113 | .0853 |
| Dibenzothiophene | * | .0153 | .0451 | .0117 |
| Phenanthrene | * | .105 | .406 | .1346 |
| Anthracene | * | .0050 | .0451 | .0067 |
| Fluoranthene | * | .0240 | .181 | .0277 |
| Pyrene | * | .0189 | .0903 | .0165 |
| Benz[a]anthracene | * | <.0015 | <.0226 | <.0029 |
| Chrysene | * | <.0017 | <.0226 | .0034 |
| Cyclopenta[c,d]pyrene | * | <.0013 | 0 | <.0027 |
| Benzofluoranthenes | * | <.0015 | <.0226 | <.0029 |
| Benzo[e]pyrene | * | <.0015 | <.0226 | <.0029 |
| Benzo[a]pyrene | * | <.0001 | <.0226 | 0 |
| Indeno[1,2,3,-c,d]pyrene | * | 0 | <.0226 | 0 |
| Benzo[g,h,i,]perylene | * | 0 | 0 | 0 |
| Dibenzo[a,h]anthracene | * | 0 | 0 | 0 |

* There is no data associated with this time.
0 There was no mass detected for this compound; therefore, the concentation is considered zero.

TABLE A-2. CONCENTRATIONS OF TARGET PAH COMPOUNDS ($\mu g/m^3$) MEASURED IN CHAMBERS 1 AND 3 AT INDICATED TIMES DURING RUN 2

J79 (idle) CHAMBER #1

| | Sampling Time (CDT) | | | |
|---|---|---|---|---|
| Compound Name | 9.83 | 10.58 | 15.42 | 17.42 |
| Naphthalene | 123 | * | 29.5 | 28.1 |
| Acenaphthylene | 4.94 | * | .199 | .128 |
| Dibenzothiophene | .477 | * | .0347 | .0072 |
| Phenanthrene | 1.73 | * | .711 | .182 |
| Anthracene | .152 | * | .0087 | .0029 |
| Fluoranthene | .333 | * | .0607 | .0216 |
| Pyrene | .289 | * | .0433 | .0120 |
| Benz[a]anthracene | <.0064 | * | <.0087 | <.0022 |
| Chrysene | .0148 | * | <.0087 | <.0024 |
| Cyclopenta[c,d]pyrene | <.0027 | * | <.0087 | <.0022 |
| Benzofluoranthenes | <.0072 | * | <.0087 | <.0022 |
| Benzo[e]pyrene | <.0045 | * | <.0087 | <.0022 |
| Benzo[a]pyrene | .0011 | * | 0 | 0 |
| Indeno[1,2,3,-c,d]pyrene | .0020 | * | 0 | 0 |
| Benzo[g,h,i,]perylene | .0052 | * | 0 | 0 |
| Dibenzo[a,h]anthracene | 0 | * | 0 | 0 |

J79 (idle) CHAMBER #3

| | | | | |
|---|---|---|---|---|
| Naphthalene | * | 128 | 3.29 | 44.2 |
| Acenaphthylene | * | 5.14 | 1.23 | .854 |
| Dibenzothiophene | * | .498 | .065 | .0163 |
| Phenanthrene | * | 1.80 | 0.81 | .413 |
| Anthracene | * | .159 | .0086 | .0065 |
| Fluoranthene | * | .347 | .106 | .0350 |
| Pyrene | * | .300 | .090 | .0217 |
| Benz[a]anthracene | * | <.0067 | <.0086 | <.0021 |
| Chrysene | * | .0154 | <.0086 | <.0025 |
| Cyclopenta[c,d]pyrene | * | <.0028 | <.0086 | <.0019 |
| Benzofluoranthenes | * | <.0074 | <.0086 | <.0019 |
| Benzo[e]pyrene | * | <.0047 | <.0086 | <.0019 |
| Benzo[a]pyrene | * | .0012 | 0 | 0 |
| Indeno[1,2,3,-c,d]pyrene | * | .0021 | 0 | 0 |
| Benzo[g,h,i,]perylene | * | .0054 | 0 | 0 |
| Dibenzo[a,h]anthracene | * | 0 | 0 | 0 |

* There is no data associated with this time.
0 There was no mass detected for this compound; therefore, the concentration is considered zero.

TABLE A-3. CONCENTRATIONS OF TARGET PAH COMPOUNDS ($\mu g/m^3$) MEASURED IN CHAMBERS 1 AND 3 AT INDICATED TIMES DURING RUN 3

TF33-3 (idle) CHAMBER #1

| | Sampling Time (CDT) | | | | | | | |
|---|---|---|---|---|---|---|---|---|
| Compound Name | 8.41 | 9.17 | 10.95 | 11.23 | 12.17 | 13.5 | 15.0 | 16.5 |
| Naphthalene | 409 | * | 188 | * | 178 | * | 173 | 111 |
| Acenaphthylene | 4.09 | * | 3.23 | * | 1.51 | * | 1.34 | .646 |
| Dibenzothiophene | .340 | * | .302 | * | .089 | * | .031 | .0151 |
| Phenanthrene | 3.40 | * | 6.82 | * | 3.29 | * | 2.35 | .729 |
| Anthracene | .390 | * | .114 | * | .027 | * | .0314 | .0079 |
| Fluoranthene | .419 | * | .255 | * | .151 | * | .141 | .0318 |
| Pyrene | .526 | * | <.182 | * | .110 | * | .0942 | .0196 |
| Benz[a]anthracene | .0724 | * | <.0163 | * | <.0137 | * | <.0157 | <.0039 |
| Chrysene | <.0885 | * | <.0184 | * | <.0137 | * | <.0157 | <.0042 |
| Cyclopenta[c,d]pyrene | <.0504 | * | .0013 | * | 0 | * | 0 | 0 |
| Benzofluoranthenes | <.1039 | * | .0039 | * | 0 | * | 0 | <.0039 |
| Benzo[e]pyrene | <.0441 | * | .0038 | * | 0 | * | 0 | <.0040 |
| Benzo[a]pyrene | .0378 | * | .0040 | * | 0 | * | 0 | .0004 |
| Indeno[1,2,3,-c,d]pyrene | .0567 | * | .0052 | * | 0 | * | 0 | <.0004 |
| Benzo[g,h,i,]perylene | .0787 | * | .0074 | * | 0 | * | 0 | <.0004 |
| Dibenzo[a,h]anthracene | .0019 | * | <.0013 | * | 0 | * | 0 | 0 |

TF33-3 (idle) CHAMBER #3

| | | | | | | | | |
|---|---|---|---|---|---|---|---|---|
| Naphthalene | * | 521 | * | 144 | * | 179 | * | 204 |
| Acenaphthylene | * | 5.21 | * | 4.38 | * | 3.19 | * | 1.66 |
| Dibenzothiophene | * | .433 | * | .104 | * | .0658 | * | .0862 |
| Phenanthrene | * | 4.32 | * | 2.50 | * | 2.44 | * | 1.85 |
| Anthracene | * | .497 | * | .0483 | * | .0282 | * | .0257 |
| Fluoranthene | * | .533 | * | .305 | * | .188 | * | .382 |
| Pyrene | * | .669 | * | .188 | * | .0846 | * | .218 |
| Benz[a]anthracene | * | .0921 | * | <.0119 | * | <.0094 | * | .0106 |
| Chrysene | * | .112 | * | <.0195 | * | .0094 | * | .0198 |
| Cyclopenta[c,d]pyrene | * | <.0641 | * | <.0159 | * | <.0094 | * | <.0042 |
| Benzofluoranthenes | * | <.130 | * | .0078 | * | 0 | * | <.0076 |
| Benzo[e]pyrene | * | <.0560 | * | .0048 | * | 0 | * | <.0053 |
| Benzo[a]pyrene | * | .0481 | * | .0034 | * | 0 | * | .0038 |
| Indeno[1,2,3,-c,d]pyrene | * | .0721 | * | .0127 | * | 0 | * | .0038 |
| Benzo[g,h,i,]perylene | * | .100 | * | .0093 | * | 0 | * | .0028 |
| Dibenzo[a,h]anthracene | * | .0024 | * | .0102 | * | 0 | * | .0042 |

* There is no data associated with this time.
0 There was no mass detected for this compound; therefore, the concentration is considered zero.

TABLE A-4. CONCENTRATIONS OF TARGET PAH COMPOUNDS ($\mu g/m^3$) MEASURED IN CHAMBERS 1 AND 3 AT INDICATED TIMES DURING RUN 4

TF33-3 (75% power) CHAMBER #1

| | Sampling Time (CDT) | | | | | | |
|---|---|---|---|---|---|---|---|
| Compound Name | 7.58 | 8.78 | 10.38 | 10.87 | 12.22 | 13.75 | 16.83 |
| Naphthalene | * | 2.25 | * | 7.08 | * | 14.8 | 10.1 |
| Acenaphthylene | * | .0823 | * | .103 | * | .235 | .180 |
| Dibenzothiophene | * | .0395 | * | .0387 | * | .0723 | .0099 |
| Phenanthrene | * | .634 | * | .529 | * | .795 | .334 |
| Anthracene | * | .0370 | * | .0220 | * | <.0181 | .0137 |
| Fluoranthene | * | .103 | * | .103 | * | .0903 | .0350 |
| Pyrene | * | .103 | * | .0808 | * | .0542 | .0197 |
| Benz[a]anthracene | * | <.0045 | * | .0147 | * | <.018 | <.0022 |
| Chrysene | * | <.0052 | * | .0294 | * | <.0181 | .0064 |
| Cyclopenta[c,d]pyrene | * | <.0041 | * | 0 | * | 0 | 0 |
| Benzofluoranthenes | * | <.0045 | * | .0387 | * | <.0181 | 0 |
| Benzo[e]pyrene | * | <.0045 | * | .0387 | * | <.0181 | 0 |
| Benzo[a]pyrene | * | <.0004 | * | .0441 | * | <.0181 | 0 |
| Indeno[1,2,3,-c,d]pyrene | * | 0 | * | .0294 | * | <.0181 | 0 |
| Benzo[g,h,i,]perylene | * | <.0004 | * | .0387 | * | <.0181 | 0 |
| Dibenzo[a,h]anthracene | * | 0 | * | .0588 | * | .0181 | 0 |

TF33-3 (30% power) CHAMBER #3

| | | | | | | | |
|---|---|---|---|---|---|---|---|
| Naphthalene | 21.5 | * | 12.9 | * | 11.0 | 12.0 | 5.67 |
| Acenaphthylene | 0.746 | * | .0819 | * | 0 | 0 | .0957 |
| Dibenzothiophene | .149 | * | .0585 | * | .0390 | .0417 | .0085 |
| Phenanthrene | 1.19 | * | 1.18 | * | 1.03 | .723 | .151 |
| Anthracene | .0497 | * | <.0117 | * | <.0130 | .0139 | .0075 |
| Fluoranthene | .271 | * | .105 | * | .0779 | .0974 | .0241 |
| Pyrene | .342 | * | .0468 | * | .0280 | .0417 | .0102 |
| Benz[a]anthracene | <.0191 | * | <.0117 | * | <.0130 | <.0139 | <.0010 |
| Chrysene | <.0284 | * | .0117 | * | <.0130 | <.0139 | .0019 |
| Cyclopenta[c,d]pyrene | .0552 | * | 0 | * | 0 | 0 | 0 |
| Benzofluoranthenes | <.0293 | * | .0117 | * | <.0130 | <.0139 | 0 |
| Benzo[e]pyrene | <.0138 | * | <.0117 | * | <.0130 | <.0139 | 0 |
| Benzo[a]pyrene | .0099 | * | <.0117 | * | <.0130 | <.0139 | 0 |
| Indeno[1,2,3,-c,d]pyrene | .0055 | * | <.0117 | * | <.0130 | <.0139 | 0 |
| Benzo[g,h,i,]perylene | .0122 | * | <.0117 | * | <.0130 | 0 | 0 |
| Dibenzo[a,h]anthracene | <.0003 | * | <.0117 | * | <.0130 | 0139 | 0 |

* There is no data associated with this time.
0 There was no mass detected for this compound; therefore, the concentration is considered zero.

TABLE A-5. CONCENTRATIONS OF TARGET PAH COMPOUNDS ($\mu g/m^3$) MEASURED IN CHAMBERS 1 AND 3 AT INDICATED TIMES DURING RUN 5

TF33-7 (30% power) CHAMBER #1

| | Sampling Time (CDT) | | | | | | | |
|---|---|---|---|---|---|---|---|---|
| Compound Name | 8.00 | 8.80 | 10.85 | 11.05 | 12.92 | 14.08 | 15.33 | 17.20 |
| Naphthalene | * | 10.2 | * | 21.5 | * | 13.5 | 10.7 | 4.47 |
| Acenaphthylene | * | .602 | * | .485 | * | .158 | .0451 | .216 |
| Dibenzothiophene | * | .145 | * | .121 | * | .129 | .135 | .0237 |
| Phenanthrene | * | 1.46 | * | 2.29 | * | .716 | .542 | .157 |
| Anthracene | * | .112 | * | .0135 | * | .100 | .0150 | .0184 |
| Fluoranthene | * | .500 | * | .188 | * | .143 | .135 | .0276 |
| Pyrene | * | .602 | * | .135 | * | .0716 | .0752 | .0130 |
| Benz[a]anthracene | * | <.0412 | * | <.0135 | * | .0143 | <.0150 | <.0106 |
| Chrysene | * | .0602 | * | .0269 | * | .0143 | <.0150 | <.0137 |
| Cyclopenta[c,d]pyrene | * | .0430 | * | 0 | * | 0 | 0 | .0054 |
| Benzofluoranthenes | * | <.0384 | * | <.0135 | * | .0287 | <.0150 | <.0047 |
| Benzo[e]pyrene | * | <.0171 | * | <.0135 | * | .0287 | <.0150 | <.0054 |
| Benzo[a]pyrene | * | <.0194 | * | <.0135 | * | <.0143 | 0 | <.0019 |
| Indeno[1,2,3,-c,d]pyrene | * | <.0092 | * | <.0135 | * | .0430 | <.0104 | <.0045 |
| Benzo[g,h,i,]perylene | * | .0102 | * | 0 | * | .0430 | 0 | .0019 |
| Dibenzo[a,h]anthracene | * | .0112 | * | <.0135 | * | .0573 | <.0301 | <.0118 |

TF33-7 (idle) CHAMBER #3

| | | | | | | | | |
|---|---|---|---|---|---|---|---|---|
| Naphthalene | 629 | * | 509 | * | 378 | * | 441 | 189 |
| Acenaphthylene | 44.9 | * | 2.30 | * | 1.08 | * | .943 | 7.45 |
| Dibenzothiophene | .390 | * | .364 | * | .162 | * | .152 | .0142 |
| Phenanthrene | 8.22 | * | 9.58 | * | 5.26 | * | 4.26 | 1.06 |
| Anthracene | 1.02 | * | .255 | * | .135 | * | .213 | .0043 |
| Fluoranthene | .463 | * | .352 | * | .243 | * | .213 | .0328 |
| Pyrene | .481 | * | .206 | * | .135 | * | .122 | .0185 |
| Benz[a]anthracene | <.0220 | * | .0121 | * | .0135 | * | .0152 | <.0041 |
| Chrysene | <.0310 | * | .170 | * | .0270 | * | .0304 | <.0042 |
| Cyclopenta[c,d]pyrene | <.0391 | * | 0 | * | 0 | * | 0 | <.0034 |
| Benzofluoranthenes | <.130 | * | <.0121 | * | <.0135 | * | <.0152 | 0 |
| Benzo[e]pyrene | <.0584 | * | 0 | * | <.0135 | * | <.0152 | 0 |
| Benzo[a]pyrene | .0584 | * | <.0121 | * | .0135 | * | <.0152 | 0 |
| Indeno[1,2,3,-c,d]pyrene | .103 | * | <.0121 | * | .0270 | * | <.0152 | 0 |
| Benzo[g,h,i,]perylene | .157 | * | 0 | * | .0270 | * | 0 | 0 |
| Dibenzo[a,h]anthracene | .0090 | * | .0485 | * | .0539 | * | .0456 | 0 |

* There is no data associated with this time.
0 There was no mass detected for this compound; therefore, the concentration is considered zero.

TABLE A-6. CONCENTRATIONS OF TARGET PAH COMPOUNDS ($\mu g/m^3$) MEASURED IN CHAMBERS 1 AND 3 AT INDICATED TIMES DURING RUN 6

TF33-7 (30% power) CHAMBER #1

| | Sampling Time (CDT) | | | | | | | | |
|---|---|---|---|---|---|---|---|---|---|
| Compound Name | 7.92 | 8.63 | 10.38 | 12.2 | 12.2 | 14.0 | 15.6 | 16.8 | 18.0 |
| Naphthalene | * | 26.6 | 19.7 | * | * | 8.24 | * | 5.34 | 3.85 |
| Acenaphthylene | * | 1.03 | .234 | * | * | .108 | * | .0741 | .0545 |
| Dibenzothiophene | * | .0997 | .0739 | * | * | .0266 | * | .0297 | .0140 |
| Phenanthrene | * | 2.56 | 1.11 | * | * | .903 | * | .549 | .146 |
| Anthracene | * | .0484 | .0370 | * | * | .0266 | * | .0148 | .0047 |
| Fluoranthrene | * | .458 | .136 | * | * | .159 | * | .104 | .0302 |
| Pyrene | * | .476 | .0863 | * | * | .0930 | * | .0593 | .0154 |
| Benz[a]anthracene | * | <.0247 | <.0123 | * | * | <.0133 | * | <.0148 | <.0038 |
| Chrysene | * | .0347 | .0123 | * | * | <.0133 | * | <.0148 | .0039 |
| Cyclopenta[c,d]pyrene | * | <.0406 | 0 | * | * | 0 | * | 0 | <.0035 |
| Benzofluoranthrenes | * | <.0343 | 0 | * | * | 0 | * | 0 | <.0039 |
| Benzo[e]pyrene | * | <.0159 | 0 | * | * | 0 | * | 0 | <.0038 |
| Benzo[a]pyrene | * | .0111 | 0 | * | * | 0 | * | 0 | <.0003 |
| Indeno[1,2,3-c,d]pyrene | * | .0148 | 0 | * | * | 0 | * | 0 | 0 |
| Benzo[g,h,i]perylene | * | .0166 | 0 | * | * | 0 | * | 0 | 0 |
| Dibenzo[a,h]anthracene | * | .0066 | 0 | * | * | 0 | * | 0 | 0 |

TF33-7 (30% power) CHAMBER #3

| | | | | | | | | | |
|---|---|---|---|---|---|---|---|---|---|
| Naphthalene | 23.3 | * | 23.8 | 23.8 | 27.7 | 13.7 | 9.65 | * | 9.69 |
| Acenaphthylene | 0.908 | * | .132 | .235 | .0932 | .0762 | .0701 | * | .0271 |
| Dibenzothiophene | .0875 | * | .0528 | .118 | .124 | .0305 | .0175 | * | .0084 |
| Phenanthrene | 2.25 | * | 2.24 | 4.11 | 3.11 | 1.05 | .474 | * | .164 |
| Anthracene | .0425 | * | .0264 | .0588 | .0821 | .0305 | .0175 | * | .0053 |
| Fluoranthene | .402 | * | .159 | .793 | .311 | .152 | .0701 | * | .0298 |
| Pyrene | .418 | * | .0924 | .969 | .156 | .0914 | .0351 | * | .0159 |
| Benz[a]anthracene | <.0217 | * | <.0132 | <.0294 | <.0311 | <.0152 | <.0175 | * | <.0043 |
| Chrysene | .0305 | * | <.0132 | <.0294 | <.0311 | <.0152 | <.0175 | * | <.0048 |
| Cyclopenta[c,d]pyrene | <.0357 | * | 0 | 0 | 0 | 0 | 0 | * | <.0043 |
| Benzofluoranthenes | <.0301 | * | 0 | 0 | 0 | 0 | 0 | * | <.0048 |
| Benzo[e]pyrene | <.0139 | * | 0 | 0 | 0 | 0 | 0 | * | <.0039 |
| Benzo[a]pyrene | .0097 | * | 0 | 0 | 0 | 0 | 0 | * | 0 |
| Indeno[1,2,3-c,d]pyrene | .0130 | * | 0 | 0 | 0 | 0 | 0 | * | 0 |
| Benzo[g,h,i]perylene | .0146 | * | 0 | 0 | 0 | 0 | 0 | * | 0 |
| Dibenzo[a,h]anthracene | .0058 | * | 0 | 0 | 0 | 0 | 0 | * | 0 |

* There is no data associated with this time.
0 There was no mass detected for this compound; therefore, the concentration is considered zero.

TABLE A-7. CONCENTRATIONS OF TARGET $NO_2$-PAH COMPOUNDS ($ng/m^3$) MEASURED IN CHAMBERS 1 AND 3 AT INDICATED TIMES DURING RUN 1

J79 (30% power) CHAMBER #1

| | Sampling Time (CDT) | | | |
|---|---|---|---|---|
| COMPOUND NAME | 8.68 | 9.25 | 11.43 | 17.5 |
| 2-Nitro-1-naphthol | 438 | * | * | 48.9 |
| 4-Hydroxy-3-nitrobiphenyl | 30.1 | * | * | 43.7 |
| 1-Nitronaphthalene | 6.77 | * | * | 20.3 |
| Nitronaphthalene isomer | 7.78 | * | * | 14.9 |
| 9-Nitroanthracene | .552 | * | * | .587 |
| 9-Nitrophenanthrene | .131 | * | * | .195 |
| Nitroanthracene/phenanthrene | .0812 | * | * | .144 |
| 3-Nitrofluoranthene | 0 | * | * | .0462 |
| 1-Nitropyrene | .0861 | * | * | .123 |
| 6-Nitrochrysene | .0267 | * | * | .0128 |
| Di-Nitropyrene isomer | 0 | * | * | 0 |

J79 (30% POWER) CHAMBER #3

| | | | | |
|---|---|---|---|---|
| 2-Nitro-1-naphthol | * | 478 | * | 179 |
| 4-Hydroxy-3-nitrobiphenyl | * | 32.9 | * | 5.65 |
| 1-Nitronaphthalene | * | 7.39 | * | 8.82 |
| Nitronaphthalene isomer | * | 8.50 | * | 5.07 |
| 9-Nitroanthracene | * | .802 | * | .781 |
| 9-Nitrophenanthrene | * | .143 | * | .205 |
| Ni.anthracene/phenanthrene | * | .0886 | * | .117 |
| 3-Nitrofluoranthrene | * | 0 | * | .0245 |
| 1-Nitropyrene | * | .0940 | * | .0560 |
| 6-Nitrochrysene | * | .0290 | * | .0053 |
| Di-Nitropyrene isomer | * | 0 | * | 0 |

* There is no data associated with this time.
0 There was no mass detected for this compound; therefore, the concentration is considered zero.

TABLE A-8. CONCENTRATIONS OF TARGET $NO_2$-PAH COMPOUNDS ($ng/m^3$) MEASURED IN CHAMBERS 1 AND 3 AT INDICATED TIMES DURING RUN 2

J79 (idle) CHAMBER #1

| | Sampling Time (CDT) | | | |
|---|---|---|---|---|
| COMPOUND NAME | 9.83 | 10.58 | 15.42 | 17.42 |
| 2-Nitro-1-naphthol | 2506 | * | 511 | 142 |
| 4-Hydroxy-3-nitrobiphenyl | 9.75 | * | 9.54 | 1.86 |
| 1-Nitronaphthalene | 22.6 | * | 52.9 | 16.1 |
| Nitronaphthalene isomer | 17.8 | * | 65.0 | 17.8 |
| 9-Nitroanthracene | 1.53 | * | .494 | .292 |
| 9-Nitrophenanthrene | .568 | * | 0 | .186 |
| Nitroanthracene/phenanthrene | .568 | * | 0 | .117 |
| 3-Nitrofluoranthene | .130 | * | 0 | .0145 |
| 1-Nitropyrene | .691 | * | 0 | .0041 |
| 6-Nitrochrysene | .0718 | * | 0 | 0 |
| Di-Nitropyrene isomer | 0 | * | 0 | 0 |

J79 (idle) CHAMBER #3

| | | | | |
|---|---|---|---|---|
| 2-Nitro-1-naphthol | * | 2606 | 1062 | 886 |
| 4-Hydroxy-3-nitrobiphenyl | * | 10.1 | 29.4 | 9.68 |
| 1-Nitronaphthalene | * | 23.5 | 114 | 63.9 |
| Nitronaphthalene isomer | * | 18.5 | 106 | 50.2 |
| 9-Nitroanthracene | * | 1.59 | 1.55 | .827 |
| 9-Nitrophenanthrene | * | .591 | .547 | .273 |
| Ni.anthracene/phenanthrene | * | .591 | .106 | .171 |
| 3-Nitrofluoranthrene | * | .131 | 0 | .0348 |
| 1-Nitropyrene | * | .719 | 0 | .0366 |
| 6-Nitrochrysene | * | .0745 | 0 | 0 |
| Di-Nitropyrene isomer | * | 0 | 0 | 0 |

* There is no data associated with this time.
0 There was no mass detected for this compound; therefore, the concentration is considered zero.

TABLE A-9. CONCENTRATIONS OF TARGET $NO_2$-PAH COMPOUNDS ($ng/m^3$) MEASURED IN CHAMBERS 1 AND 3 AT INDICATED TIMES DURING RUN 3

TF33-3 (idle) CHAMBER #1

| | Sampling Time (CDT) | | | | | | | |
|---|---|---|---|---|---|---|---|---|
| COMPOUND NAME | 8.41 | 9.17 | 10.95 | 11.23 | 12.17 | 13.5 | 15.0 | 16.5 |
| 2-Nitro-1-naphthol | 2052 | * | 992 | * | 878 | * | 581 | 78.7 |
| 4-Hydroxy-3-nitrobiphenyl | 17.0 | * | 4.82 | * | 23.3 | * | 22.0 | 1.46 |
| 1-Nitronaphthalene | 6.77 | * | 15.0 | * | 91.9 | * | 45.5 | 15.4 |
| Nitronaphthalene isomer | 12.9 | * | 18.0 | * | 32.9 | * | 29.8 | 13.0 |
| 9-Nitroanthracene | 1.10 | * | 2.68 | * | .933 | * | 1.11 | .530 |
| 9-Nitrophenanthrene | .586 | * | 1.58 | * | .357 | * | .330 | .456 |
| Nitroanthracene/phenanthrene | .469 | * | .563 | * | 0 | * | 0 | .276 |
| 3-Nitrofluoranthene | .302 | * | .335 | * | 0 | * | 0 | .0118 |
| 1-Nitropyrene | .148 | * | .348 | * | 0 | * | 0 | .0083 |
| 6-Nitrochrysene | 0 | * | 0 | * | 0 | * | 0 | 0 |
| Di-Nitropyrene isomer | 0 | * | 0 | * | 0 | * | 0 | 0 |

TF33-3 (idle) CHAMBER #3

| | | | | | | | | |
|---|---|---|---|---|---|---|---|---|
| 2-Nitro-1-naphthol | * | 2607 | * | 1457 | * | 207 | * | 420 |
| 4-Hydroxy-3-nitrobiphenyl | * | 21.6 | * | 15.8 | * | 4.51 | * | 4.16 |
| 1-Nitronaphthalene | * | 8.60 | * | 33.0 | * | 31.0 | * | 104 |
| Nitronaphthalene isomer | * | 16.4 | * | 23.4 | * | 43.2 | * | 92.7 |
| 9-Nitroanthracene | * | 1.40 | * | 3.81 | * | .893 | * | 3.17 |
| 9-Nitrophenanthrene | * | .744 | * | 2.08 | * | .460 | * | 2.11 |
| Ni.anthracene/phenanthrene | * | .596 | * | 1.24 | * | .0584 | * | .975 |
| 3-Nitrofluoranthrene | * | .384 | * | .364 | * | 0 | * | .0831 |
| 1-Nitropyrene | * | .188 | * | .729 | * | 0 | * | .208 |
| 6-Nitrochrysene | * | 0 | * | 0 | * | 0 | * | .0113 |
| Di-Nitropyrene isomer | * | 0 | * | 0 | * | 0 | * | 0 |

* There is no data associated with this time.
0 There was no mass detected for this compound; therefore, the concentration is considered zero.

TABLE A-10. CONCENTRATIONS OF TARGET $NO_2$-PAH COMPOUNDS ($ng/m^3$) MEASURED IN CHAMBERS 1 AND 3 AT INDICATED TIMES DURING RUN 4

TF33-3 (75% power) CHAMBER #1

| | Sampling Time (CDT) | | | | |
|---|---|---|---|---|---|
| COMPOUND NAME | 7.58 | 8.78 | 10.87 | 13.75 | 16.83 |
| 2-Nitro-1-naphthol | * | 230 | 323 | 434 | 528 |
| 4-Hydroxy-3-nitrobiphenyl | * | 15.2 | 9.55 | 19.9 | 5.64 |
| 1-Nitronaphthalene | * | 7.61 | 8.82 | 14.6 | 9.71 |
| Nitronaphthalene isomer | * | 4.81 | 7.35 | 7.59 | 9.21 |
| 9-Nitroanthracene | * | 2.80 | .713 | .9439 | .512 |
| 9-Nitrophenanthrene | * | .152 | .147 | .668 | .587 |
| Nitroanthracene/phenanthrene | * | .132 | .206 | .831 | .385 |
| 6-Nitrofluoranthene | * | 0 | .125 | .831 | .328 |
| 1-Nitropyrene | * | .115 | .0514 | .416 | .0788 |
| 6-Nitrochrysene | * | 0 | 0 | 0 | 0 |
| Di-Nitropyrene isomer | * | 0 | 0 | 0 | 0 |

TF33-3 (30% power) CHAMBER #3

| | | | | | |
|---|---|---|---|---|---|
| 2-Nitro-1-naphthol | 1757 | * | * | | 179 |
| 4-Hydroxy-3-nitrobiphenyl | 18.5 | * | * | | 2.55 |
| 1-Nitronaphthalene | 19.6 | * | * | | 16.4 |
| Nitronaphthalene isomer | 14.2 | * | * | | 18.6 |
| 9-Nitroanthracene | 22.9 | * | * | | .440 |
| 9-Nitrophenanthrene | .804 | * | * | | .344 |
| Ni.anthracene/phenanthrene | .511 | * | * | | .241 |
| 3-Nitrofluoranthrene | .635 | * | * | | .638 |
| 1-Nitropyrene | .218 | * | * | | .0220 |
| 6-Nitrochrysene | 0 | * | * | | 0 |
| Di-Nitropyrene isomer | 0 | * | * | | 0 |

* There is no data associated with this time.
0 There was no mass detected for this compound; therefore, the concentration is considered zero.

TABLE A-11. CONCENTRATIONS OF TARGET $NO_2$-PAH COMPOUNDS ($ng/m^3$) MEASURED IN CHAMBERS 1 AND 3 AT INDICATED TIMES DURING RUN 5

TF33-7 (30% power) CHAMBER #1

| | Sampling Time (CDT) | | |
|---|---|---|---|
| COMPOUND NAME | 8.0 | 8.80 | 17.2 |
| 2-Nitro-1-naphthol | * | 842 | 98.9 |
| 4-Hydroxy-3-nitrobiphenyl | * | 47.2 | 5.98 |
| 1-Nitronaphthalene | * | 18.7 | 138 |
| Nitronaphthalene isomer | * | 15.8 | 82.0 |
| 9-Nitroanthracene | * | 22.7 | .522 |
| 9-Nitrophenanthrene | * | 1.17 | .559 |
| Nitroanthracene/phenanthrene | * | .504 | .358 |
| 3-Nitrofluoranthene | * | .116 | 0 |
| 1-Nitropyrene | * | 1.71 | 0 |
| 6-Nitrochrysene | * | .190 | 0 |
| Di-Nitropyrene isomer | * | 0 | 0 |

TF33-7 (idle) CHAMBER #3

| | | | |
|---|---|---|---|
| 2-Nitro-1-naphthol | 2404 | * | 134 |
| 4-Hydroxy-3-nitrobiphenyl | 15.2 | * | 2.27 |
| 1-Nitronaphthalene | 7.91 | * | 29.6 |
| Nitronaphthalene isomer | 8.79 | * | 17.3 |
| 9-Nitroanthracene | 1.21 | * | .400 |
| 9-Nitrophenanthrene | .364 | * | .210 |
| Ni.anthracene/phenanthrene | .838 | * | .204 |
| 3-Nitrofluoranthrene | .144 | * | .0339 |
| 1-Nitropyrene | .234 | * | .0237 |
| 6-Nitrochrysene | .0584 | * | 0 |
| Di-Nitropyrene isomer | 0 | * | 0 |

* There is no data associated with this time.
0 There was no mass detected for this compound; therefore, the concentration is considered zero.

TABLE A-12. CONCENTRATIONS OF TARGET $NO_2$-PAH COMPOUNDS ($ng/m^3$) MEASURED IN CHAMBERS 1 AND 3 AT INDICATED TIMES DURING RUN 6

TF33-3 (30% power) CHAMBER #1

| | Sampling Time (CDT) | | | | | | | | |
|---|---|---|---|---|---|---|---|---|---|
| COMPOUND NAME | 7.92 | 8.63 | 10.38 | 12.2 | 12.2 | 14.0 | 15.6 | 16.8 | 18.0 |
| 2-Nitro-1-naphthol | * | 1219 | 505 | * | * | 531 | * | 90.5 | 61.0 |
| 4-Hydroxy-3-nitrobiphenyl | * | 23.2 | 35.7 | * | * | 51.8 | * | 13.2 | 9.37 |
| 1-Nitronaphthalene | * | 18.8 | 27.1 | * | * | 63.8 | * | 25.2 | 106 |
| Nitronaphthalene isomer | * | 13.9 | 30.8 | * | * | 97.0 | * | 44.5 | 70.6 |
| 9-Nitroanthracene | * | 40.3 | 3.08 | * | * | 2.39 | * | 1.07 | .295 |
| 9-Nitrophenanthrene | * | 4.17 | .981 | * | * | 1.40 | * | .311 | .221 |
| Nitroanthracene/phenanthrene | * | .776 | .579 | * | * | .452 | * | .341 | .257 |
| 3-Nitrofluoranthene | * | .307 | 1.83 | * | * | 1.99 | * | .623 | .237 |
| 1-Nitropyrene | * | 1.40 | .518 | * | * | 1.86 | * | .816 | .0305 |
| 6-Nitrochrysene | * | .111 | .370 | * | * | 1.59 | * | 0 | 0 |
| Di-Nitropyrene isomer | * | 0 | 0 | * | * | 0 | * | 0 | 0 |

TF33-7 (30% power + EKMA/NOX) CHAMBER #3

| | | | | | | | | |
|---|---|---|---|---|---|---|---|---|
| 2-Nitro-1-naphthol | 1070 | * | 964 | 2703 | 1274 | 153 | * | 77.7 |
| 4-Hydroxy-3-nitrobiphenyl | 20.4 | * | 68.0 | 267 | 121 | 12.1 | * | 6.04 |
| 1-Nitronaphthalene | 16.5 | * | 47.5 | 176 | 118 | 47.3 | * | 25.9 |
| Nitronaphthalene isomer | 12.2 | * | 35.7 | 167 | 99.4 | 49.1 | * | 19.4 |
| 9-Nitroanthracene | 35.3 | * | 13.2 | 11.2 | 11.5 | .614 | * | .519 |
| 9-Nitrophenanthrene | 3.66 | * | 3.17 | 3.82 | 3.42 | .737 | * | .333 |
| Ni.anthracene/phenanthrene | .681 | * | 1.19 | 1.85 | 1.24 | .684 | * | .190 |
| 3-Nitrofluoranthrene | .268 | * | 1.10 | 4.11 | 4.04 | .333 | * | .0581 |
| 1-Nitropyrene | 1.23 | * | .489 | 4.70 | 2.55 | .561 | * | .0244 |
| 6-Nitrochrysene | .0972 | * | .357 | 4.70 | 3.11 | 0 | * | 0 |
| Di-Nitropyrene isomer | 0 | * | 0 | 0 | 0 | 0 | * | 0 |

* There is no data associated with this time.
0 There was no mass detected for this compound; therefore, the concentrarion is considered zero.


(The reverse of this page is blank.)

# APPENDIX B

## TOTAL ION CHROMATOGRAMS AND IDENTIFICATION OF MAJOR PEAKS IN SILICA GEL FRACTIONS OF A SELECTED ENGINE EXHAUST SAMPLE (TF33-P7, IDLE EXHAUST)

TABLE B-1. THE MAJOR COMPONENTS TENTATIVELY IDENTIFIED IN THE ALIPHATIC FRACTION, SAMPLE CODE: X038

| Peak Number[a] | Scan Number | Tentatively Identified Compound Name |
|---|---|---|
| 1 | 242 | C1, benzene |
| 2 | 253 | C2, cyclohexane |
| 3 | 273 | Long chain alkane |
| 4 | 321 | C2, cyclohexane |
| 5 | 359 | Long chain alkane |
| 6 | 373 | C2, benzene |
| 7 | 411 | Long chain alkane + C2, benzene |
| 8 | 465 | Long chain alkane |
| 9 | 516 | Long chain alkane + C3, benzene |
| 10 | 528 | C3, benzene |
| 11 | 515 | C3, benzene + aliphatic alcohol |
| 12 | 614 | Long chain alkane |
| 13 | 623 | C3, benzene |
| 14 | 635 | C4, cyclohexane |
| 15 | 680 | Long chain alkane + C4, cyclohexane |
| 16 | 746 | Aliphatic alcohol |
| 17 | 789 | C4, benzene |
| 18 | 890 | Long chain alkane |
| 19 | 910 | Long chain alkane |
| 20 | 931 | Long chain alkane |
| 21 | 1022 | Long chain alkane |
| 22 | 1065 | Long chain alkane |
| 23 | 1211 | Long chain alkane |
| 24 | 1349 | Long chain alkane |
| 25 | 1480 | Long chain alkane |

(a) The total ion current chromatogram is presented in Figure B-1.

TABLE B-2. THE MAJOR COMPONENTS TENTATIVELY IDENTIFIED IN THE AROMATIC FRACTION, SAMPLE CODE: X038

| Peak Number[a] | Scan Number | Tentatively Identified Compound Name |
|---|---|---|
| 1 | 226 | Mixture |
| 2 | 253 | Hydroxybenzaldehyde |
| 3 | 262 | Benzeneacetaldehyde |
| 4 | 268 | Dihydrobenzofuran |
| 5 | 306 | Benzaldehyde |
| 6 | 317 | Ethenylbenzaldehyde |
| 7 | 322 | C4, benzene |
| 8 | 327 | Formylbenzonitrile |
| 9 | 334 | C2, benzaldehyde |
| 10 | 341 | C4, benzene |
| 11 | 375 | Aliphatic alcohol |
| 12 | 383 | C3, benzaldehyde |
| 13 | 389 | C1, benzeneacetic acid |
| 14 | 417 | C3, benzaldehyde |
| 15 | 468 | Biphenyl |
| 16 | 504 | C4, benzene |
| 17 | 595 | Naphthalenecarboxaldehyde |
| 18 | 648 | Fatty acid ester |
| 19 | 1610 | Phthalate |

(a) The total ion current chromatogram is presented in Figure B-2.

TABLE B-3. THE MAJOR COMPONENTS TENTATIVELY IDENTIFIED IN THE MODERATE POLAR FRACTION ($CH_2Cl_2$ FRACTION), SAMPLE CODE: X038

| Peak Number(a) | Scan Number | Tentatively Identified Compound Name |
|---|---|---|
| 1 | 205 | Cyclic alkene |
| 2 | 220 | Phenol |
| 3 | 248 | Benzenemethanol |
| 4 | 256 | C1, phenol |
| 5 | 295 | C2, phenol |
| 6 | 344 | Phenyl azetidine |
| 7 | 349 | Benzenedicarboxaldehyde |
| 8 | 386 | Dihydroindenone |
| 9 | 438 | Hydroxymethylbenzoic acid |
| 10 | 460 | Ethenylnaphthalene |
| 11 | 484 | Dihydronaphthalenone |
| 12 | 490 | Ethylidenebenzacetaldehyde |
| 13 | 550 | C1, benzofuranone or isomer |
| 14 | 555 | C1, dihydronaphthalene |
| 15 | 570 | C1, dihydronaphthalene |
| 16 | 582 | Nitrophenol |
| 17 | 634 | C1, nitrophenol |
| 18 | 652 | C1, nitrophenol |
| 19 | 1547 | Phthalate |

(a) The total ion current chromatogram is presented in Figure B-3.

TABLE B-4. THE MAJOR COMPONENTS TENTATIVELY IDENTIFIED IN THE POLAR FRACTION (MeOH FRACTION), SAMPLE CODE: X038

| Peak Number[a] | Scan Number | Tentatively Identified Compound Name |
|---|---|---|
| 1 | 240 | Benzenemethanol |
| 2 | 264 | Aliphatic alcohol |
| 3 | 280 | C2, phenol |
| 4 | 287 | Benzoic acid |
| 5 | 334 | Phenylpropenal |
| 6 | 365 | Quinoline |
| 7 | 376 | Dihydroindenone |
| 8 | 407 | C2, benzoic acid |
| 9 | 416 | C2, benzoic acid |
| 10 | 423 | C2, benzoic acid |
| 11 | 428 | Hydroxymethylbenzoic acid |
| 12 | 433 | C1, phenyl propenal |
| 13 | 442 | C1, phenyl propenal |
| 14 | 450 | Hydroxymethylbenzaldehyde |
| 15 | 540 | C2, benzenedicarboxaldehyde |
| 16 | 571 | Nitrophenol |
| 17 | 611 | Tetrahydronaphthalenediol |
| 18 | 624 | C1, nitrophenol |
| 19 | 642 | C1, nitrophenol |
| 20 | 1542 | Phthalate |

(a) The total ion current chromatogram is presented in Figure B-4.

TABLE B-5. THE MAJOR COMPONENTS TENTATIVELY IDENTIFIED IN THE AROMATIC FRACTION, SAMPLE CODE: F038

| Peak Number[a] | Scan Number | Tentatively Identified Compound Name |
|---|---|---|
| 1 | 206 | Trichloropropene |
| 2 | 245 | Acetophenone |
| 3 | 408 | C3-benzaldehyde |
| 4 | 422 | Hydroxymethoxybenzoic acid |
| 5 | 435 | Long chain alkane |
| 6 | 445 | Biphenyl |
| 7 | 470 | C2, naphthalene |
| 8 | 491 | Long chain alkane |
| 9 | 526 | Long chain alkane |
| 10 | 538 | C1, biphenyl |
| 11 | 569 | Naphthalenecarboxaldehyde |
| 12 | 588 | C3, naphthalene |
| 13 | 606 | C3, naphthalene |
| 14 | 626 | Long chain alkane |
| 15 | 648 | Fluorene |
| 16 | 676 | Long chain alkane |
| 17 | 686 | Biphenylol |
| 18 | 729 | Long chain alkane |
| 19 | 736 | Long chain alkane |
| 20 | 775 | C1, fluorene |
| 21 | 811 | Fluorenone |
| 22 | 834 | Long chain alkane |
| 23 | 844 | Long chain alkane |
| 24 | 859 | Phenanthrene |
| 25 | 869 | Anthracene |
| 26 | 937 | Long chain alkane |
| 27 | 976 | C2, phenanthrene |

TABLE B-5. THE MAJOR COMPONENTS TENTATIVELY IDENTIFIED IN THE AROMATIC FRACTION, SAMPLE CODE: F038 (CONCLUDED)

| Peak Number[a] | Scan Number | Tentatively Identified Compound Name |
|---|---|---|
| 28 | 1003 | Cyclopenta[d,e,f]phenanthrene or isomer |
| 29 | 1038 | Long chain alkane |
| 30 | 1136 | Long chain alkane |
| 31 | 1148 | Fluoranthene |
| 32 | 1203 | Pyrene |
| 33 | 1300 | Unknown, possible -N- containing compound |
| 34 | 1549 | Phthalate |

(a) The total ion current chromatogram is presented in Figure B-5

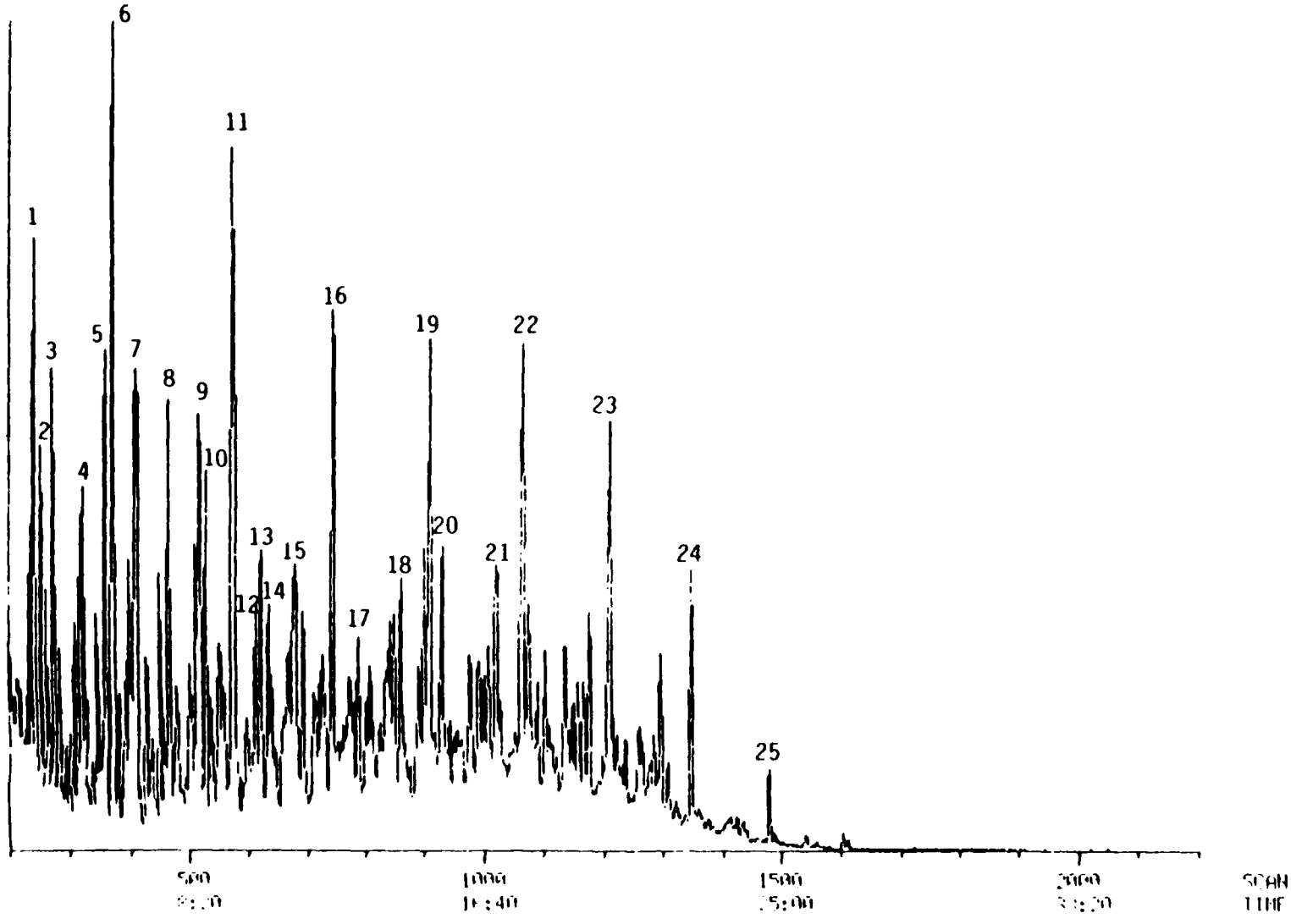


Figure B-1 Total Ion Current Chromatogram of the Aliphatic Fraction from X038

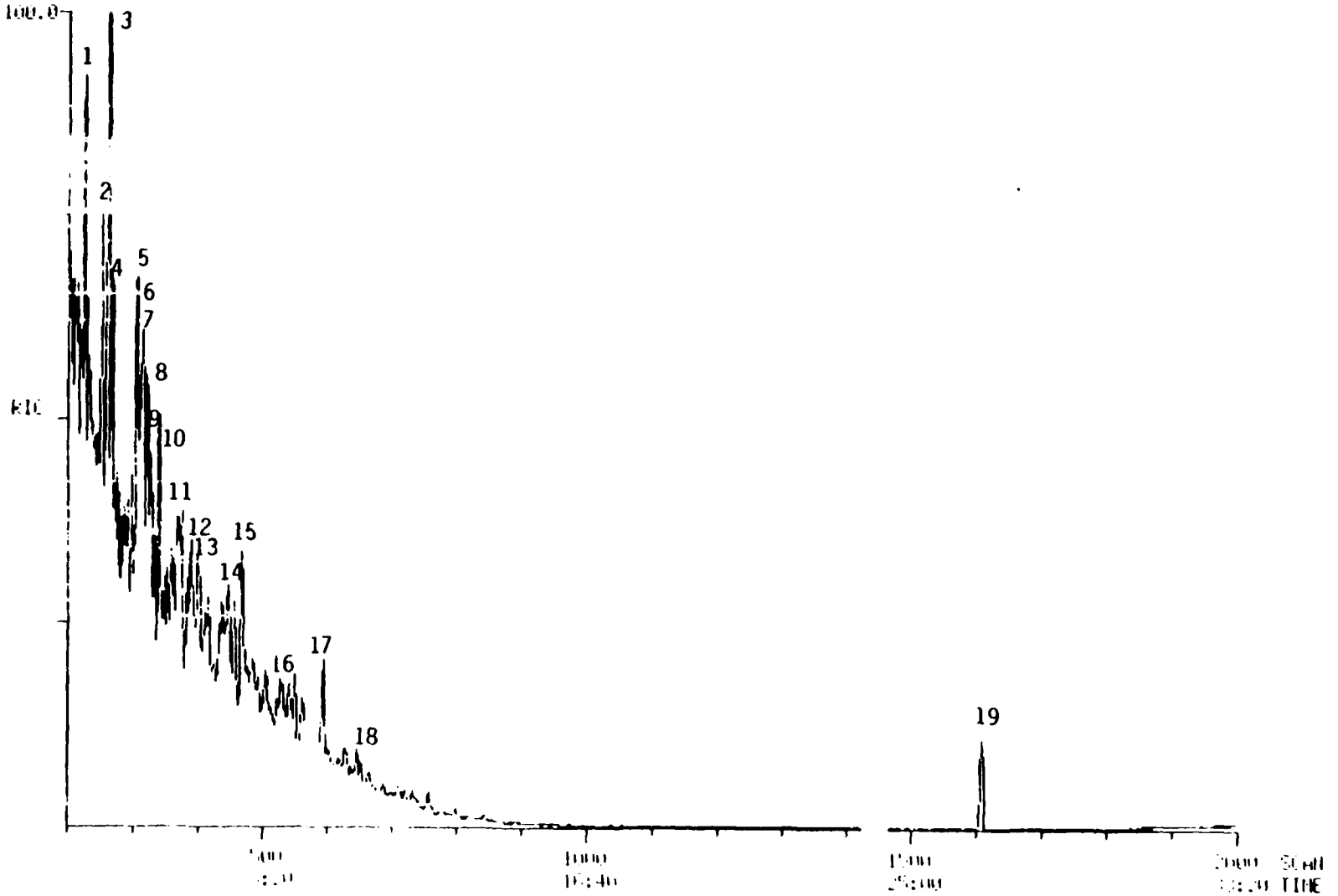


Figure B-2 Total Ion Current Chromatogram of the Aromatic Fraction from X038

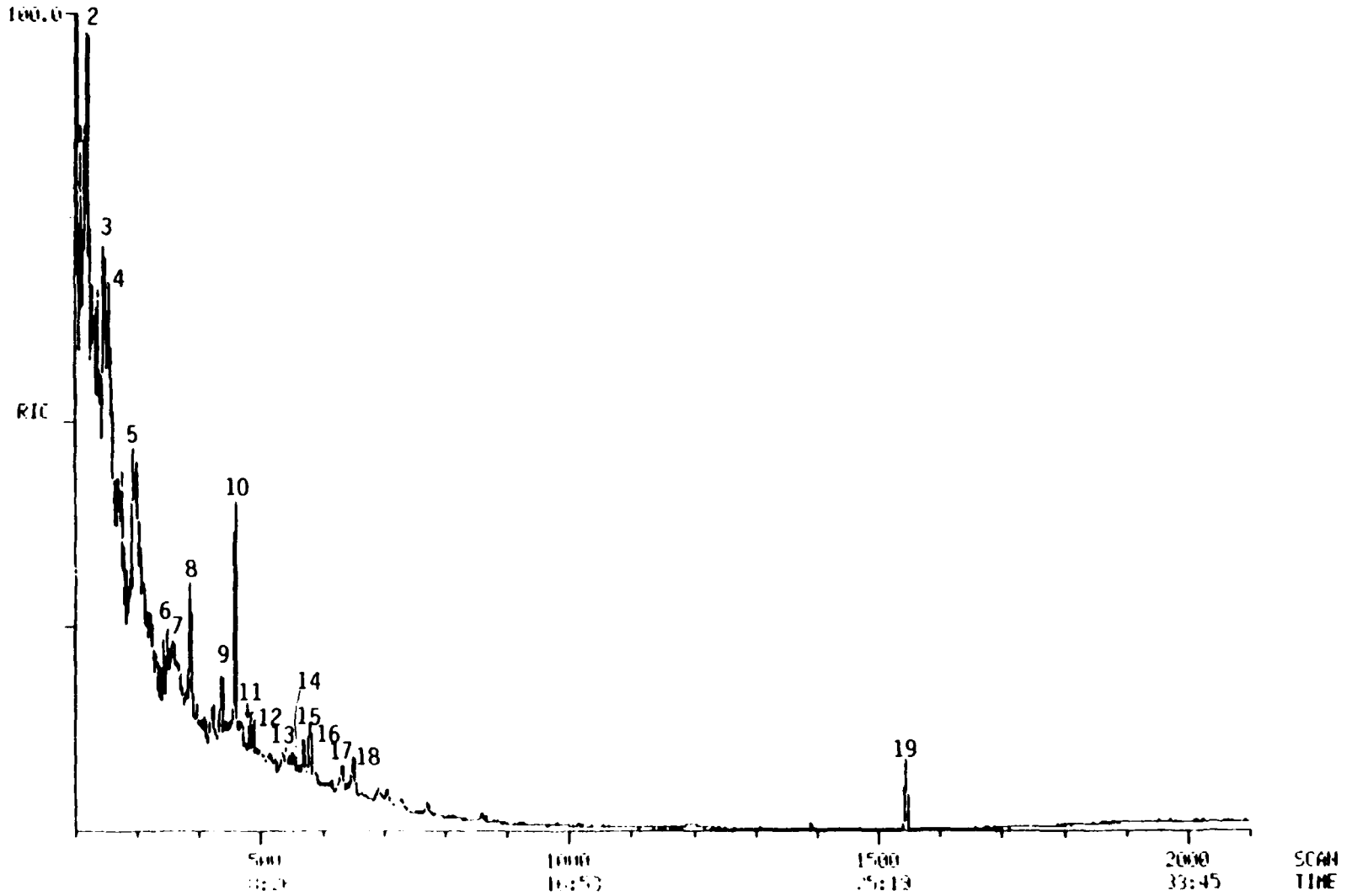


Figure B-3 Total Ion Current Chromatogram of the Moderate Polar Fraction from X038

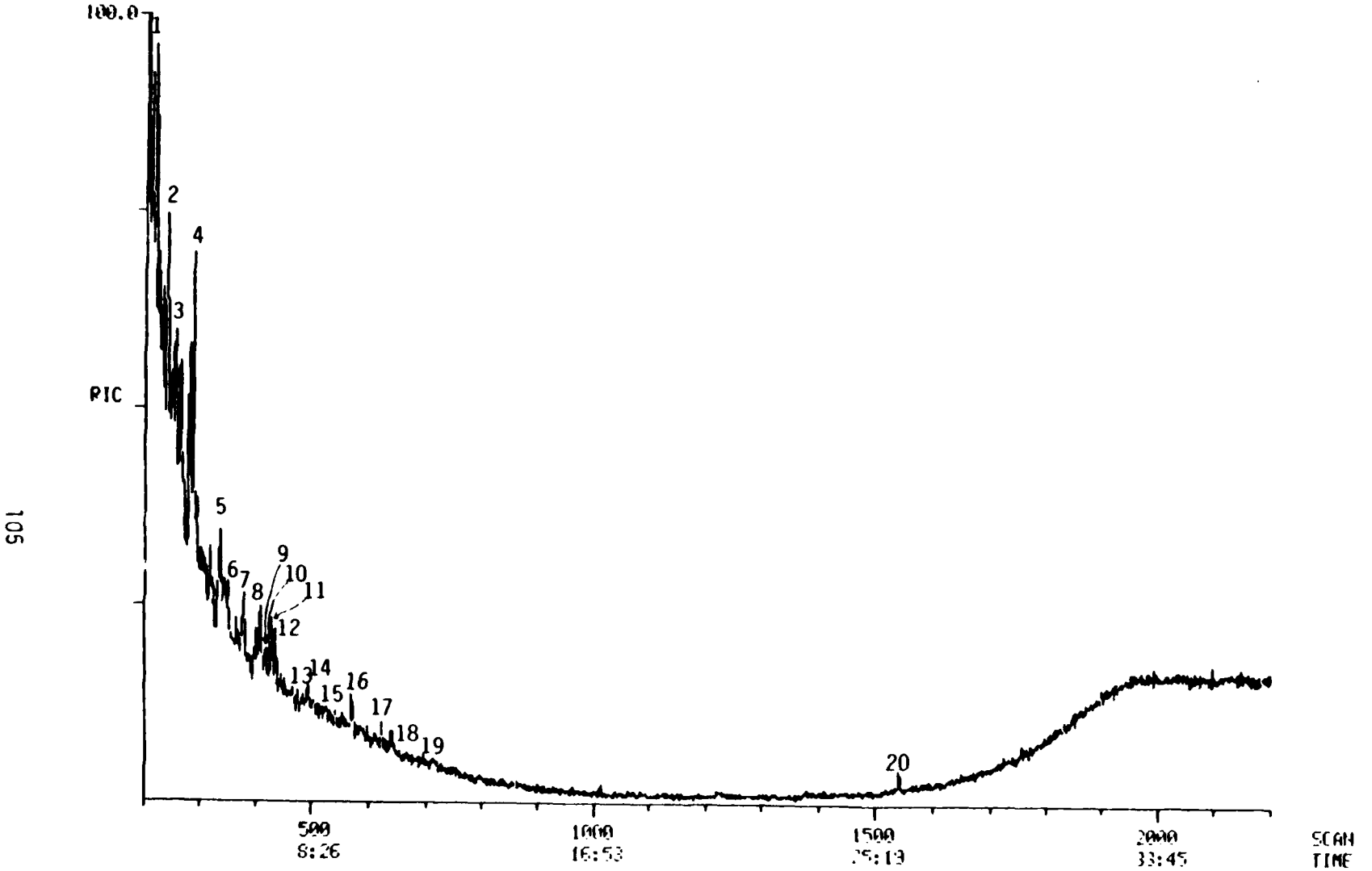


Figure B-4 Total Ion Current Chromatogram of the Polar Fraction from X038

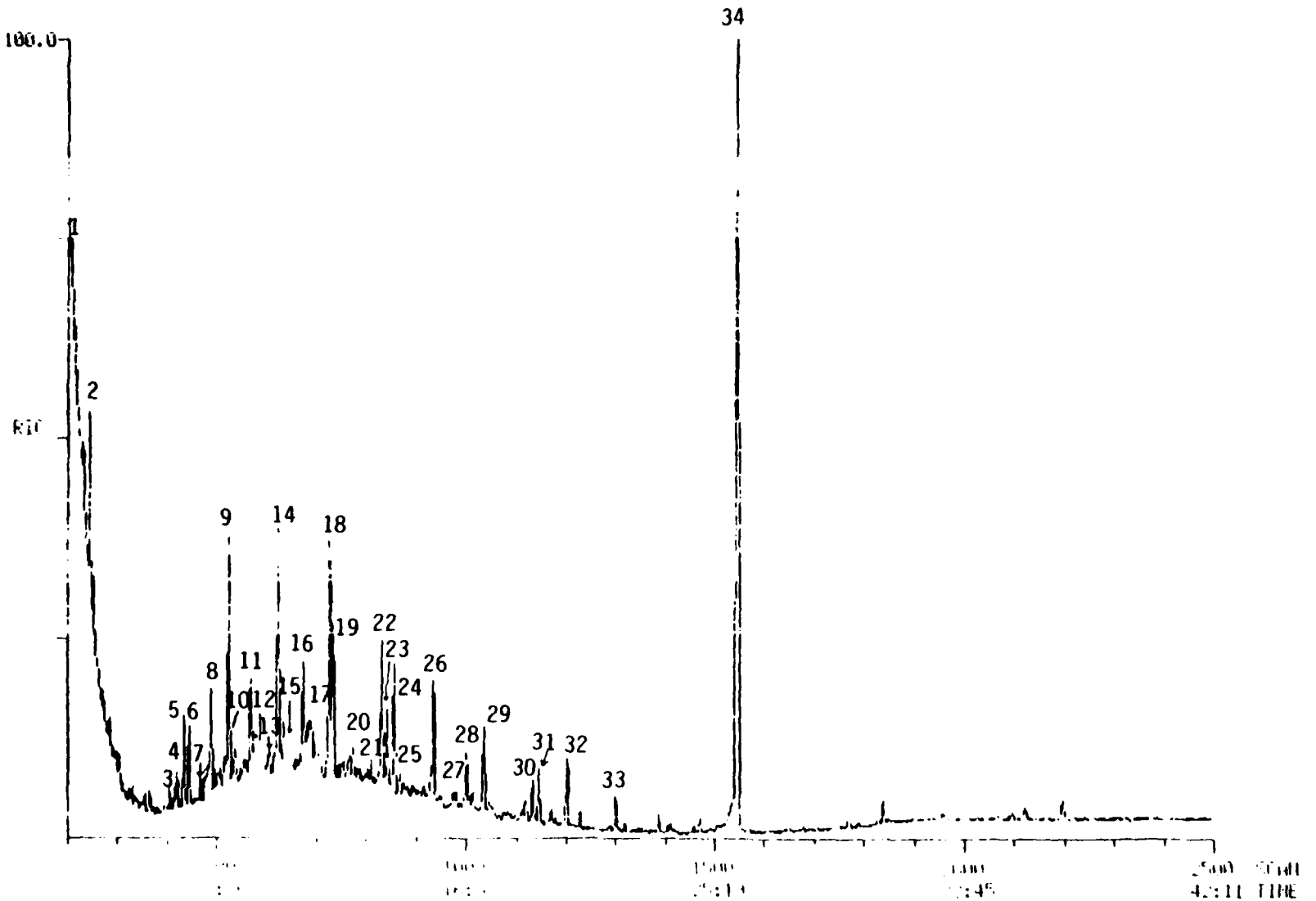


Figure B-5 Total Ion Current Chromatogram of the Aromatic Fraction from F038